Faculdade de Engenharia da Universidade do Porto

Instituto de Ciências Biomédicas Abel Salazar da Universidade do Porto

Implementing translational steps for the clinical application of stromal-vascular cells spheroids

Margarida Alves Simas

Dissertation for the Master Degree in Bioengineering – Molecular Biotechnology

Supervisor: Tália Figueiredo, PhD

Co-supervisor: Cristina Barrias, PhD

June 2019

© Margarida Simas, 2019

“Happiness can be found, even in the darkest of times, if one remembers to turn on the light”

Albus Dumbledore

This page was intentionally left on blank.

Abstract

Cell therapies (CT), together with the high throughput (HT) production of pre-vascularized spheroids, are likely to play a pivotal role in the next generation of healthcare, owing to their potential of providing novel treatments for currently unmet human diseases and injuries. Pre-vascularized spheroids can be used alone, for bottom-up assembly of macrotissues, or in combination with three-dimensional (3D) scaffolds. Spheroids have been showing promise for regenerative medicine (RM), since they favor dynamic cell–cell and cell–matrix interactions, namely though the production of extracellular matrix (ECM) components and improved release of growth factors (GF) and cytokines, which may provide protection against the harsh *in vivo* environment, favoring cell survival and function upon implantation.

Endothelial cell (EC) spheroids usually show poor integrity and viability, but this can be overcome by co-culturing these cells with stromal cells, which promote increased production of ECM and growth factor release. In such co-culture 3D environment, EC can form primitive tubular-like structures, representing a promising approach in tissue engineering (TE). Still, further applications of spheroids in CT depend on the ability to produce them in high amounts, in a short period of time, and/or having them promptly available to delivery. The latter approach would require cryopreservation, a technology that aims to storage biological tissues while maintaining its functional properties once retrieved. However, until now, only few protocols have been successfully established for cryopreserving tissue engineered constructs.

In this context, the present study aimed at producing stromal-vascular cell spheroids in a HT manner and characterize them; and establishing a methodology for their cryopreservation. Experiments have been done under xeno-free (XF) conditions, which represent another important translation step. Outgrowth endothelial cells (OEC) were co-cultured with Mesenchymal stem cells (MSC) in a 1:1 ratio, and with neonatal human dermal fibroblasts (HDFn) in a 5:1 ratio, in agarose micromolds. HDFn-OEC spheroids were cultured for 7 days, and their morphology along with cell organization were evaluated. In HDFn-OEC spheroids OEC organized in two different ways; as a monolayer at spheroids surface, or as clusters at the core, which eventually sprouted into tubular-like structures overtime.

Spheroids were cryopreserved 18 h after cell seeding, using two cryopreservation techniques: Slow Freezing and Vitrification. Different protocol variations were tested, and different

cryocarriers were used, namely cryovials, agarose molds and nylon mesh. Once retrieved, spheroids that underwent vitrification were exposed to a sucrose dilution solution while Slow freezing spheroids were just washed in fresh medium.

MSC-OEC spheroids cryopreserved in cryovials and agarose molds exhibited low metabolic activity and sprout potential post-thawing. HDFn-OEC spheroids cryopreserved in agarose molds demonstrated capacity to sprout, with Slow freezing cryopreserved spheroids having an enhanced viability, as compared to vitrification. Moreover, cells were able to migrate out of the spheroids and proliferate. HDFn-OEC spheroids vitrified in nylon mesh did not show any sprouting potential. HDFn-OEC spheroids cryopreserved by Slow freezing exhibited enhanced sprout potential and production of ECM components (collagen type I). Furthermore, HDFn-OEC spheroids showed more viability from cryopreservation than MSC-OEC spheroids.

This study demonstrated that vitrification approaches, as described in the literature, are not the best approach to spheroids cryopreservation. Nevertheless, this study provided new insights into the process, which will be important for future optimizations that should be attempted to achieve higher cryopreservation success rates.

Aknowledgments

First of all, I would like to express my deepest gratitude to my supervisor Tália Figueiredo and thank her for her support, patience, dedication and for helping me in my (small) path to become a scientist.

To my professor and co-supervisor, Cristina Barrias, for accepting me in her incredible group and for all the guidance.

To all members of Bioengineered 3D Microenvironments group, for welcoming me with open arms, for the company and friendships. I will never forget to bring you queijadas.

To my friends whom have been my best friends in Porto for 6 years: Teresa, Carolina, Teresa M., Joana, Rute. May our paths never diverge.

To all people I knew in MIB, thanks for the laughs, the shared memories and friendships.

A special thanks to my childhood best friends: Margarida, Marta and Raquel. Thank you for all the support and friendship over these years and for celebrating each other's victories as our own.

To my amazing cousins, whom I've shared a house for the last 3 years: thank you isn't enough. You were the best roommates I have ever had.

A very special thanks to my boyfriend, Pedro, for not letting me give up, and for always believing in me.

And finally, to my parents and brothers, for allowing me to pursue my goals and being always there for me, through good and bad.

The research described in this thesis was financially supported by:

Project ANGIONICHE funded by POCI via FEDER (POCI-01-0145-FEDER-028744) and by FCT via OE (PTDC/BTM-MAT/28744/2017).

This page was intentionally left on blank.

Table of contents

List of figures

List of tables

This page was intentionally left on blank.

Abbreviations

List of abbreviations

AELC	Alginate-Encapsulated Liver Cells
BM-	Bone marrow derived
BSA	Bovine Serum Albumin
CIDOCD	Cryopreservation-induced delayed-onset cell death
Col I	Collagen Type I
CPA	Cryoprotectant Additive
CPS	Closed Pulled Straw
CT	Cell Therapy
DAH	Differential Adhesion Hypothesis
DAPI	4,6-diamidino-2-phenylindole
DMSO	Dimethyl Sulfoxide
EC	Endothelial Cell
ECM	Extracellular Matrix
EG	Ethylene Glycol
EGF	Endothelial Growth Factor
EM	Electron Microscopy
EPC	Endothelial Progenitor Cells
ES1	Equilibrium Solution 1
ES2	Equilibrium Solution 2
EtOH	Ethanol

EX/EM	Excitation/Emission
FBS	Fetal Bovine Serum
FGF	Fibroblast Growth Factor
GF	Growth factor
HDF	Human Dermal Fibroblast
HDFn	Neonatal Human Dermal Fibroblast
hMSC	Human Mesenchymal Stem Cells
HUVEC	Human Umbilical Vein Endothelial Cell
HT	High throughput
IGF	Insulin-like growth factor
LN	Liquid Nitrogen
LT	Liquidus Tracking
MCS	Multicellular Spheroid
MDS	Minimum Drop Size
MSC	Mesenchymal Stem Cell
MVC	Minimum Volume Cooling
npCPA	Non-permeating Cryoprotectant Additive
OEC	Outgrowth Endothelial Cell
ON	Overnight
OPS	Open Pulled Straw
PBS	Phosphate Buffer Saline
pCPA	Permeating Cryoprotectant Additive
PD	1,2 - propanediol
PECAM-1	Platelet endothelial cell adhesion molecule - 1
PEG	Polyethylene Glycol
PFA	Paraformaldehyde
P/S	Penicillin/Streptomycin
RM	Regenerative Medicine

RGD	Arginine-Glycine-Aspartate
RT	Room Temperature
RWV	Rotating wall vessel
SCC	Supplement for Cell Culture
SF	Slow Freezing
SFS	Slow Freezing solution
SFC	Serum free cocktail
TE	Tissue Engineering
Tg	Glass Transition Temperature
VE	Vascular-endothelial
VEGF	Vascular Endothelial Growth Factor
VS	Vitrification Solution
vWF	von Willebrand Factor
XF	Xeno-Free
2D	Two-dimensional
3D	Three-dimensional

This page was intentionally left on blank.

Chapter 1

Introduction

1.1. General Introduction

Tissue engineering aims to develop new strategies to overcome the limited efficiency of conventional treatments or organ transplantation. Several advances have been made in the fields of TE and RM, which generally make use of cells, scaffolding biomaterials and bioactive agents, alone or in combination (Annabi *et al.*, 2017; Aurora *et al.*, 2018; Syed-Picard *et al.*, 2018). CT is a RM approach which consists in the delivery of stem, progenitor, primary and/or genetic modified cells as a therapeutic strategy, namely to facilitate tissue repair/regeneration. Several studies have been done using CT. For instance, a randomized controlled trial has been performed in patients with critical limb ischemia, showing that autologous transplant of bone marrow-derived (BM-) mononuclear cells can safely and effectively induce neo-vascularization (Tateishi-Yuyama *et al.*, 2002). BM-MSC delivered intravenously in animal ischemic stroke models increased expression of neurotrophic factors, reduced apoptosis and promoted neural progenitor cells proliferation (J. Chen, Li, *et al.*, 2003; Y. Li *et al.*, 2002). The transplanted cells also contributed to angiogenesis by angiogenic GF secretion (J. Chen, Zhang, *et al.*, 2003). However, the traditionally administration mode of CT, by single-cell delivery, usually shows a short-term effect, due to low cell survival and persistence at the target site, which consequently leads to low engraftment rates (Mohamadnejad *et al.*, 2007; Peng *et al.*, 2011).

On the other hand, upon implantation, cell survival in large scaffold-based or scaffold-free 3D constructs depends on how quickly appropriate blood supply is established. *In vivo*, nutrients and oxygen diffused from capillaries, which distance from cells does not exceed 100-200 μm. The same is required in TE constructs (Jain *et al.*, 2005), where these are provided to cells through medium supply under static or dynamic culture conditions. However, upon tissue constructs implantation, cell survival is impaired, especially in large 3D constructs of clinically relevant size, due to insufficient diffusion of oxygen and nutrients if neo-vascularization is not rapidly established. In this context, pre-vascularized constructs have emerged as a potential therapeutic strategy in RM. This strategy consists on promoting

endothelial organization in to tubular-like structures within TE constructs, before their implantation (Laschke & Menger, 2016). The aim is to stimulate rapid inosculation of these vascular beds with the host vasculature, creating a new vascular network that will promote tissue survival and engraftment.

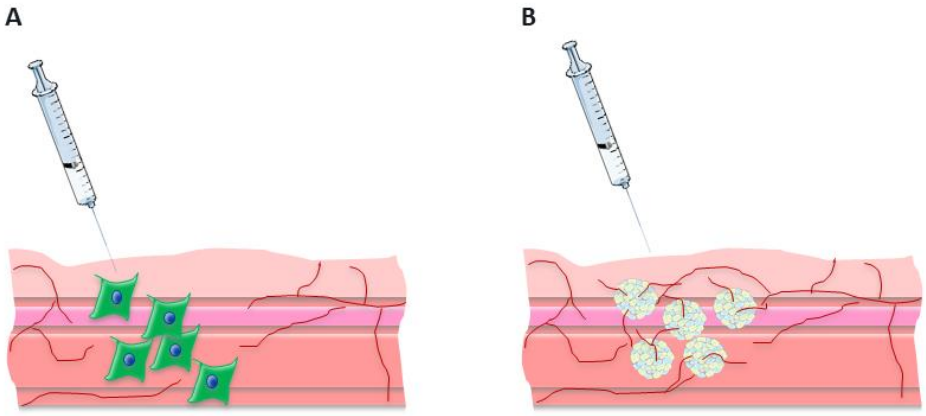

Figure 1 - Single cell suspension versus pre-vascularized 3D constructs delivery. (A) In single cell delivery, cells are not able to organize and produce ECM leading to low engraftment rates, which in turn causes lack of neo-vascularization and ultimately cell death. (B) In pre-vascularized spheroids delivery, the pre-existent vascular like network will promote spheroids integration to the host vasculature, resulting in higher rates of cell survival upon implantation.

1.2. Multicellular spheroids (MCS)

In RM, spheroids have become very popular, as an alternative to single-cell administration, since they promote a dynamic 3D environment retaining cell-cell as well as, cell-matrix interactions (Laschke & Menger, 2017). Studies in pulp regeneration (Dissanayaka *et al.*, 2014), hepatic ischemia-reperfusion (Sun *et al.*, 2018), heart failure (Noguchi *et al.*, 2016) and bone tissue engineering (Heo *et al.*, 2019) have reported the use of pre-vascularized spheroids. Furthermore, comparing to single-cell suspensions, spheroids are able to produce and accumulate endogenous ECM (J. M. Kelm *et al.*, 2010), higher amounts of pro-angiogenic factors (J. M. Kelm *et al.*, 2005) and have increased protection against hypoxia and oxidative stress (Zhao *et al.*, 2016). All this, in the end, will contribute to improve microtissue engraftment.

While along the past century, cells cultured in two-dimensions (2D) have been the gold standard for *in vitro* studies, they fall short in mimic the *in vivo* environment (Laschke & Menger, 2017). Therefore, 3D cell culture models, have been gathering increasing interest among the scientific community since they provide more representative spatial, biological, biochemical and biophysical conditions (Abbott & Kaplan, 2015; Pampaloni, 2007; Schmeichel & Bissell, 2003; Schwartz & Chen, 2013). Thus, the use of spheroids culture has also become a popular form of *in vitro* 3D culture.

1.2.1. Spheroids assembly and organization

Whenever anchorage-dependent cells are seeded under non-adhesive culture conditions, they spontaneously self-aggregate into compact, microtissue structures (so called spheroids). The process of spheroid formation highly depends in cell-cell adhesion. One of the most accepted concepts is "The Differential Adhesion Hypothesis" (DAH). DAH claims that under certain conditions, monodispersed cells tend to minimize the surface free energy, by maximizing intercellular interactions, spontaneously aggregating into more stable spherical clusters (Foty & Steinberg, 2005). This self-aggregation occurs due to long-chain ECM fibers with multiple Arginin-Glycine-Aspartate (RGD) motifs that bind to integrins in cell membranes (Salmenpera *et al.*, 2008). This cell-cell contact triggers of cadherin over expression, leading to cadherin accumulation in the membrane surface which causes cells to form compact microtissues (Cui *et al.*, 2017; Duguay *et al.*, 2003). In fact, it has been reported that, contrarily to cadherin expression in mouse fibroblasts, cells with inhibited cadherin expression failed to form compact spheroids, which demonstrates the key role of these cell adhesion molecules on spheroids assembly (Dittrich *et al.*, 2018).

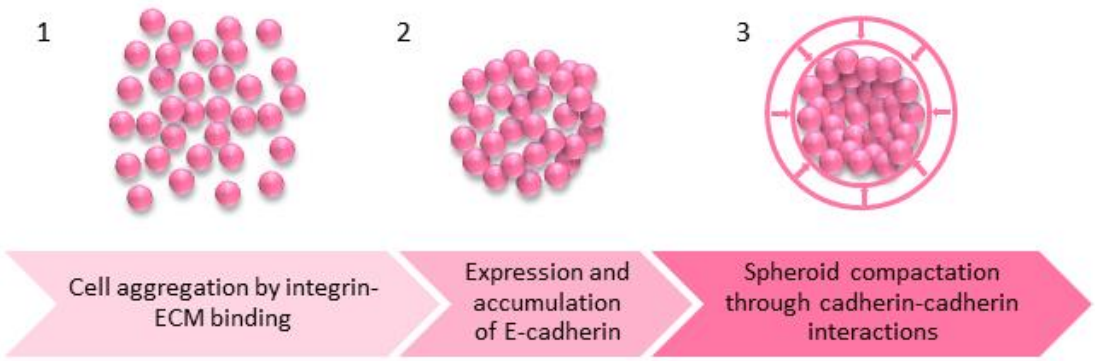

Figure 2 - Spheroid formation process model. Spheroid formation can be divided into three stages: (1) formation of loose cell aggregates via integrin-ECM binding; (2) a delay period for cadherin expression and accumulation; (3) formation of compact spheroids through homophilic cadherin-cadherin interactions. Adapted from (Benien & Swami, 2014).

In co-culture spheroids, cells organization takes place according to the expression levels of cadherin. If cells have the same cadherin expression levels, they tend to form randomly mixed spheroids (Duguay *et al.*, 2003). On the other hand, if cells have different cadherin expression levels, following DAH, cells with increased cadherin expression will surround the other cell population, forming a concentric spheroid (Foty & Steinberg, 2004, 2005). Cells cytoskeleton also contributes in spheroids formation, providing cellular structural stability due to expansion of actin microfilaments (Tzanakakis *et al.*, 2001).

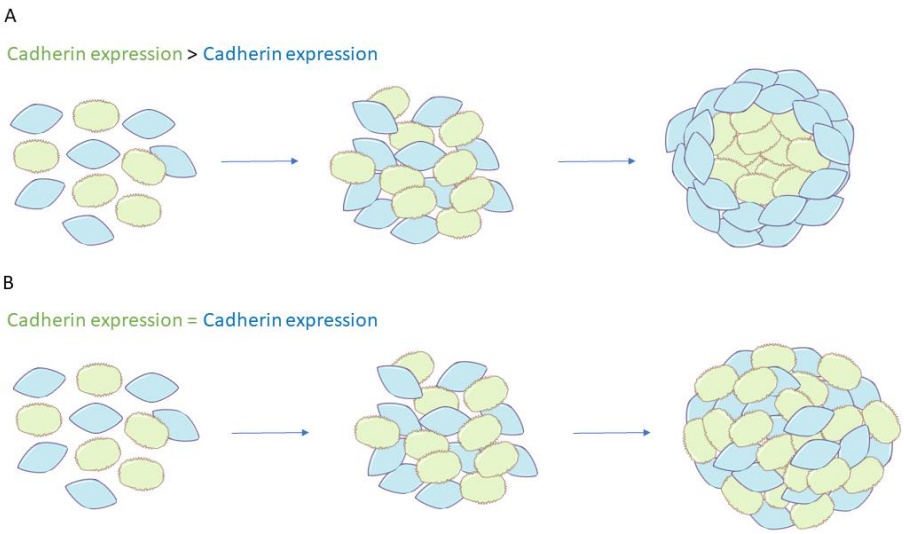

Figure 3 - Mechanisms underlying spheroids formation. In spheroids, cells organize according to their cadherin expression. (A) Cells with higher cadherin expression tend to migrate towards the center of the spheroid as for cells with lower cadherin expression stay at the surface, forming a concentric layer. (B) When cells have similar cadherin expression, a randomly mixed spheroid is formed.

Depending on their size, spheroids may display a three-zoned structure: 1) proliferating zone which contains cells active with intact nuclei and abundant microvilli; 2) quiescent zone, where cells with shrunk nuclei, sunken-in membranes and with minimal minimum metabolic activity; 3) necrotic zone, where cells have disintegrated nuclei and membranes and die due to lack of nutrients (Curcio *et al.*, 2007). As previously mentioned, in an avascular tissue, nutrients and oxygen supply for cells in spheroids should be between 100-200 µm distance. Therefore, a spheroid with a size above 300 µm in diameter will have diffusion limitation, resulting also in metabolic waste accumulation in the inner layer of spheroids, and leading to development of a necrotic core (Mueller-Klieser, 1984).

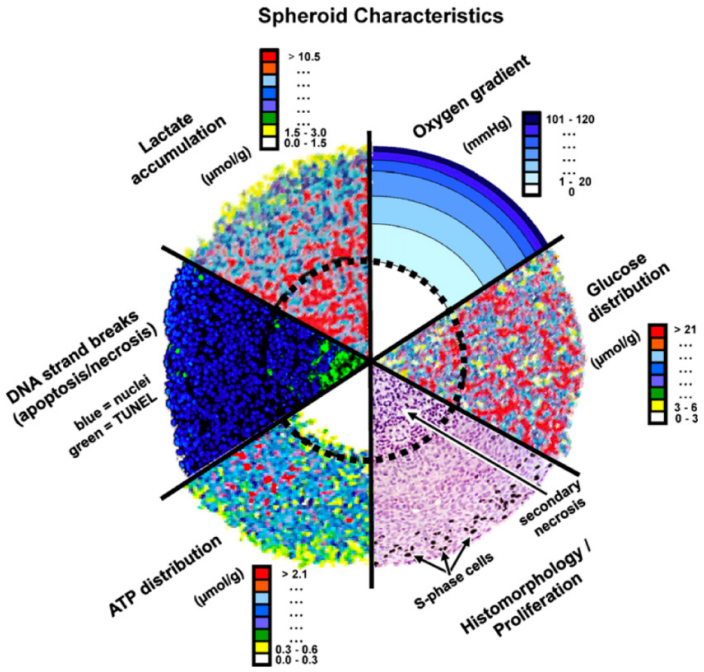

Figure 4 - Spheroid characteristics. Combination of analytical images of spheroid median sections studied with different technologies: autoradiography, the tunnel assay, bioluminescence imaging, and probing with oxygen microelectrodes. Together these measurements enable the concentric arrangement of cell proliferation, viability and the microenvironment in large spheroids to be understood. Figure retrieved from Hirschhaeuser et al. (Hirschhaeuser *et al.*, 2010).

1.2.2. Spheroid production

When producing spheroids, the main requisite is to prevent cells from attaching to the culture substrate, forcing their aggregation into multicellular clusters. Still, there are other requirements to take in account such as, high production efficiency, spheroid size uniformity, reproducibility, and suitability for the intended applications (R. Z. Lin & Chang, 2008). It is also important to avoid possible damage or deleterious influence on cellular physiology (R. Z. Lin & Chang, 2008). Multiple techniques have been used to generate multicellular microtissues. These are (1) pellet cultures (figure 5A) (Jahn *et al.*, 2010); (2) cultivation in gyratory shakers, roller bottles and spinner flasks (figure 5B) (Brophy *et al.*, 2009; Han *et al.*, 2006); (3) microgravity modulators (Figure 5C) (Becker & Souza, 2013; Grimm *et al.*, 2014); (4) culture in non-adhesive hydrogels (Figure 5E) (Q. Li *et al.*, 2011; Vantangoli *et al.*, 2015); (5) hanging-drop cultures Figure 5F) (J. M. Kelm *et al.*, 2006); (6) magnetic levitation (Figure 5D) (Souza *et al.*, 2010) and (7) droplet microfluidics (Figure 5G) (Chan *et al.*, 2013).

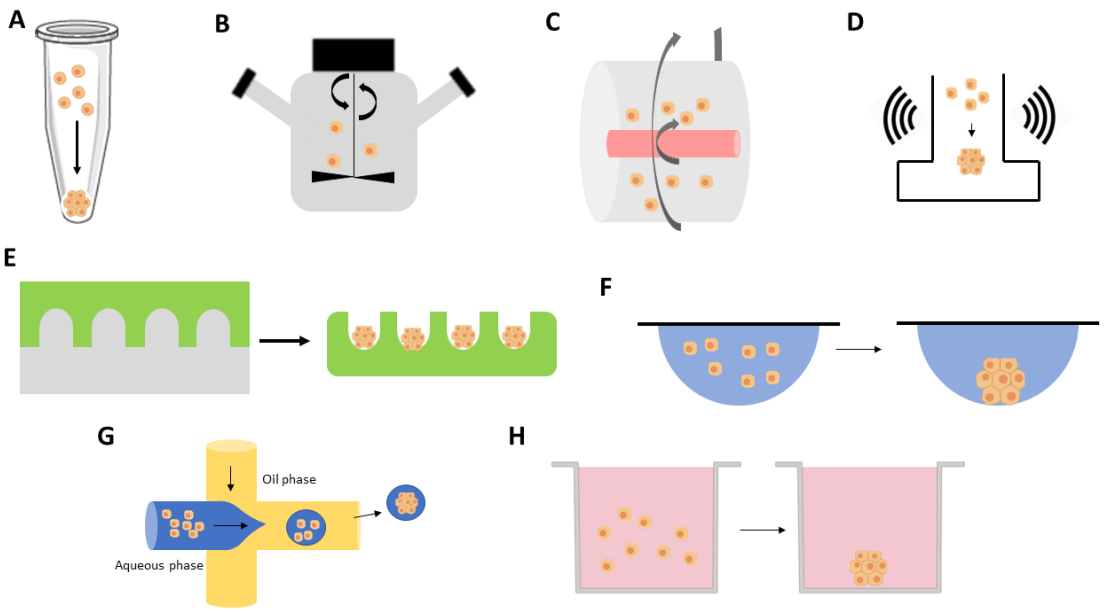

Figure 5 - Different techniques for spheroids production. (A) Pellet cultures, (B) gyratory flasks, (C) microgravity modulators, (D) magnetic levitation, (E) non-adhesive culture hydrogels, (F) hanging-drop culture, (G) droplet microfluidics and (H) non-adhesive culture vessels: culture well coated with non-adhesive film.

Table 1.1 – Comparison between common methodologies for spheroid production. Adapted from Lin et al (R. Z. Lin & Chang, 2008).

Method	Description	Advantages	Disadvantages	References
Pellet cultures	Cell seeding in well plates, centrifugation tubes or Eppendorf tubes. Cells can form spheroids over time or by centrifugation.	Simple to perform; Rapid aggregation of large number of cells.	Shear force; Difficult to scale up.	(Jahn *et al.*, 2010; Qihao *et al.*, 2007)
Gyratory shakers, roller bottles and spinner flasks	Cells are inoculated in the device. Spheroid diameter can be controlled by tuning cell-seeding density, medium composition, spinning rate and culture time.	Commercially available; Produces large amounts; Long-term culture; Co-culture of different cell types; Dynamic control of culture conditions.	Require specialized equipment; Produced spheroids are heterogeneous in size and shape; Strong shear force used may affect cell physiology.	(Lazar *et al.*, 1995; Nyberg *et al.*, 2005; Song *et al.*, 2004)
Microgravity modulators	Rotating wall vessel (RWV) has a central silicone membrane that delivers oxygen via diffusion. The vessel is filled with culture media and so has no air–liquid interface. Since there are no internal moving parts, cells grow in a culture environment with low shear and low turbulence. Adherent cells are grown on microcarrier beads to provide a solid support – cells attach and cover the surface. With continued growth, cells eventually form 3D aggregate structures. As the RWV rotates, spheroids present in the fluid are in a state of free fall, but never reach the bottom of the vessel owing to the constant rotation of the RWV.	Simple to perform; Massive production; Long-term culture; Dynamic control of culture conditions; Better cell differentiation; Co-culture of different cell types.	Require specific equipment; Incompatible with real-time single-microtissues analysis.	(Becker & Souza, 2013; Ingram *et al.*, 1997; Khaoustov *et al.*, 1999)
Non-adhesive culture vessels	Cells are seeded in non-adhesive plastics or vessels can be coated with thin agarose films or hydrophobic polymers. Also, non-adhesive micromolded hydrogels can be used: hydrogel solution is poured onto precision molds containing an array of the negative recesses. After gelation, the nonadhesive hydrogel is removed and placed on a standard culture dish.	Inexpensive; Simple to perform Easy to scale up; Micromolds are autoclavable and reused; Well-controlled spheroid size – when using micromolded hydrogels; Designed aggregate geometry; Co-culture of different cell types.	When cultured in non-adhesive plastics or coated vessels, spheroids tend to have a broad size and shape distribution.	(Hamilton *et al.*, 2001; Landry J, 1985; Q. Li *et al.*, 2011; Vantangoli *et al.*, 2015; Yuhas *et al.*, 1977)
Hanging-drop cultures	Droplets of single cell suspension (10-30µL) are	Inexpensive;	Labor intensive;	(J. M. Kelm *et al.*, 2006;

	pipetted onto a surface and then inverted upside down. Through gravity, cells concentrate at the bottom of the hanging drop, at the air-liquid interface, forming a single spheroid per drop after 1-4 days, depending on the cell type.	Simple; Well-controlled spheroid size; Fast spheroid formation; Co-culture of different cell types; Easy to trace spheroid assembly.	Difficult to scale up.	Jens M. Kelm & Fussenegger, 2004; J. M. Kelm *et al.*, 2003; Wartenberg *et al.*, 2001)
Magnetic levitation	Cells are treated with magnetic nanoparticle-containing hydrogels. Cells are then seeded onto a non-adhesive multiwell plate with an external magnet, where they levitate and assemble near the air medium interface into a spheroid.	Commercially available; Quick formation of spheroids (about 12h); Possibility to shape spheroids to the desired configuration.	Expensive.	(Souza *et al.*, 2010)
Droplet microfluidics	Cell suspension is injected into an aqueous channel, which turns into droplets upon contact with the oil phase. The water-in-oil droplets can be then cultured off-chip or stored in microchannel arrays.	High-throughput technique; Easy to scale up; Precise control over spheroid dimensions.	Inability to perform washing steps inside droplets.	(Brouzes *et al.*, 2009; Chan *et al.*, 2013; McMillan *et al.*, 2016; Rakszewska *et al.*, 2014)

1.2.3. Endothelial Cells

EC are the building blocks that give rise to newly formed vasculature. Apart from the structural role, EC also play a pivotal role in the vascularization process by paracrine and autocrine signaling by different molecules. These include, among others, von Willebrand factor (vWF), vascular endothelial (VE)-cadherin and platelet endothelial cell adhesion molecule-1 (PECAM-1 or CD31) (Fuchs et al., 2006a; Fuchs et al., 2006b; Medina *et al.*, 2010; Muller *et al.*, 2002), which are responsible to regulate cell behavior, sprouting, tubulogenesis, and ECM production (Giannotta et al., 2013; Meyer et al., 1991; Park et al., 2010; Privratsky & Newman, 2014). This milieu provides an adequate microenvironment for EC organization into capillary-like structures and subsequent formation of vascular-like networks. Taking this in consideration, spheroids that incorporate EC have been showing promise for tissue vascularization and have been widely used for assembly of pre-vascularized engineered tissues (Korff et al., 1998).

Crosstalk between EC on vessel walls and the ECM, both interstitial matrix and basement membrane, is crucial for vascular development. Different ECM components, namely fibronectin and laminin, will engage specific integrins interactions, providing a physical anchor between the cell cytoskeleton and the ECM, which also triggering important signaling pathways.

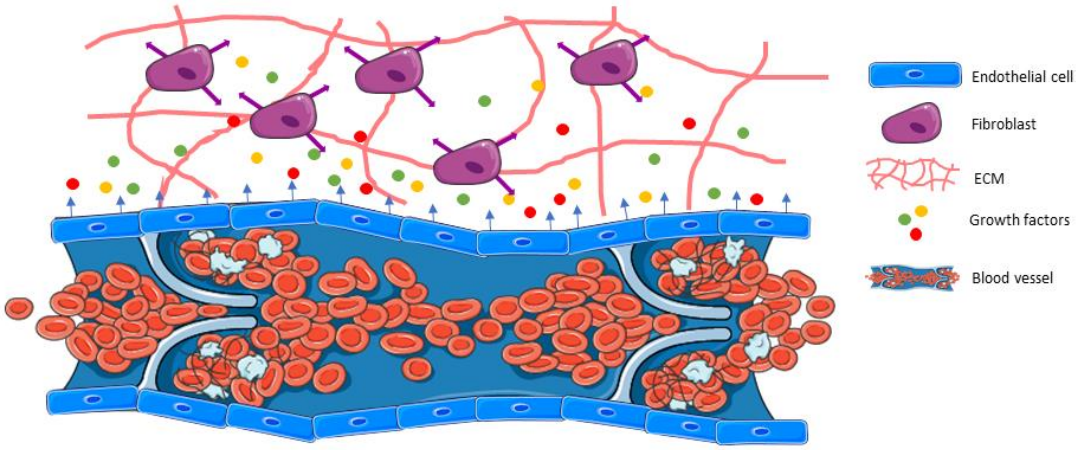

Figure 6 - EC-ECM interaction. Endothelial cells produce several GF such as vWF, VE-cadherin and PECAM-1, which will regulate cell behavior as well as ECM production.

There are different EC sources, depending on their origin and developmental stage. Endothelial progenitor cells (EPC), were first described by Asahara *et al*, as being able to participate in neo-vascularization processes, namely when recruited from the bone marrow to sites of ischemia (Asahara *et al.*, 1997). There are two main types of EPC, early EPC and late EPC, being the latter also called OEC (Lin et al., 2000Y. Lin *et al.* (2000); (Medina *et al.*, 2010). OEC can be isolated from different sources, namely from bone marrow (Shi *et al.*, 1998), umbilical cord blood (Asahara *et al.*, 1997), adipose tissue (Lin et al., 2008) and

amniotic fluid (Zhang et al., 2009), presenting some advantages over mature EC for clinical applications.

1.2.4. Stromal-vascular cell spheroids

Over the past years, many strategies using EC from different origins have been used to promote spheroids pre-vascularization. Kelm *et al.*, reported the use human umbilical vein endothelial Cells (HUVEC)-coated with human myofibroblast to create microtissues, which organized in a pre-vascular network. In 1998, Korff *et al.* demonstrated that EC multicellular spheroids prevented apoptosis and stabilized cells, when compared to 2D monocultures (Korff & Augustin, 1998). Moreover, Alajati *et al.* promoted human vasculature development in mice, by using HUVEC-based spheroids in a Matrigel-fibrin matrix with GF, proving that EC could be successfully used to form durable microvascular capillary networks (Alajati *et al.*, 2008). In 2009, Laib *et al.* developed an endothelial transplantation assay, where EC spheroids cultured *ex-vivo* were transplanted into immunosuppressed mice that could potentially be used in several angiogenesis studies (Laib *et al.*, 2009). More recently, Amann *et al.* produced a 3D angiogenesis model to study EC interactions with anti-angiogenic drugs using triple-cultures of these cells with non-small cell lung cancer cell lines and fibroblast (Amann *et al.*, 2017).

Different patterns of EC organizations within spheroids can be achieved, depending on the EC source, the cells that they are co-cultured with, their relative ratio, and other parameters such as spheroid size (J. M. Kelm *et al.*, 2005; T. Korff, et al., 2001; Stahl *et al.*, 2004). During vertebrate embryonic development, tissue morphogenesis depends on cell sorting (Foty & Steinberg, 2005). A similar process occurs in co-cultured spheroids. EC within spheroids are able to segregate and organize into tubular-like structures within the spheroid or accumulate at the core or at the periphery. For instance, a study showed that EC cultured with aortic fibroblasts or hepatocellular carcinoma cells aggregated into a concentric layer at the periphery of the spheroid. Whereas in another study, EC co-cultured with umbilical artery localized predominantly in the center of the spheroid. In addition, it was demonstrated that EC in the periphery could subsequently migrate into the inner part of the spheroids and assemble into tubular-like structures (J. M. Kelm *et al.*, 2005).

Stromal cells are involved in maintenance of tissue structure and homeostasis providing support for vascular cells, ECM production and GF secretion. MSC are a type of stromal cells characterized as an adhesive cell population present in the bone marrow and other tissues. They have been used in several studies due to their multilineage differentiation capacity, immunosuppressive properties and high expansion potential (Bianco *et al.*, 2013). Importantly, MSC spheroids were described to display enhanced anti-inflammatory and angiogenic activities, augmented differentiation and stemness potential, improved survival and delayed replicative senescence (Bartosh, 2010; Chen et al., 2013), as compared to non-

aggregated cells. However, low engraftment due to lack of vascularization, of these spheroids limit their therapeutic potential. Co-culture of MSC-EC spheroids combine the ability of EC to produce tubular-like structures, with the ECM production ability and paracrine activity of MSC, which promotes anchoring, survival and stabilization of EC. All together, these features have the potential to give rise to stable pre-vascularized microtissues.

In fact, the crosstalk between MSC and EC has been extensively described by several studies. In 2008, Au et *al*. performed co-cultures of MSC and HUVEC, showing that MSC were able to differentiate into pericytes, stabilizing the newly formed vasculature for several months (Au et al., 2008). More recently, the same was observed using MSC and EPC (Loibl *et al.*, 2014).

Moreover, Guerrero *et al*. showed that a co-culture of human progenitor-derived EC and MSC in 3D macroporous scaffolds led to an increased mRNA expression of junctional proteins, promoting osteogenesis (Guerrero *et al.*, 2013). Studies using MSC and EPC reported that MSC played a role in EPC differentiation towards an endothelial functional phenotype and formation of capillary-like structures (Duttenhoefer *et al.*, 2013). Recently, a study using co-culture spheroids of MSC and OEC in a XF culture setting demonstrated their angiogenic potential both *in vitro* and *in vivo* (Bauman et al., 2018).

Fibroblasts are stromal cells and are the main producers of ECM in native connective tissue. They synthesize key ECM components, such as collagens, elastin, fibronectin and proteoglycans, as well as ECM-degrading enzymes such as matrix metalloproteinases, which play a role in ECM remodeling. They also engage in paracrine signaling by releasing different GF, such as vascular endothelial growth factor (VEGF) and fibroblast growth factor (FGF)-2. Fibroblasts can be found in several locations within the body, since they are the main component of the stroma in different types of tissues. Human dermal fibroblasts (HDF) have been gaining interest in the vascularization field. HDF, like MSC, may serve as supportive cells for EC, namely through ECM deposition, allowing cell survival, maturation and stabilization, while at the same time regulating the vascularization process (Hurley et al., 2010).

The implantation of HDFn using Matrigel plugs in mice showed that HDFn induced the ingrowth of blood vessels from the host vasculature (Guerreiro *et al.*, 2012). Indeed, several *in vitro* studies have showed that fibroblasts support the assembly of EC into capillary-like structures and that the fibroblast-derived matrix is essential for lumen formation by EC (Berthod et al, 2006; Newman et al., 2011). Another study with fibroblasts and OEC have shown, *in vivo*, faster blood perfusion and anastomosis with the host vasculature (X. Chen *et al.*, 2010). Moreover, Hendrickx *et al*. reported that dermal fibroblasts sheets with OEC accelerated wound healing by incorporating into newly formed blood vessels and promoting oxygenation (Hendrickx *et al.*, 2010).

These results show that co-cultured spheroids of OEC and stromal cells should be further studied and eventually could become a potent therapeutic strategy for vascularization.

However, translating this type of therapies into clinical practice still represents a huge challenge, since its production is difficult, a laborious and time-consuming process, making it hard to have an "off-the-shelf" product, which would be the optimal ultimate goal. To overcome part of these challenges, one can resort to cell/tissue cryopreservation. Cryopreservation consists in using very low temperatures (usually from -135 to -196ºC) to preserve structurally and functionally biological material, such as living cells and tissues. Even though, cryopreservation being an old and widely used technique, there is not much done in the TE field. Nevertheless, there are some studies which used tissue cryopreservation, such as, hepatocyte spheroids cryopreservation (Magalhaes *et al.*, 2008), alginate-fibrin beads with MSC (Bhakta *et al.*, 2009), stem cell-laden core-shell microfibers (Tian *et al.*, 2019) and even articular cartilage (David E. Pegg *et al.*, 2006).

1.3. Cryopreservation

Cryopreservation is the preservation of biological material for certain periods of times at sub-zero temperatures. It involves the use of cryoprotectant additives (CPA) (Meryman, 1971), which will prevent ice crystals formation and consequently damage of cells/tissue (Argyle *et al.*, 2016). Firsts reports of cell cryopreservation appeared around 1950s, when Polge successfully cryopreserved cock spermatogoa (Polge *et al.*, 1949). Later, embryos were also cryopreserved (Trounson & Mohr, 1983), followed by oocytes cryopreservation, giving rise to successful pregnancies (C. Chen, 1986; van Uem *et al.*, 1987).

There are two different techniques for performing cryopreservation: controlled **slow freezing** and rapid cooling by **vitrification**. The main difference between both is that slow freezing results in a liquid changing to a solid state, forming ice crystals, where vitrification results in a non-crystalline amorphous solid (Argyle *et al.*, 2016).

1.3.1. Cryoprotectant additives (CPA)

Almost all cells and tissues are made of approximately 80% water. When cooled to below zero temperatures, water leads to the formation of ice crystals. This represented the first challenge in cryopreservation, because this ice formation leads to loss of cells/ECM integrity and functionality. The firsts reports of the use of CPA goes back to 1949 when Polge and co-workers showed that adding 10-20% of glycerol to cock spermatozoa enabled cell survival after prolonged freezing at -80ºC (Polge *et al.*, 1949). Later, Lovelock and Bishop discovered that dimethyl sulfoxide (DMSO) protected cells against ice injury (Lovelock & Bishop, 1959).

CPA are usually classified according to their cell membrane penetrating rate: those with a sufficiently low molecular mass are able to quickly penetrate through cell membrane, being designated as permeating CPA (pCPA). Those who have higher molecular weights and are slower in crossing membranes are non-permeating CPA (npCPA) (Fahy & Wowk, 2015; Karow, 1969). pCPA include methanol, ethanol, DMSO, ethylene glycol (EG), 1,2-propanediol (PD) and propylene glycol, among others. The npCPA are usually sugars (glucose, sucrose and dextrose); polymers (dextran, polyethylene glycol (PEG) and ficoll) or proteins (albumin, gelatin and others). Due to its molecular weight, glycerol is in the threshold of both types of CPA, however it is usually considered a pCPA (Karow, 1969).

Each CPA has its own properties and can have different behavior when mixed with other CPA. Several studies have showed that mixing different CPA, especially, mixing pCPA and npCPA can lead to higher cryoprotective activity (Kasai *et al.*, 1992; L. L. Kuleshova *et al.*, 1999; Kuleshova *et al.*, 2001; Mukaida *et al.*, 1998). Generally, pCPA cause osmotic dehydration by entering the cell and forcing water to come out to maintain its normal volume (D. E. Pegg, 1984). However, this efflux of water happens at a faster rate than the influx of pCPA, resulting in an initial cell osmotic stress and shrinkage until equilibrium volume is reached.

npCPA do not enter cell membrane but cause cellular dehydration by increasing the osmolality of the cryopreservation solution (Sieme *et al.*, 2016).

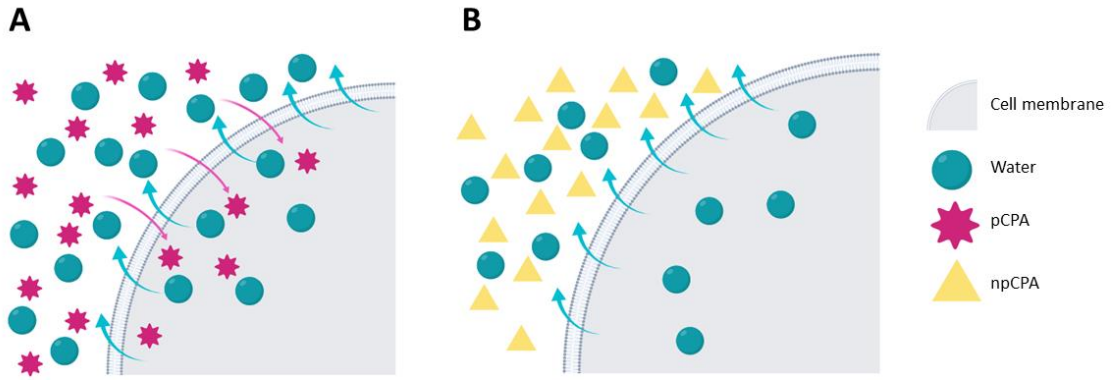

Figure 7 - CPA action on cells. (A) Permeating CPA influx at first is lower than water outflux. (B) Non permeating CPA increase osmolality of the outside solution forcing water to come out of the cell.

Even though CPA are used to increase post-cryopreservation cell viability, there are still adverse effects associated. CPA, unlike most traditional drugs, which are delivered in low concentrations with a specific target, are delivered in higher concentrations with multiple actions, with both active and passive targeting. This is predominantly seen when using pCPA, as they are associated with higher toxicity. pCPA penetrate cell membrane and can interfere with several biological and enzymatic processes (Elliott *et al.*, 2017). Concentrations of pCPA used in the process will tend to accumulate in intracellular components. When warming or thawing, cells will have a major uptake of water, which can destroy homeostatic mechanisms, such as membrane barrier characteristics (Meryman & Hornblower, 1972; Sloviter, 1951; Whittingham *et al.*, 1972). Therefore, it is important to choose wisely the solution in which cells will be thawed. The use of osmotic buffers, usually sugars, in the initial cryopreservation solution will attenuate the water influx during CPA exposure. For example, sucrose was used for hepatocyte spheroids cryopreservation (Magalhaes *et al.*, 2008), while other studies also reported the use of sucrose (Bhakta *et al.*, 2009; Pope *et al.*, 1986; Quinn & Kerin, 1986).

1.3.2. Slow freezing

Slow freezing involves exposing tissue or cells to sub-zero temperatures in a controlled rate, with the use of low concentration CPA. Generally, slow freezing starts with cooling the sample, in the presence of CPA, to temperatures between – 5°C and -7°C for several minutes to reach equilibration. Then to initiate extracellular freezing, sample is cooled in a programmable freezing device until between - 30°C and - 65°C in a slow rate of 0.3-0.5 °C/min. Finally, samples are stored in liquid nitrogen (LN) (Saragusty & Arav, 2011). The use of a freezing solution at very slow cooling rate ensures that freezing will take place only outside cells, resulting in an efflux of active water from cells, and their gradual dehydration,

until they reach the temperature at which the intracellular matrix vitrifies (Mazur, 1963; Saragusty & Arav, 2011).

This technique is very well established, and several studies demonstrate its efficacy (Boldt *et al.*, 2003; Borini *et al.*, 2004; Porcu *et al.*, 1997; Tucker *et al.*, 1998; Winslow *et al.*, 2001). However, the need to use a controlled rate freezer makes it not practical and expensive. Also, the major challenge of this technique is to prevent ice formation during cryopreservation in order to maintain tissue integrity and prevent toxic concentration of solutes, while preserving organelles functionality and overall tissue viability (Konc *et al.*, 2014).

Uncontrolled freezing [cooling in two subsequent steps in common freezers (- 20°C and - 80 °C)] is a variation of slow freezing and it was firstly described in 1987 (Stiff *et al.*, 1987). This technique is cheaper and simpler, since no specific equipment is required. However, it is viewed as more detrimental for biological samples, especially if sensitive cells are being used. Nevertheless, several studies have used uncontrolled freezing with good results (Choi *et al.*, 2001; Feremans *et al.*, 1996; Galmes *et al.*, 2007; Makino *et al.*, 1991; Rosenfeld *et al.*, 1994).

1.3.3. Vitrification

Vitrification is defined as glass-like solidification and/or complete avoidance of ice crystal formation during cooling and warming (Kuleshova *et al.*, 2007). The first successful report of vitrification was described in 1984 (Fahy *et al.*, 1984) and later demonstrated in mouse embryos by Rall and Fahy in 1985 (Rall & Fahy, 1985). Since that, several studies have been made to further optimize vitrification protocols.

There are a few factors that should be considered in vitrification: 1) cooling and warming rate, 2) sample viscosity and 3) volume (Yavin & Arav, 2007). Cooling rate is one of factors that distinguish vitrification from slow freezing. The Arav equation (1.1) (Yavin & Arav, 2007) demonstrates that increasing cooling, warming rates, sample viscosity and decreasing volume of the sample, increases, independently, the probability of vitrification.

$$\text{Probability of Vitrification} = \frac{\text{Cooling and warming rate} \times \text{Viscosity}}{\text{Volume}} \qquad (1.1)$$

1) In vitrification, cooling rates are rapid and usually achieved with LN. However, the cooling rate of the sample does not entirely depend on LN, but also on the sample volume, size and composition. Samples can be frozen in LN (-196 ºC), in LN vapor phase (-180 to -140 ºC) or in LN slush (-210 ºC). LN slush is formed by VitMaster (A. Arav *et al.*, 2000), a device that reduces LN temperature by applying negative pressure. It has been suggested that using LN

slush to decrease significantly cooling rate, as well as low volume samples (below 1 µL) would reduce the probability of chilling injury and ice formation, without the need to use high concentrations of CPA (A. Arav *et al.*, 2002). Several studies have shown that cooling in LN slush leads to higher post-thawing survival rates (up to 37%) (Beebe *et al.*, 2005; Cai *et al.*, 2005; Cuello *et al.*, 2004; V. Isachenko *et al.*, 2001; Lee *et al.*, 2007; Papis *et al.*, 2009; Santos *et al.*, 2006; Seki & Mazur, 2009). However, this system requires specialized equipment, making it less practical to use.

2) Sample viscosity depends on the CPA type and concentration as well as other additives used in the vitrification solutions. As CPA concentration increases, so does viscosity of the solution: the higher the CPA concentration, the higher the glass transition temperature (Tg) (Saragusty & Arav, 2011). Each CPA has its own Tg, penetrating rate and toxicity. Mixing different CPA will affect the solution behavior, and consequently its viscosity. As Tg increases, solution toxicity tends to decrease, however, is important to keep CPA concentration to a minimum, since it could have toxic and hypertonic effects on cells (Yavin & Arav, 2007).

3) Sample volume is one of the biggest struggles when using TE constructs. It is known that the lower the volume, the less amount of liquid that needs to be vitrified, increasing the probability of an efficient vitrification (A. Arav *et al.*, 2002; Yavin & Arav, 2007). This is one of the reasons why embryo/single cells vitrification has become so successful whereas tissue cryopreservation remains challenging. Since, cells and tissues are made of approximately 80% water, the bigger the biological sample, the higher water content and increased probability to form cryoinjury.

There are several methods used in vitrification (table 1.2) and they are mainly divided in two categories: Open Vitrification (or Surface techniques) and Closed Vitrification (or Tubing techniques).

1.3.3.1. Open *vs.* Closed Vitrification

In Open Vitrification samples are in direct contact with low volumes of LN placed inside capillary devices (Argyle *et al.*, 2016; Saragusty & Arav, 2011). This technique allows a high cooling rate and an equally high warming rate, since it is an open system. However, there is the risk of cross-contamination between the sample and LN (Argyle *et al.*, 2016). To overcome this, the use of vapour phase LN has increased, since it contains a lower density of environmental airborne contaminants and avoids direct contact between sample and LN (Cobo *et al.*, 2010). In closed vitrification, samples are in indirect contact with LN. This type of vitrification can also achieve high cooling rates and has the advantage of being a closed system, which means there is less probability of contamination (Criado *et al.*, 2011; Vajta *et al.*, 2015). As shown in table 1.2, there are several techniques to perform both open and

closed vitrification, however, some of them are more used due to their higher success rates and/or process simplicity.

Table 1.2 – Different types of open and closed vitrification techniques.

Open Vitrification Technique	Reference	Closed Vitrification Technique	Reference
EM grid	(Martino *et al.*, 1996; Steponkus *et al.*, 1990)	**Plastic straw**	(Rall & Fahy, 1985)
Minimum drop size (MDS)	(A. Arav & Zeron, 1997)	**Closed pulled straw (CPS)**	(S. U. Chen *et al.*, 2001)
Cryotop	(Hamawaki *et al.*, 1999; M. Kuwayama *et al.*, 2005)	**Flexipet-denuding pipette**	(Liebermann *et al.*, 2002)
Cryoloop	(M. Lane *et al.*, 1999; Michelle Lane *et al.*, 1999)	**Open pulled straw (OPS)**	(Vajta *et al.*, 1998)
Hemi-straw	(Vanderzwalmen *et al.*, 2000)	**Superfine OPS**	(Vladimir Isachenko *et al.*, 2003)
Solid surface	(Dinnyés *et al.*, 2000)	**Cryotip**	(Masashige Kuwayama *et al.*, 2005)
Cryoleaf	(Chian *et al.*, 2005)	**Pipette tip**	(Leno *et al.*, 2008)
Direct cover vitrification	(M.-Y. Wu *et al.*, 2006)	**High security vitrification device**	(Camus *et al.*, 2006)
Fiber plug	(Muthukumar *et al.*, 2008)	**Sealed pulled straw**	(Amir Arav *et al.*, 2009)
Vitrification spatula	(Tsang & Chow, 2009)	**Rapid-i**	(G Larman *et al.*, 2006)
Cryo-E	(Petyim *et al.*, 2009)		
Plastic blade	(Sugiyama *et al.*, 2010)		
Vitri-Inga	(Paixao *et al.*, 2010)		
Nylon mesh	(Matsumoto *et al.*, 2001)		

Cryotop®

The Cryotop® method is a modification of the minimum volume cooling (MVC) from Hamawaki et al (Hamawaki *et al.*, 1999). In this method, samples are equilibrated and washed in vitrification solutions, and then placed in a reduced volume, one by one on top of a fine polypropylene strip attached to a hard-plastic handle. The device is then immediately vertically submerged in LN and the strip is covered with a hard-plastic cover to further protect samples during LN storage. For thawing, the hard-plastic is removed when samples are still inside the LN and then the fine polyproline strip is placed in a sucrose solution at 37ºC (M. Kuwayama *et al.*, 2005). Even though it is originally an open vitrification device from Kitazato Supply Co, the company has developed a modified version of the original product - Cryotop® - SC – Closed System. In this product, the device is sealed within a straw, avoiding direct contact of the samples with LN (Kitazato).

McGill Cryoleaf™

McGill Cryoleaf™ was developed at McGill University and is commercially available. McGill Cryoleaf™ is composed by two segments: an outer cover and the Cryoleaf™. This device is used according to the manufacturer's specifications: first the outer layer is removed and plunged in liquid nitrogen, to allow air bubbles to come out. Then, cells are placed in the McGill Cryoleaf™ with the minimum volume possible and are inserted directly into LN. While still in LN, the protective layer is slide down to cover cells and finally, the outer cover is inserted onto the device. For thawing, while still inside the LN container, the outer cover is removed, the protective layer is slide up and the McGill Cryoleaf™ is transferred immediately to the warming medium (Origio).

Cryoloop™

In the Cryoloop™ method a small nylon loop is attached to a holder and equipped with a container. First, the nylon loop is immersed in the vitrification solution, cells are transferred into the loop with the help of a dissecting microscope, after being rinsed several times in vitrification solution. The cap is then inserted and is plunged in LN (Mukaida *et al.*, 2003).

Cryotip®

CryoTip® device consists of a plastic straw with a thin part connected to a thick part, equipped with a moving protective metal sleeve (Masashige Kuwayama *et al.*, 2005). In this method, cells are loaded in approximately 1 µL volume solution onto the thin part. The straw is then sealed at both ends and the protective metal sleeve are placed on top the thin part. Finally, the straw is plunged into LN. Being Cryotip® a closed system, it avoids potential cross-contamination during cryopreservation process and storage in LN.

Rapid-i™

Rapid-i™ is a closed vitrification device composed by a plastic stick with a capillary sized hole. After cells being transferred between vitrification solutions, the outer straw is placed in LN and the stainless-steel rod removed. Rapid-i™ device is put under a microscope, and cells are loaded into the tiny hole. Rapid-i™ is vertically placed into the pre-cooled outer straw, the top of the outer straw is sealed and finally, Rapid-i™ is moved into LN (Desai *et al.,* 2013).

1.3.4. Liquidus-Tracking

Liquidus-tracking (LT) (David E. Pegg *et al.*, 2006) is a recent vitrification technique, which is based in the liquidus tracking curve of CPA concentration. The goal is to vitrify samples by avoiding crystallization of ice without having to introduce high concentrations of CPA at temperatures above zero. As CPA concentration increases, sample temperature decreases, thus achieving high enough CPA concentration to avoid ice nucleation. This technique was performed on ovine articular cartilage (David E. Pegg *et al.*, 2006).

Liquidus-Tracking appears as an alternative to the minimum volume devices. As previously mentioned, the probability of vitrification increases when sample volume decreases. Taking this into consideration, almost every device described so far uses the minimum volume possible as a pre-requisite. However, this becomes highly limiting when it comes to tissue vitrification. Most tissues have complex composition (cells, ECM) and large size, which often leads to inefficient cryopreservation.

Each CPA solution has an associated liquidus-curve, which defines the equilibrium melting point temperature – the higher sub-zero temperature in which, ice crystals and liquid can co-exist (Puschmann *et al.*, 2014). By adding gradually CPA into the solution and cooling it above its freezing point, solution toxicity is reduced. With this method there is no need to perform rapid cooling, which is desirable when vitrifying larger volumes. Even though the process seems simple, it greatly relies on the use of programmable freezers, which are not a standard equipment in a common laboratory (Puschmann *et al.*, 2014; Puschmann *et al.*, 2017). Nevertheless, some studies have been performed in alginate-encapsulated liver cells (AELC) (Puschmann *et al.*, 2017), human cartilage allografts (Kay *et al.*, 2015) and articular cartilage (Yu *et al.*, 2013).

1.3.5. Cryopreservation of multicellular spheroids

The clinical application potential of CT and TE constructs would greatly benefit from having readily available, i.e. “off-the-shelf”, cell-based products. Cryopreservation is an essential tool towards this end. As already mentioned, while cell cryopreservation may be already difficult, tissue or organ cryopreservation is even more challenging. Tissues usually have in

their composition several important components other than cells, that could have a profound impact in the cryopreservation process. As mentioned above, there is a possibility of cryoinjury within intracellular components, additionally ice formation outside cells can occur. These two events can affect more dramatically the viability of multicellular tissues than single cells. It is important to maintain cell-cell interactions and cell-matrix interactions to preserve tissue integrity and functionality, which could be disrupted by mechanical or chemical injury during the process (Hunt, 1984; D. E. Pegg, 2010; Pollock *et al.*, 1986; Rall, 1987; M. J. Taylor & Pegg, 1983).

In the cryopreservation of multicellular aggregates or tissues, vitrification is usually recommended. Like cells, in spheroids pCPA will replace intracellular water together with npCPA for further dehydration. Moreover, the thawing process should be quick in order to avoid ice crystals formation (Kuleshova *et al.*, 2007). In spheroids, and especially in pre-vascularized spheroids, maintaining endothelial organization and viability are the two main priorities, so avoiding ice formation during cryopreservation is imperative (D. E. Pegg, 2015).

CPA choice is also a key factor: it is essential to have a vitrification solution both stable and non-toxic to the tissue. Therefore, type of CPA, its concentration and the exposure time are three important factors that should be studied and considered when vitrifying spheroids. It was reported that EG-based solutions are less toxic to cells, when compared with DMSO, having a three-fold higher cell viability (Valdez *et al.*, 1992). Also, the addition of npCPA such as ficoll and sucrose have showed higher survival rates. Recently, vitrification solutions made of pCPA and npCPA have shown high success in vitrifying. A baby was born from a previous vitrified oocyte using a vitrification solution of 40% EG and 0,6 M sucrose (L. Kuleshova *et al.*, 1999). Since then, several works were done using this solution as a carrier solution (Bhakta *et al.*, 2009; Gouk *et al.*, 2006; Magalhaes *et al.*, 2008; Tan *et al.*, 2007; Y. Wu *et al.*, 2007). One of these works was performed on hepatocyte spheroids (Magalhaes *et al.*, 2008), where spheroids were exposed to three different vitrification solutions, with increased EG concentration and a final solution of EG and sucrose, resulting in the maintenance of spheroids viability and integrity .

Recently, Tian *et al.* performed vitrification on stem cell-laden core-shell microfibers using very low CPA concentration. Tian used several different CPA solutions containing EG, PD, trehalose and dextran and exposed microfibers for 15 minutes at 4ºC. Tian also studied the importance of the cryocarrier, with two different groups: cryovial and nylon mesh. In the nylon mesh group survival rates were up to 85%-89%, which was more than 7 times higher than in the cryovial group. This study suggests that not only CPA concentration and time of exposure is important, but also, and perhaps more critical, the device used for cryopreservation (Tian *et al.*, 2019).

1.4. Main Goals

Pre-vascularized spheroids show promise as a cell therapy strategy, as promoting neo-vascularization is a major priority in the tissue engineering and regenerative medicine fields However, in order to more easily translate these therapies into the market and the clinics, successful cryopreservation strategies are essential tools. Furthermore, in this type of applications, the use of growth media supplemented with animal origin components, such as foetal bovine serum, may compromise the post-implantation safety of patients. In that context, the main goals of this study were the generation, expansion and cryopreservation of vascular-stromal pre-vascularized spheroids, in a high-throughput manner and under XF conditions. For that, two main tasks were developed:

Task 1 - Production and characterization of vascular-stromal spheroids, with dermal fibroblasts as the stromal component, under XF conditions;

Task 2 - Cryopreservation of co-cultured spheroids by optimization of different cryopreservation protocols: Slow Freezing, Vitrification and Liquidus-Tracking.

Chapter 2

Materials and Methods

2.1. Cell Culture

Human Bone Marrow Mesenchymal Stem Cells (hMSC) (PT-2501, Lonza) were were used between passages 4 and 8, cultured in Dulbecco's Modified Eagle Medium (α-MEM, Gibco) supplemented with 10% FBS (Gibco) and 1% v/v penicillin/streptomycin (P/S) (GIBCO).
HDFn, were used between passages 4 and 8, cultured in DMEM (Thermo Fisher Scientific) supplemented with 10% FBS (GIBCO) and 1% P/S.
OEC were isolated from human umbilical cord blood of healthy donors, according to protocols approved by the UC Davis Stem Cell Research Oversight Committee, as reported previously (Williams *et al.*, 2015) and were a kind gift from Eduardo Silva (UC Davis UCB). All blood donors were kept anonymous, so the need for written consent was waived. Cells between passages 4 and 8 were used for experiments. OEC's expand medium was prepared as already reported by us (Bauman *et al.*, 2018). Briefly, MCDB131 basal medium (Standard) was supplemented with 5% FBS (Biowest), 1% of Pen/Strep, 2 mM L-glutamine (Biowest), 1 µg/ml ascorbic acid, 0.2 µg/ml hydrocortisone and the following GF (2ng/ml VEGF, 20ng/ml IGF-1R, 10ng/ml FGF and 5ng/ml EGF). A similar formulation was prepared with the base of a serum-free cocktail (SFC) and a 10ng/ml VEGF concentration. The XF Supplement for cell culture (SCC) was prepared by reconstitution of the freeze-dried product in MCDB131, followed by filtration (0.2 µm). All supplements were reconstituted in 0.1% human serum albumin solution in phosphate buffered saline (PBS, pH 7.4).
Cells were routinely cultured in T75 flasks at 37 °C under a 5% v/v CO_2 humidified atmosphere and passaged upon reaching 70-80% and 80-90% confluence for OEC and HDFn/MSC, respectively. Culture medium was changed every 2 days for OEC and 4 days for HDFn and MSC.

2.2. Co-culture spheroids generation

2.2.1. Agarose micromolds preparation

Agarose microwells were prepared by using commercially available micromolds (MicroTissues, Inc). Agarose (SeaKem® LE Agarose, Lonza) was sterilized (autoclave, 30 min at 140°C in dry cycle) and dissolved in 0.9% w/v NaCl at a final concentration of 2% w/v under microwave heating. The molten agarose was filtered (0.2 µm, filtropur S0.2, Sarstedt) and 500 µL of agarose solution were poured into each mold (Figure 8B). When cooled down, the casted microwell arrays were carefully transferred to a 12-well cell culture plate (353043, Falcon®) (Figure 8C) and equilibrated with 1,5 mL of Standard or XF medium overnight (ON).

2.2.2. Cell seeding

MSC-OEC (1:1 ratio) spheroids were prepared with a total number of 4000 cells per spheroid and HDFn-OEC (5:1 ratio) spheroids with 12000 cells per spheroid. After expansion, cells were counted using a Neubauer chamber, centrifuged at 1200 rpm for 5 min and resuspended at the desired concentration. Culture medium was removed from the agarose molds and 200 µL of cell suspension was loaded (Figure 8D). After 30 min at room temperature (RT), 2 mL of Standard or XF medium were added to the outside of the agarose molds and incubated at 37°C. Medium was changed every 2 days and spheroids were collected at days 1,2,4 and 7, depending on the experimental setup.

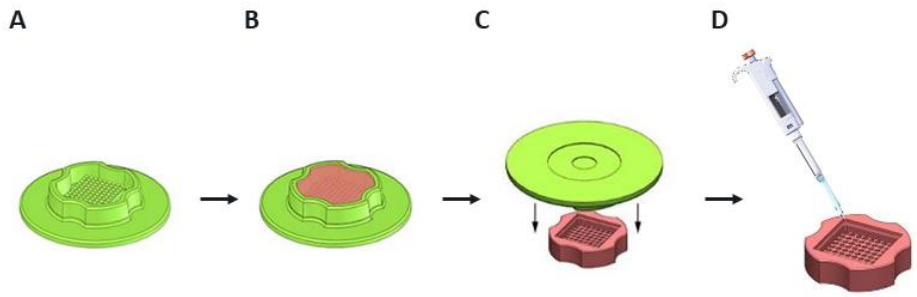

Figure 8 - Agarose mold preparation and cell seeding illustration. 2% Agarose was loaded in the mold. After gelling, agarose mold comes out and the next day, cells were seeded on top of the agarose mold. Image removed from MicroTissues, Inc.

2.3. HDFn-OEC spheroids characterization

2.3.1. Metabolic activity

For assessing spheroids metabolic activity, a resazurin assay was performed. Spheroids were collected from molds on days 1, 4 and 7 and moved to a 96-well plate. 300 µL of resazurin was diluted in fresh Standard or XF medium to a work dilution of 20% (v/v). Resazurin was added into each well and incubated for 2h at 37ºC. Supernatant was transferred to a 96-well black plate and fluorescence was measured in a microplate reader (Synergy Mx, BioTek) at 530nm/590nm (EX/EM) wavelengths. Replicates were normalized to the number of spheroids per well.

2.3.2. Spheroids processing

For immunohistochemical characterization, spheroids were fixed within the agarose molds using 4% (w/v) paraformaldehyde (PFA) for 1h at RT and washed with PBS. 200 µL of molten HistoGelTM (HG-4000-012, ThermoFisher) were carefully added on top of the agarose mold to prevent spheroid loss. After gelling, arrays were placed inside histological cassettes, immersed in PBS and processed using an automatic rotational tissue processor (STP-120-1, MICROTOM). Molds were then paraffin-embedded in an EC-350 embedding center. Paraffin blocks were cut in a Leica RM2255 microtome into 5 µm sections for immunohistochemical analysis. Paraffin embedded sections were mounted on Normafrost - coated glass slides (VWR), dried overnight at 37ºC and then kept at RT until use.

2.3.2.1 - Immunohistochemistry

Paraffin-embedded sections were deparaffinized in xylene 3X for 5 min and rehydrated in 100%, 96%, 70% and 50% EtOH dilutions series for 5 min each and finally washed in distilled water for 5 min. For antigen retrieval, spheroid sections were incubated in a steam cook for 30 min in 10 mM sodium citrate buffer, pH=6 or 10 mM Tris-1 mM EDTA buffer, pH=9. Samples were then kept in the antigen retrieval solutions for 20 min at RT and washed 3X in PBS for 5 min each. Samples were permeabilized in PBS 0.25% v/v TritonTM X-100 (X100, SIGMA) for 10 min under agitation followed by blocking in PBS supplemented with 10% v/v FBS for 1h at RT. Primary antibody dilutions were prepared in PBS supplemented with 5% v/v FBS ON at 4ºC (table 2.4). Sections were then washed 3X in PBS for 5 min each, secondary antibody (table 2.5) was also prepared in PBS supplemented with 5% v/v FBS and incubated for 1h at RT. Finally, slides were washed 3X in PBS for 5 min each and mounted using mounting medium with DAPI. Z-series optical sections were collected using a Zeiss AxioImager Z1 (Carl Zeiss, Germany) equipped with an AxioCam MR ver.3.0.

2.4. Spheroids cryopreservation

2.4.1. Preparation of cryopreservation solutions with Standard and XF medium

Cryopreservation solutions were prepared in both Standard and XF medium:

Table 2.1 – Cryopreservation conditions tested and respective cryopreservation solutions.

Condition	Solution
Slow-Freezing	Slow Freezing solution (SFS): 10% v/v DMSO (D2650, Sigma)
Vitrification	Equilibrium solution 1 (ES1): 10% v/v EG (324558, Sigma) Equilibrium solution 2 (ES2): 25% v/v EG Vitrification solution (VS): 40% v/v EG + 0,6 M sucrose (27483.294, VWR)
Liquidus-Tracking	20% v/v DMSO 30% v/v DMSO 40% (v/v) DMSO + 10% w/v glucose (G-7528, Sigma) 50% (v/v) DMSO + 10% w/v glucose 60% (v/v) DMSO + 10% w/v glucose 70% (v/v) DMSO + 10% w/v glucose

All solutions containing sucrose or glucose were filtered (0.2 µm, filtropur S0.2, Sarstedt).

Table 2.2 – Seven different conditions were tested in both Standard and XF medium.

Standard	XF
Control	
Vitrification	
Vitrification – Slow Freezing	
Slow-Freezing	
Vitrification CPA Cytotoxicity control	
Liquidus Tracking	
LT CPA Cytotoxicity control	

2.4.2. Protocol Optimizations

2.4.2.1. Agarose molds ability to maintain integrity

Agarose molds were prepared as previously mentioned and cryopreservation solutions were prepared in basal MCDB131 medium. Increased concentrations of 5 mL of EG solutions (two wells per solution were used) were added to a 6-well plate (353046, Falcon®). First, two agarose molds were placed inside the wells containing the 10% v/v EG solution (one mold per well) and then transferred from one solution to another (with 5 min of incubation in each solution). This experiment was performed at RT. For DMSO solutions, agarose molds were incubated with the solutions for several days at RT and at -20ºC. Agarose molds were then washed with PBS and their integrity was evaluated.

2.4.2.2. Liquidus-Tracking Optimization

To determine how much time it takes for each solution to reach a specific temperature, agarose molds and LT solutions were prepared. 4 mL of each solution was added to 10 mL flasks. A thermometer (Z257400, Sigma-Aldrich) was attached to the flask and placed in the -20ºC or -80ºC freezer depending on the solution: 20%, 30% and 40% DMSO time points were tested in -20ºC freezer and 50%, 60% and 70% DMSO in the -80ºC. 50%, 60% and 70% DMSO solutions were kept overnight in -20ºC freezer before the experiment.

Table 2.3 – Solutions ideal temperatures

% v/v DMSO solution	Initial temperature	Final Temperature
20	RT	-5ºC
30	RT	-5ºC
	-5ºC	-10ºC
40	RT	-10ºC
	-10ºC	-20ºC
50	-20ºC	-30ºC
60	-20ºC	-30ºC
	-30ºC	-40ºC
70	-20ºC	-40ºC

2.4.3. Cooling and cryopreservation of spheroids

On day 1 after cell seeding, spheroids were cryopreserved and stored in either cryovials (368632, Thermo Scientific), agarose molds or in a 100 μm pore size nylon mesh.

2.4.3.1. Cryovial group

Spheroids were removed from agarose molds (Figure 9A) and put in 1 mL Eppendorf tubes. For Vitrification, spheroids were exposed to ES1, ES2 and VS (500 μL each) for 5 min each, with centrifugation at 20x g for 1 m between each solution (Figure 9B). During the 5 min, up and down pipetting was performed to allow diffusion of the solution through the spheroids. Finally, spheroids in VS solution were transferred to cryovials and 500 μL of fresh VS was added (Figure 9D). Cryovials were transferred and stored in LN vapor phase for a week (Figure 9F). For Slow-freezing, spheroids were transferred to a 1 mL Eppendorf tube and exposed to 500 μL of SF solution for 3 min (Figure 9C). Next, spheroids were transferred to cryovials and 500 μL of SF solution was added. Cryovials were stored in a Mr Frosty and left ON in a -80ºC freezer (Figure 9E). The next day, cryovials were stored in LN vapor phase and left for 1 week (Figure 9F).

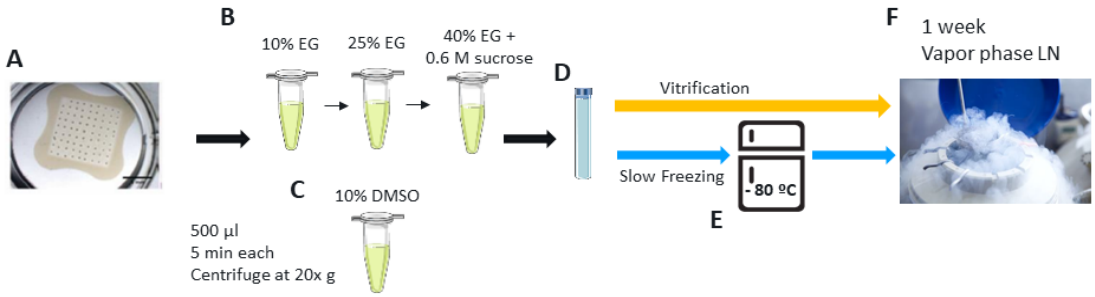

Figure 9 - Schematic view of the cryovial group protocol. Spheroids are retrieved from molds (A), then exposed to the different cryopreservation solutions (B, C). Next, are pipetted onto cryovials (D), Vitrification spheroids are transferred to LN (F) and Slow-Freezing spheroids are stored in Mr Frosty at -80ºC overnight (E) and then to LN (F).

2.4.3.1. Agarose molds group

In Vitrification, medium was removed from wells and spheroids, while still in the agarose molds, and were exposed to 2 mL of ES1, then to ES2 and finally to VS, for different timepoints (3 and 5 min) (Figure 10A). Thereafter, spheroids, still inside the agarose molds, were moved to flasks with 4 mL of VS and stored in LN vapor phase (Figure 10BD). For Slow Freezing conditions, spheroids were exposed to SF for 3 min and then moved to flasks with 4 mL of SF and placed in a -80ºC freezer on a Mr Frosty apparatus ON (Figure 10ABC). The day after, flasks were moved to LN vapor phase (Figure 10D). As for Vitrification-SF, the protocol is the same as Vitrification except for immediate storage in LN, instead, spheroids were kept in a Mr Frosty, -80ºC, ON and put in LN vapor phase the day after, as in Slow Freezing. For

Liquidus-Tracking condition, spheroids were exposed to 6 DMSO increasing concentration solutions for the time required (figure 10E). For the first 3 concentrations (20%, 30% and 40%), spheroids were incubated in -20ºC freezer (Figure 10F) and for the final 3 incubation took place in -80ºC freezer (Figure 10G). For each transfer, 12-well plate was placed inside a thermic box with ice to prevent drops of temperature. After reaching -40ºC in 70% DMSO solution, spheroids were transferred and stored in LN vapor phase (Figure 10D).

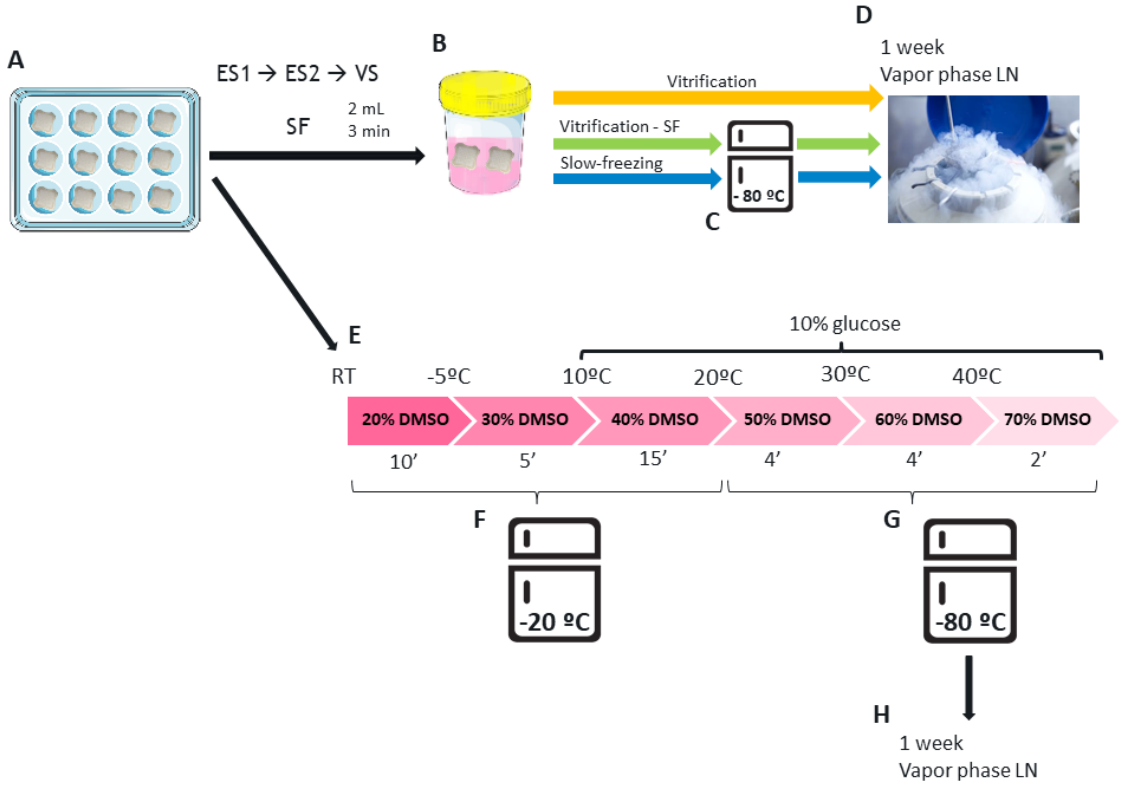

Figure 10 - Schematic view of the agarose molds group protocol. Spheroids still in the molds (A) were exposed to different cryopreservation solutions (A, E). Vitrification spheroids were transferred to 10 mL flasks (B) and then to LN (D). Slow-Freezing and Vitrification-SF spheroids were stored in Mr Frosty at -80ºC O.N (C) and then transferred to LN (D). In LT protocol, the first 3 solutions exposure occured in -20ºC freezers (F) and the last 3 in the -80ºC (G). Spheroids were then moved to flasks (B) and stored in LN (H).

2.4.3.1. Nylon mesh group

Histology cassettes were sterilized for 1h in UV light and nylon mesh for 30 min in freshly prepared 70% ethanol followed by 1h in UV light. A previously embedded in VS nylon mesh was placed inside the histology cassette (Figure 11A). After spheroid exposure to the cryopreservation solutions while still in the agarose molds, spheroids were retrieved and pipetted on top of the nylon mesh (Figure 11B). Next, a second nylon mesh was put on top of the spheroids. Cassette was then closed and placed inside a sterile petri dish with parafilm all around and stored in LN vapor phase (Figure 11C).

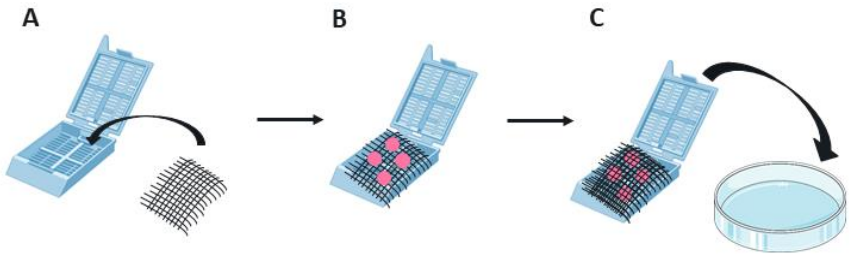

Figure 11 - Nylon mesh and spheroids assembly. First embedded in VS nylon mesh was placed inside the histology cassette (A). Spheroids were removed from agarose mold and placed on top of nylon mesh (B), A second embedded in VS nylon mesh was placed on top of the spheroids (C). Finally, cassette was closed and stored inside a petri dish.

2.4.4. Thawing of spheroids

Spheroids of all conditions were transferred from LN to a 37ºC water bath. Then, Vitrification, Vitrification-SF and Nylon Mesh spheroids were exposed to 1M sucrose solution for 5 min and a stepwise dilution was performed (5 min in each solution): 0,7 M → 0,525 M → 0,375 M → 0,175 M → 0 M. All dilution solution was removed, and spheroids were washed with 2 mL of fresh medium, moved to fresh agarose molds and incubated for 18 h at 37°C under a 5% v/v CO_2. In Slow Freezing conditions, all SF solution was removed, replaced with fresh medium. Spheroids were then transferred to fresh agarose molds and incubated at 37°C under a 5% v/v CO_2 for 18 h and 42 h.

2.4.5. CPA Cytotoxicity Control

For Vitrification CPA cytotoxicity control, after exposure to vitrification solutions, spheroids were treated with 1M sucrose for 5 min and then subsequent dilutions.
For LT CPA cytotoxicity control, when reaching 70% DMSO solution in -40ºC, spheroids were exposed to reverse DMSO concentrations solutions for 4 min each at RT.

2.5. Spheroids metabolic activity and sprouting potential assay

2.5.1. Resazurin Assay

For the resazurin assay, taking in account the assay, spheroids were collected from molds on days 1 and 2 for Control and CPA Cytotoxicity Control conditions and 18 h and 42 h post-thawing for cryopreservation conditions and moved to a 96-well plate. 300 µL of resazurin diluted in fresh Standard or XF medium to a work dilution of 20% v/v resazurin was added into each well and incubated for 2h at 37ºC. Supernatant was transferred to a 96-well black plate and fluorescence was measured in a microplate reader (Synergy Mx, BioTek) at 530nm/590nm (EX/EM) wavelengths. Replicates were normalized to the number of spheroids.

2.5.2. Fibrin Sprouting Assay

To evaluate spheroids viability, a fibrin sprouting assay was performed on spheroids days 1 and 2 for Control and Vitrification CPA Cytotoxicity Control conditions and 18 h and 42 h post-thawing for cryopreservation conditions, depending on the assay.

To prepare fibrin gels, fibrinogen (4 mg/ml Sigma) solution was prepared. A first solution of fibrinogen in 0.9% NaCl, mixed with aprotinin (60mg/ml Sigma) and Standard or XF medium was added to a second solution of thrombin (2 µg/ml Sigma), which was diluted in PBS homogenized (Figure 12A) and added to ibidi chambers (ibidi). Fibrin was left to polymerize for 30 min at 37 °C under a 5% v/v CO_2 humidified atmosphere, to form a first layer (Figure 12B). A second layer of fibrin gel now containing the spheroids resuspended in medium of solution A, was placed on top of the first layer (Figure 12C). After 30 min, 500 µL of Standard and XF medium were added to the ibidi chambers. Spheroids were left in a fibrin for 72 h with medium changes every 24h. At the end of the 72 h, spheroids were fixed with 4% v/v PFA in PBS 1x for 1h at RT and washed with PBS. Immunofluorescence in the fibrin gels was performed to analyze the spheroids sprouting potential and ECM deposition. Sections were permeabilized in 0.25% v/v Triton X-100 (X100, Sigma) for 20 min, blocked with 2% v/v BSA in PBS for 1h at RT. Primary antibody dilutions were prepared in PBS supplemented with 1% (v/v) BSA and left for 2h at RT and then ON at 4ºC (table 2.4). Sections were then washed with PBS and incubated with the corresponding fluorochrome-conjugated secondary antibodies (Alexa-Invitrogen) (table 2.5) for 4h at RT. Nuclei were counterstained with 4',6-diamidino-2-phenylindole (DAPI) for 30 min. VectaShield (H-1000, Vector) was added to image the samples. The samples were acquired using a Z-step pf 11 µm with Leica TCS SP5 AOBS spectral confocal microscope (Leica Microsystems, Germany).

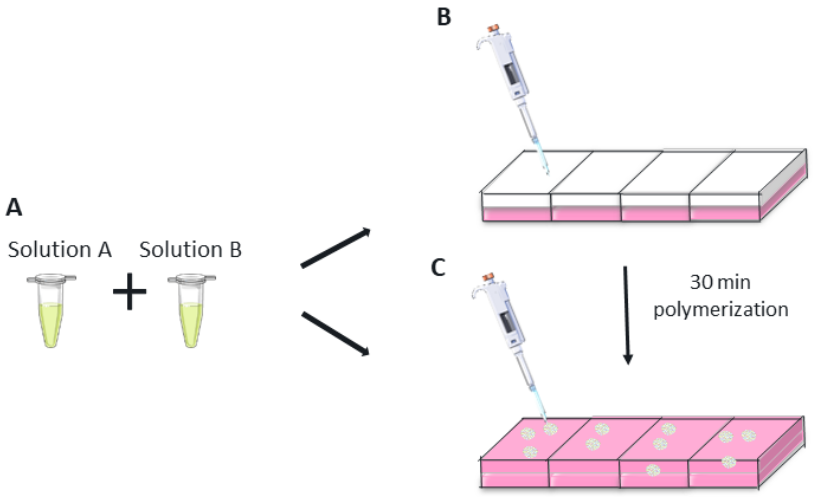

Figure 12 – Fibrin sprouting assay preparation protocol. Solutions A and B were prepared (A). First layer of fibrin gel was formed in the ibidi chamber (B) 30 min polymerization, second layer containing spheroids was added (C).

Table 2.4 - Primary antibodies used for immunostaining analysis.

Targeted antigen	Species source	Reference	Manufacturer	Antibody dilution
CD31	Mouse	M0785	Dako	1:100
CD90	Sheep	AF2067	R&D	1:50
Collagen I	Rabbit	600-401-103-0.5	Rockland	1:150
Vimentin	Mouse	Sc-6260	Santacruz	1:100

Table 2.5 – Secondary antibodies used for immunostaining analysis

Secondary Antibody	Primary Antibody	Primary Antibody Source	Manufacture /Reference	Antibody dilution
Alexa Fluor® 488	CD31 /Vimentin	Mouse	ThermoFisher A11059	1:500
Alexa Fluor® 594	Collagen	Rabbit	ThermoFisher A11702	1:500
Alexa Fluor® 594	CD90	Sheep	ThermoFisher A11016	1:500

Chapter 3

Results

3.1. Generation and characterization of stromal-vascular cells spheroids under XF conditions

The majority of growth media used in TE are supplemented with components of animal origin, such as FBS, which may compromise the post-translational safety of patients and present several other drawbacks (Tekkatte *et al.*, 2011). In that context, a novel XF supplement SCC was described to generate and support the functionality of MSC-OEC spheroids. Bauman *et al* reported that MSC-OEC spheroids at a 1:1 ratio cultured in XF medium were able to maintain morphology and function and promoted the formation of vascular-like structures more efficiently than in Standard FBS-supplemented medium. Furthermore, they showed that ECs tend to organize in the periphery of the spheroid and form a vascular-like network inside over time (Bauman *et al.*, 2018).

In the present study, we tried to investigate the feasibility of using the same XF medium with a different stromal cell type, namely dermal fibroblasts (HDFn). After preliminary screening experiments to define the best cell ratio, HDFn-OEC spheroids were co-cultured at a 5:1 ratio and metabolic activity, spheroid size, and OEC spatial organization were characterized, after 1, 4 and 7 days.

At day 1, cells were already assembled in spheroids with a size of approximately 400-490 µm in diameter, which progressively decreased reaching around 300-350 µm by day 7, both in Standard and XF conditions (Figure 13AB). It was also observed an outer layer of cells detaching from the spheroids, likely to be OEC as previously observed (Bauman *et al.*, 2018), that increased over time (Figure 13A).

The metabolic activity was determined for HDFn-OEC spheroids using the resazurin assay, throughout the culture time. In XF medium, metabolic activity was always lower that in Standard medium, decreasing continuously until day 7, while in Standard medium it stabilized around day 4 (Figure 13C).

To study endothelial organization, we performed immunofluorescence in paraffin-embedded sections to access the expression of CD31, an EC specific marker. At day 1, HDFn are distributed homogenously throughout the spheroid, where OEC exhibit two different localizations: some were randomly distributed inside the spheroid, while others started organizing in an outer monolayer. OEC at the periphery initially adopted a cuboidal shape, more evident in XF conditions (Figure 13D), which turned into a more flattened morphology over time. At day 4, clusters of OEC inside the spheroids could be observed, under both conditions, and by day 7 tubular-like structures started to sprout from those clusters (Figure 13D).

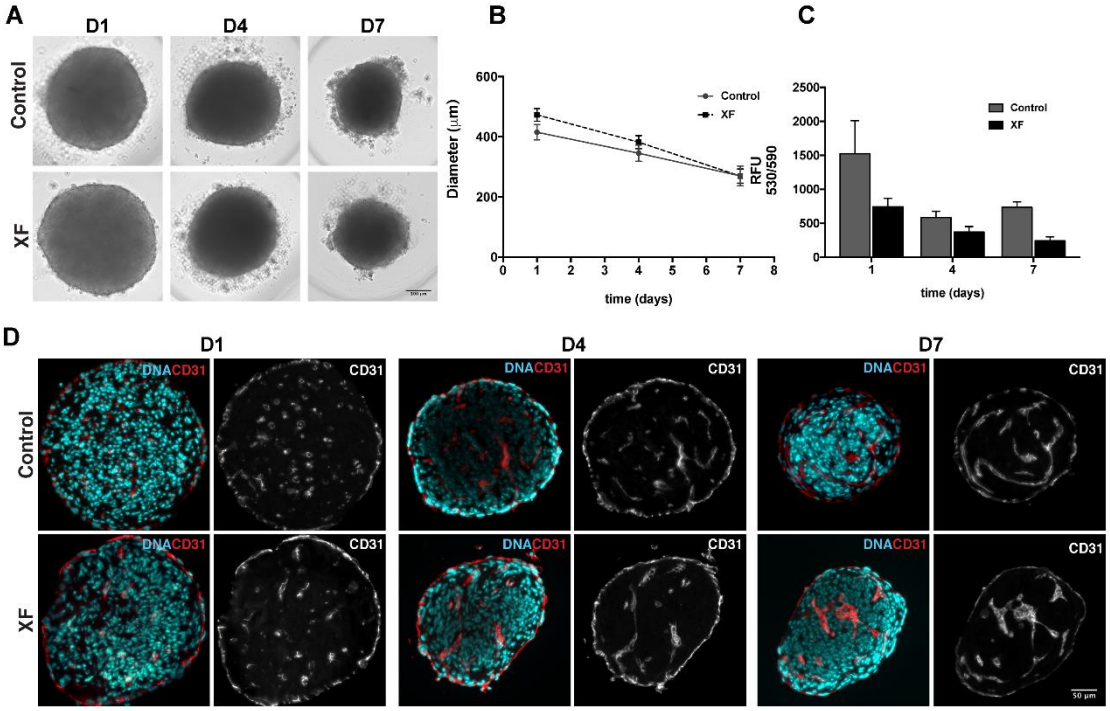

Figure 13 - Generation and characterization of HDFn-OEC spheroids. (A) Brightfield images of HDFn OEC spheroids in culture at different timepoints (1, 4 and 7 days). (B) Spheroid diameter was determined by outlining spheroid area in brightfield images using ImageJ software. (C) Metabolic activity for HDFn-OEC spheroids (n=2 independent experiments). RFU stands for relative fluorescence units. (D) Immunostaining of CD31 (red) and counterstained with DAPI (blue) in 5 μm paraffin-embedded sections of HDFn-OEC spheroids. Images were taken with a 20X objective. Scale bar 50 μm.

3.2. Cryopreservation of MSC-OEC spheroids

Besides the presence of animal-derived components in products for regenerative medicine, another major roadblocks for translation lies on the difficulty to adequately preserve these structures. Thus, herein, some cryopreservation techniques/protocols were designed and tested, which would facilitate storage/transport of spheroids and increase their potential for future clinical applications. For this part of the project, we started by using MSC-OEC

spheroids as these spheroids had been previously developed at the group, and were better characterized, while HDFn-OEC spheroids were used at later stage.

3.2.1. Cryopreservation in cryovials

Spheroids were removed from agarose molds and cryopreserved as cell suspension in cryovials. Based on the work of Magalhaes (Magalhaes *et al.*, 2008) MSC-OEC spheroids were produced and vitrified using the same cryopreservation approach: 10% v/v EG, 25% v/v EG and 40% v/v EG + 0.6 M sucrose. Since, MSC-OEC spheroids generated by us, were usually bigger (between 350-400 μm) than hepatocyte spheroids (80-100 μm) used on that study, an exposure of 5 min per solution was performed with constant up-and-down pipetting, to increase diffusion and certify that solutions penetrate through the spheroid. Slow Freezing spheroids were cryopreserved in SFS of 10% v/v DMSO. Control and CPA Cytotoxicity Control spheroids were analyzed on day 1 after seeding. Vitrification and Slow Freezing spheroids were retrieved after 1 week from LN. Upon thawing, Vitrification spheroids were exposed to a series of sucrose dilution solutions and posteriorly washed with fresh medium, while Slow Freezing spheroids were immediately transferred to fresh medium and incubated at 37 ºC for 18 h.

Metabolic Activity

Metabolic activity on CPA Cytotoxicity Control spheroids was lower, as compared to Control (Figure 14). This was somehow expected since spheroids were exposed to the vitrification solutions, which have an associated toxicity. Nevertheless, metabolic activity is considerably high, especially in the Standard medium. Upon thawing, cryopreserved spheroids were left ate 37ºC for 18 h and metabolic activity was evaluated. Vitrification spheroids had lower metabolic activity comparing with CPA Cytotoxicity Control and a slightly higher metabolic activity than Slow Freezing spheroids in Standard medium. In XF medium, it was observed the opposite, where Slow Freezing had higher metabolic activity than Vitrification spheroids (Figure 14). However, both cryopreservation conditions had very low metabolic activity comparing to Control and CPA spheroids (Figure 14).

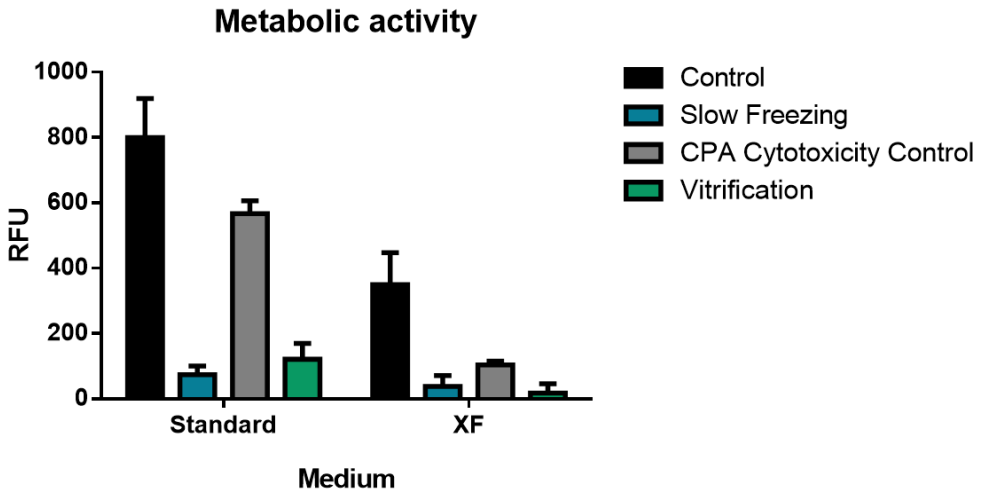

Figure 14 – **Metabolic activity assay.** Metabolic activity for MSC-OEC spheroids (n=1), from one independent experiment. RFU stands for relative fluorescence units. (B) Brightfield images of MSC-OEC spheroids after 72 h in fibrin. Scale bar 100 µm.

Spheroids sprouting potential

To further analyze the spheroids sprouting potential, spheroids after 18 h in culture pre- and post-cryopreservation were retrieved and cultured in a fibrin gel for 72 h and sprouting formation was evaluated. CPA Cytotoxicity Control spheroids were stained for endothelial cell marker CD31 and MSC membrane marker CD90 and compared with the Control.

Even though CPA Cytotoxicity Control spheroids were metabolic active, they presented very low degree of sprouting when cultured in fibrin gel (Figure 15A-5,6). The same was observed in Slow Freezing and Vitrification spheroids, with no sprouting formation, even though they presented some metabolic activity (Figure 15A-3,4,7,8).

Spheroids exhibited high expression levels of CD90 (Figure 15B), which was used as marker for stem cells. In CPA cytotoxicity control the few cells leaving spheroids were CD90 positive, for both mediums. Previous reports have shown that XF medium promotes endothelial cells sprouting (Bauman *et al.*, 2018), however in this case, no CD31 expression was detected (Figure 15B-4). The same happened in Standard medium (Figure 15B-3).

Since no sprouting were detected in brightfield images of Slow freezing and Vitrification conditions, fibrin immunofluorescence assays were not performed.

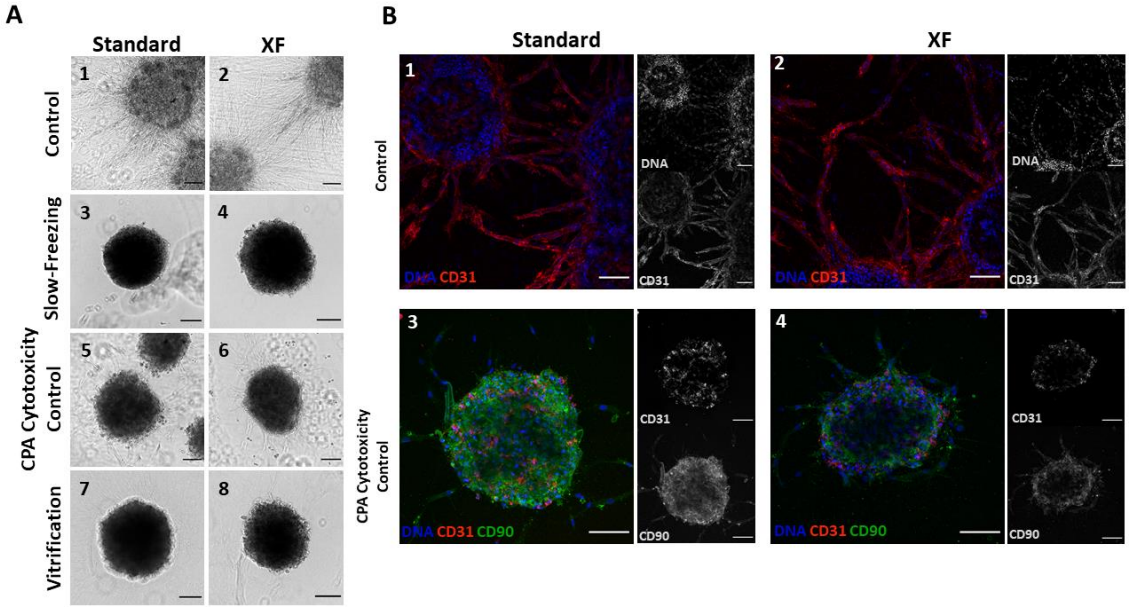

Figure 15 - Cell sprouting in MSC-OEC co-culture spheroids. (A) Brightfield images of MSC-OEC spheroids (B) Immunostaining of CD31 (red), CD90 (green) and counterstained with DAPI (blue). Images were acquired using a 20x objective. Scale bar 100 µm.

3.1.2. Cryopreservation in agarose molds

To assess if spheroids manipulation was the reason why we observed so low viability, we decided to then to cryopreservation solutions for 3 min, directly inside the agarose molds, which were transferred to 10 mL flasks (Figure 16BC). Additionally, a new condition was added to this protocol: Vitrification-Slow Freezing, to evaluate how the cooling rate affected spheroids cryopreservation. After thawing, Vitrification spheroids were exposed to the decreased sucrose solutions concentration and Slow Freezing spheroids were washed with fresh medium. Moreover, spheroids were retrieved from the old agarose molds and transferred to new ones.

Before cryopreservation procedures, we studied the impact of vitrification solutions in agarose molds integrity. Upon washing with PBS, agarose molds remained intact (Figure 16A). Yet, after thawing, almost all agarose molds were broken and the ones that were not, were very fragile (Figure 16D). This led to loss of spheroids when transferring them to new agarose molds.

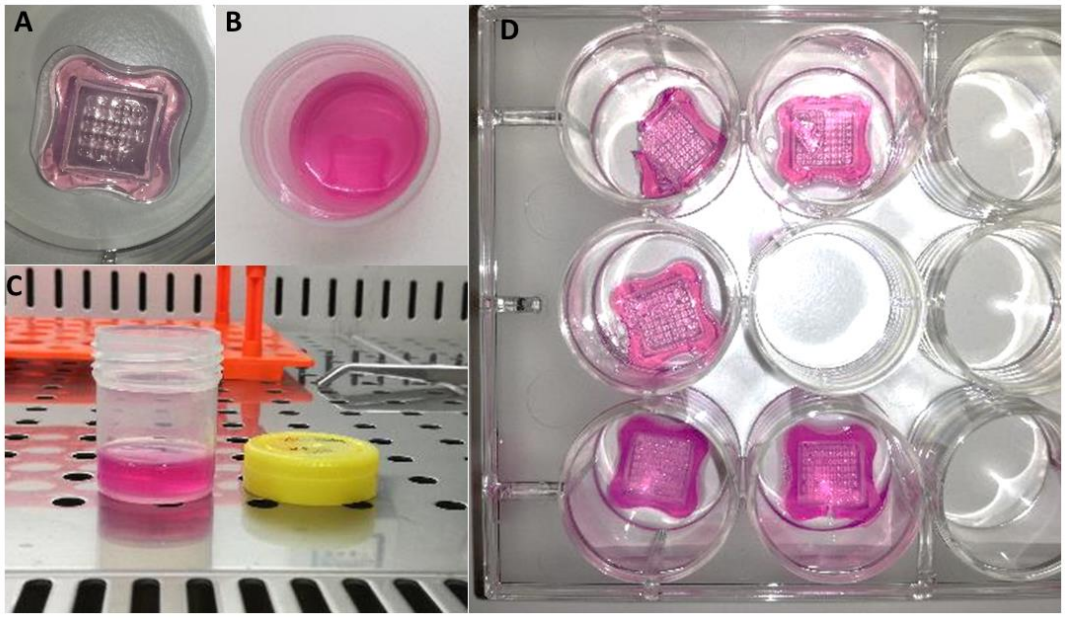

Figure 16 – Agarose molds experimental setup. (A) Agarose mol after exposure to vitrification solutions. (B) Top view (C) and side view of the flask containing cryopreservation solution and an agarose mold. (D) Agarose molds post-cryopreservation.

Spheroids diameter and integrity

To evaluate if the cryopreservation solutions were affecting spheroids diameter, brightfield images of the spheroids were taken both before cryopreservation and 18 h post-cryopreservation conditions. There were no differences between diameters for all three cryopreserved conditions and between pre- and post-cryopreservation spheroids (Figure 17B). Furthermore, spheroids apparently did not lose their integrity throughout the cryopreservation protocol (Figure 17A). This was similar for both Standard and XF medium. Interestingly, in Standard medium, Vitrification spheroids had a layer of detached cells surrounding spheroids.

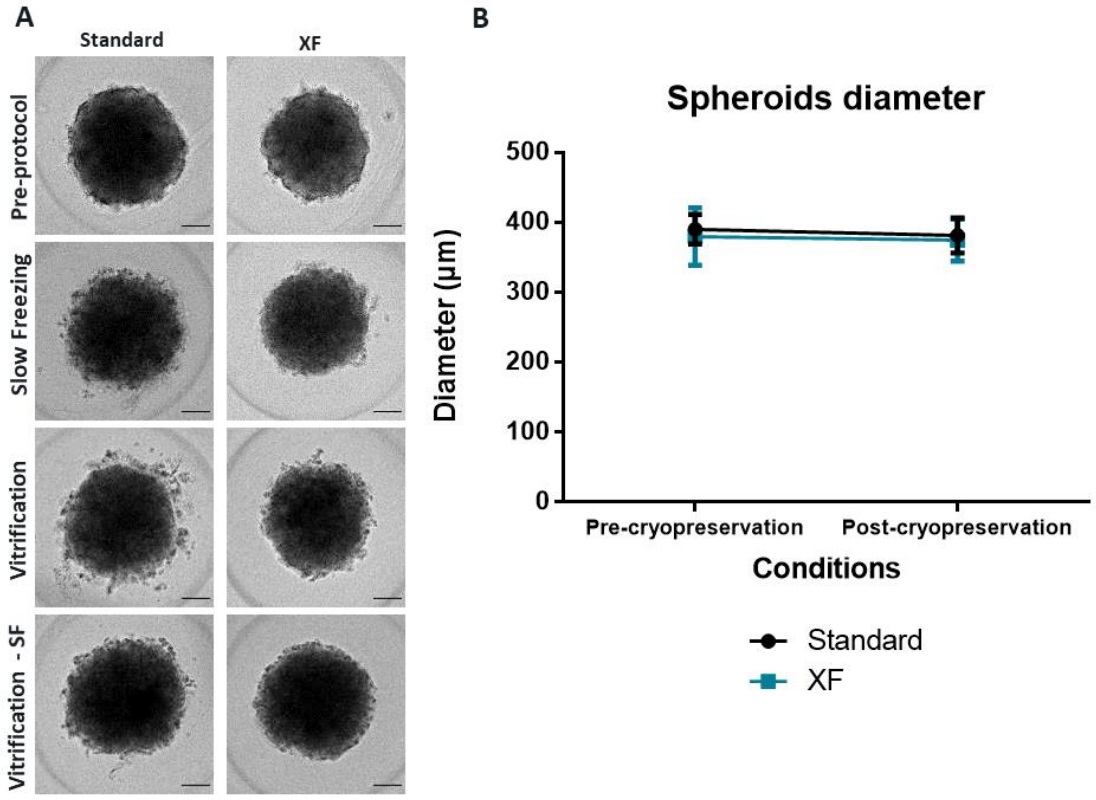

Figure 17 – MSC-OEC spheroids pre- and post-cryopreservation. (A) Brightfield images of MSC-OEC spheroids of different conditions. (B) Spheroid diameter was determined by outlining spheroid area in brightfield images using ImageJ software. Scale bar 100 µm.

Metabolic activity

The metabolic activity of CPA Cytotoxicity Control spheroids was similar to that of the Control, for both mediums. Slow Freezing spheroids presented a lower metabolic activity compared to Control, for both mediums (Figure 18). Vitrification and Vitrification-Slow Freezing spheroids presented similar metabolic activities, which suggests that the cooling rate did not affect the process. Surprisingly, Slow Freezing spheroids had higher metabolic activity than the other two cryopreservation conditions (Figure 18).

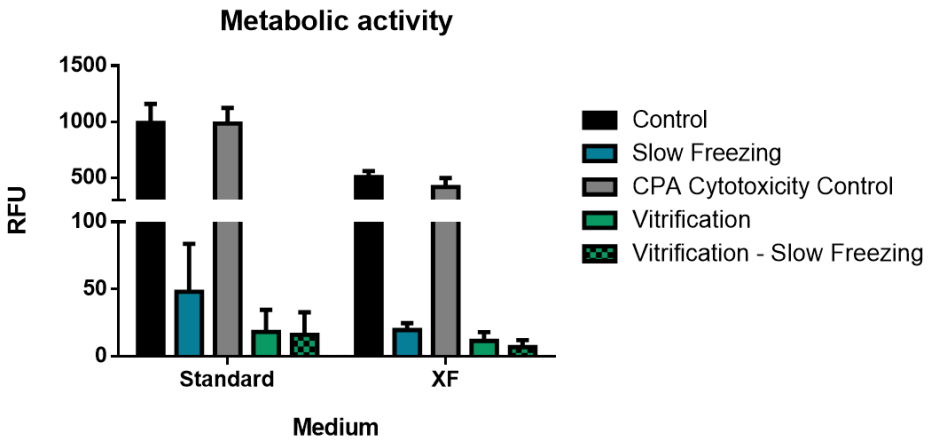

Figure 18 - Metabolic activity assay. Metabolic activity for MSC-OEC spheroids (n=2, from two independent experiments). RFU stands for relative fluorescence units.

Spheroids sprouting potential

As described previously in point 3.2.1, after 72 h in fibrin gel, MSC-OEC spheroids sprouting potential was evaluated. CPA Cytotoxicity Control spheroids showed as much sprouting as Control spheroids, for both mediums (Figure 19A-5,6). The brightfield images showed that Slow Freezing spheroids presented very low sprouting both in Standard and XF medium (Figure 19A-3,4). Nevertheless, when compared to Standard conditions, XF exhibit an increased sprouting potential (Figure 19A-4). Moreover, Vitrification and Vitrification–Slow Freezing spheroids displayed little or no sprouting. (Figure 19A-7,8,9,10).

Additionally, spheroids again were stained for EC marker CD31 and MSC marker CD90. The amount of MSC that were able sprout into the fibrin gel seems similar in Control and in CPA Cytotoxicity Control (Figure 19B). The same was not true for OEC, with the CPA Cytotoxicity Control presenting increased sprouting as compared to control (Figure 19B–3,4). The number of sprouting was slightly higher in XF medium, as compared to Standard medium.

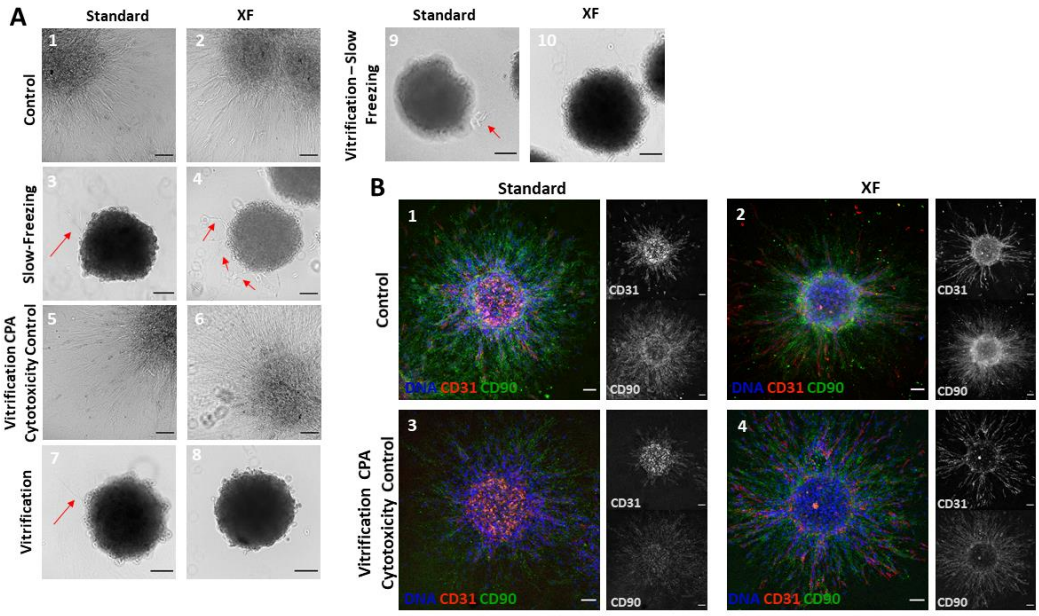

Figure 19 - MSC-OEC spheroids sprouting potential assay. (A) Brightfield images from MSC-OEC spheroids after 72 h in fibrin. Red arrows represent sprouting. (B) Immunostaining of CD31 (red), CD90 (green) and counterstained with DAPI (blue). Images were acquired using a 20x objective. Scale bar 100 µm.

3.3. Cryopreservation of HDFn-OEC spheroids

3.3.1. Cryopreservation in agarose molds

Since the previous protocols, assayed with MSC-OEC, did not provided optimal results, we decided to test LT (David E. Pegg *et al.*, 2006), a recently described vitrification technique that has shown improved outcomes (table 3.1). In order to optimize this approach to our experimental setup, several tests were performed (table 3.1). Agarose molds were placed inside 10 mL flasks with 4 mL of LT solutions and a thermometer was attached to each solution. Solutions were then placed in freezers and time was scored until solutions reached exact pre-defined temperature values.

Table 3.1 - Liquidus-Tracking time points. Different DMSO concentrated solutions were prepared and were placed in a -20 or -80ºC freezer (n=3).

% (v/v) DMSO	Initial T	Transfer at	Waiting time (min)
20 to 30	21ºC	-5ºC	10
30 to 40	-5ºC	-10ºC	5
40 to 50	-10ºC	-20ºC	15
50 to 60	-20ºC	-30ºC	4
60 to 70	-30ºC	-40ºC	4
70 to LN	-40ºC	-40ºC	2

Simultaneously, to test the impact of DMSO which is used in this method, agarose molds were left for seven days immersed in DMSO solutions of different concentrations (Figure 20A). After washing with PBS, agarose molds showed no loss of integrity (Figure 20B).

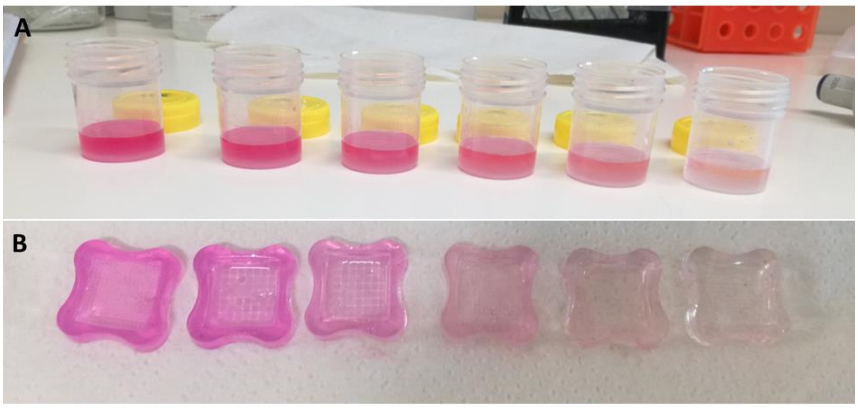

Figure 20 – DMSO solutions optimization. (A) Different DMSO solutions in 10 mL flasks with one agarose mold per flask (from 20% to 70% v/v DMSO). (B) Agarose molds after seven days exposed to DMSO solutions (from 20% to 70% v/v DMSO).

For the LT cytotoxicity control, spheroids were exposed again to the solutions in a reverse order, at RT. Spheroids were kept in LN for one week after cryopreservation, HDFn-OEC co-cultured spheroids were thaw: Vitrification and Vitrification-SF spheroids were exposed to several sucrose dilution solutions and then transferred to fresh medium, while Slow Freezing spheroids were just transferred to fresh medium. To assess if agarose molds retained toxicity due to residual cryopreservation solutions release, Vitrification and Slow Freezing spheroids were retrieved from one mold and moved to fresh agarose molds, while the other spheroids were left in the original mold.

Metabolic Activity

Metabolic activity was slightly higher in the transferred spheroids conditions (for both Slow Freezing and Vitrification spheroids) in Standard medium, which suggests that agarose molds could eventually gradually release cryopreservation solutions that may result toxic for cells (Figure 21). Both Control and CPA Cytotoxicity Control present high metabolic activity values (Figure 21). Moreover, in XF medium, cryopreserved spheroids had lower metabolic activity when compared to Standard medium. Surprisingly, Slow Freezing spheroids in Standard medium had higher metabolic activity than Vitrification spheroids. Metabolic activity of LT CPA Cytotoxicity Control was high in both mediums.

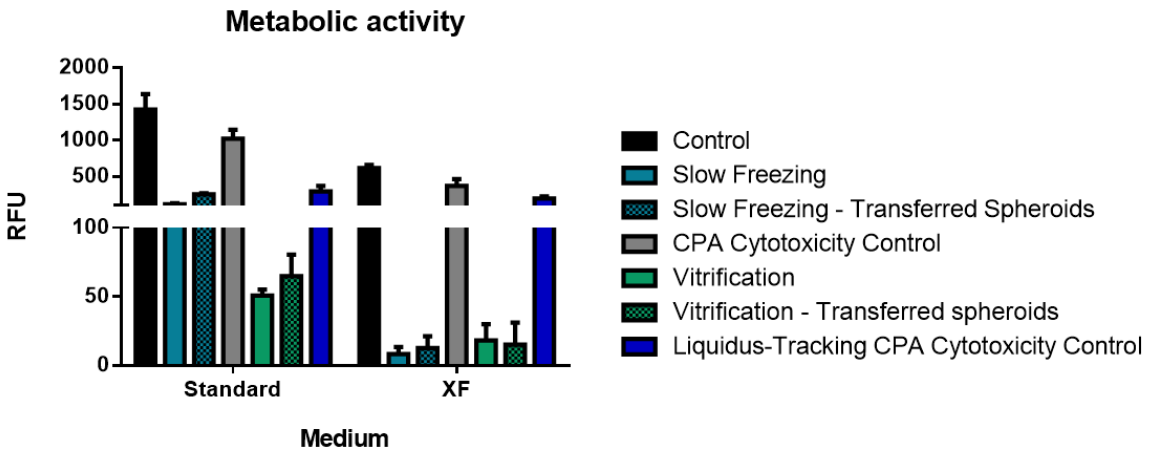

Figure 21 - Metabolic activity assay. (A) Metabolic activity for HDFn-OEC spheroids (n=1, from one independent experiment). RFU stands for relative fluorescence units.

Spheroids sprouting potential

After 72 h in fibrin gel, HDFn-OEC co-culture sprouting potential was evaluated. As observed for MSC-OEC spheroids, both Control and Vitrification CPA Cytotoxicity Control spheroids demonstrated a high level of sprouting for both mediums (Figure 22A-1,2,3,4). The brightfield images showed that Slow Freezing spheroids in original agarose molds did not sprout (Figure 24A-1,2). However, spheroids that were transferred into new agarose molds presented a higher sprouting potential (Figure 24A-3,4). Sprouting formation was also present in the Vitrification transferred spheroids condition (Figure 24A-7,8).

Despite the CPA Cytotoxicity Control used in LT had exhibited high metabolic activity, no sprouting was observed when transferred to fibrin gels (Figure 22A-5,6). This led us to not retrieve LT cryopreserved spheroids from liquid nitrogen.

Moreover, immunofluorescence in fibrin gels was performed to characterize the sprouting observed in brightfield images. In this case, spheroids were stained for CD31 as EC marker and Vimentin as HDFn marker. Additionally, COL I staining was performed to evaluate spheroids capacity to produce ECM components. Control and CPA Cytotoxicity Control spheroids showed OEC sprouting in both mediums (Figure 22B). However, Vitrification CPA Cytotoxicity Control spheroids showed less sprouts when compared to control.

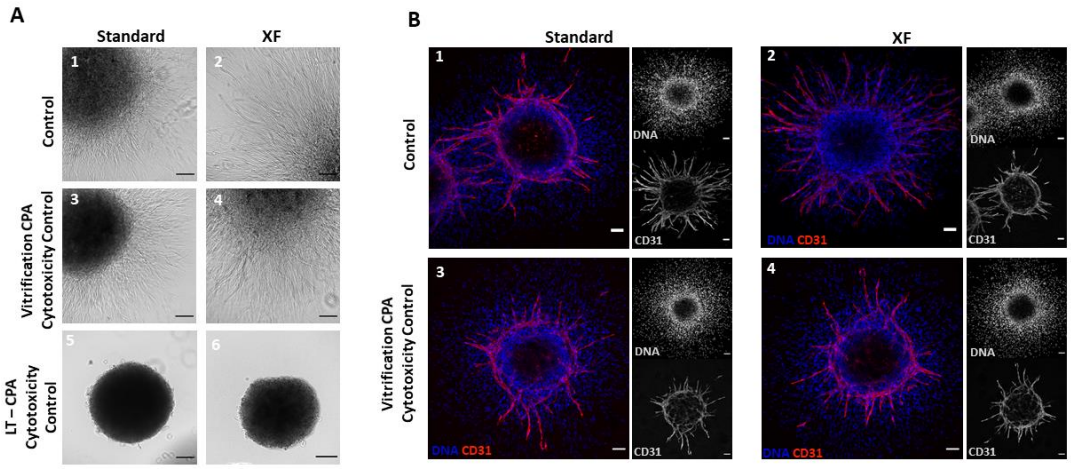

Figure 22 - HDFn-OEC co-culture spheroids sprouting assay. A) Brightfield images of HDFn-OEC spheroids after 72 h in fibrin. (B) Immunostaining of CD31 (red) and counterstained with DAPI (blue). Images were acquired using a 20x objective. Scale bar 100 µm.

Ours results showed that the majority of cells coming out of the spheroids were vimentin positive (Figure 23). Vimentin, also known as fibroblast intermediate filament protein, is required for cell migration as single cells (Battaglia *et al.*, 2018). COL I expression was detected in Control and CPA Cytotoxicity Control for both conditions, showing the ability of outward migrating fibroblasts to produce ECM. However, in XF medium, CPA Cytotoxicity Control showed a higher expression of COL I, namely near the OEC sprouts (Figure 23D).

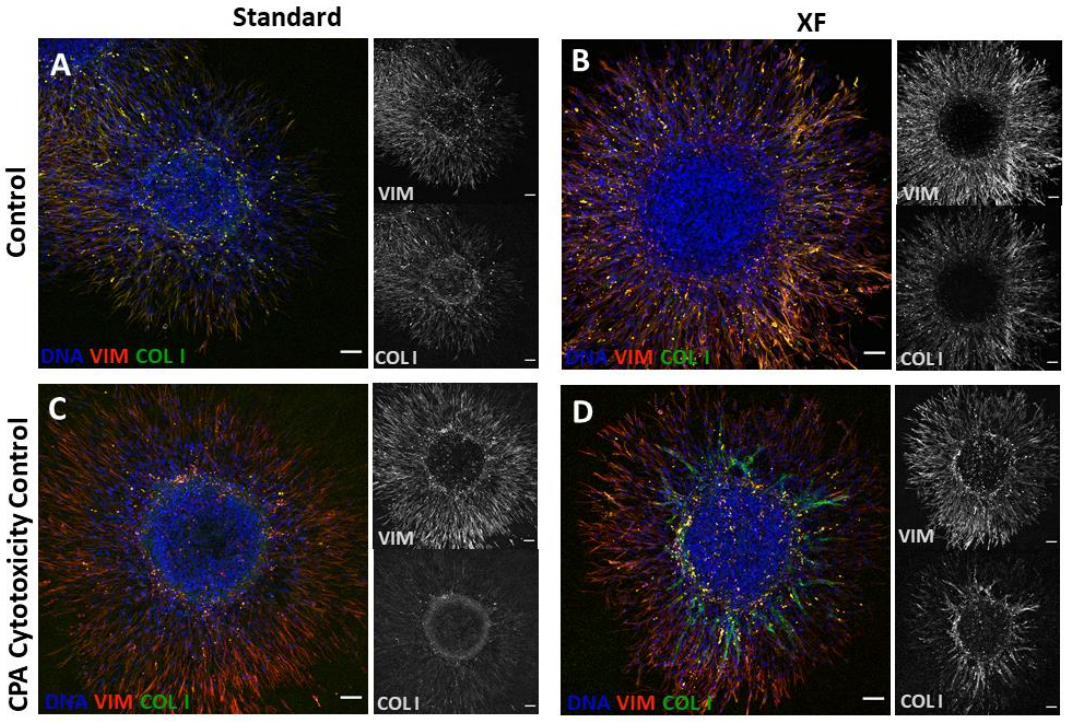

Figure 23 - Vimentin and COLI distribution in HDFn-OEC co-culture spheroids. Immunostaining of Vimentin (red), COL I (green) and counterstained with DAPI (blue). Taken with a 20x objective. Scale bar 100 µm.

In post-thawing conditions, only spheroids that were moved for new agarose molds were analyzed by immunofluorescence. Similarly, to that observed for MSC-OEC spheroids, very few OEC sprouting was seen. In fact, in Slow Freezing condition and Standard medium, no CD31 positive cells were detected outside the spheroids (Figure 24B-1). This suggested that the cells that were colonizing the fibrin gels were essentially fibroblasts (Figure 24). Interestingly, in Vitrification Transferred spheroids it was still possible to detect some OEC sprouting, but not the presence of fibroblasts (Figure 24B-3,4). In addition, it was possible to see that in both cryopreservation conditions, there was higher CD31 expression in the outer layer of the spheroids, suggesting that the outer layer of OEC was not lost during the process (Figure 24B). COL I in both conditions was expressed mainly in the periphery of the spheroids and was present in both cryopreservation conditions (Figure 24B).

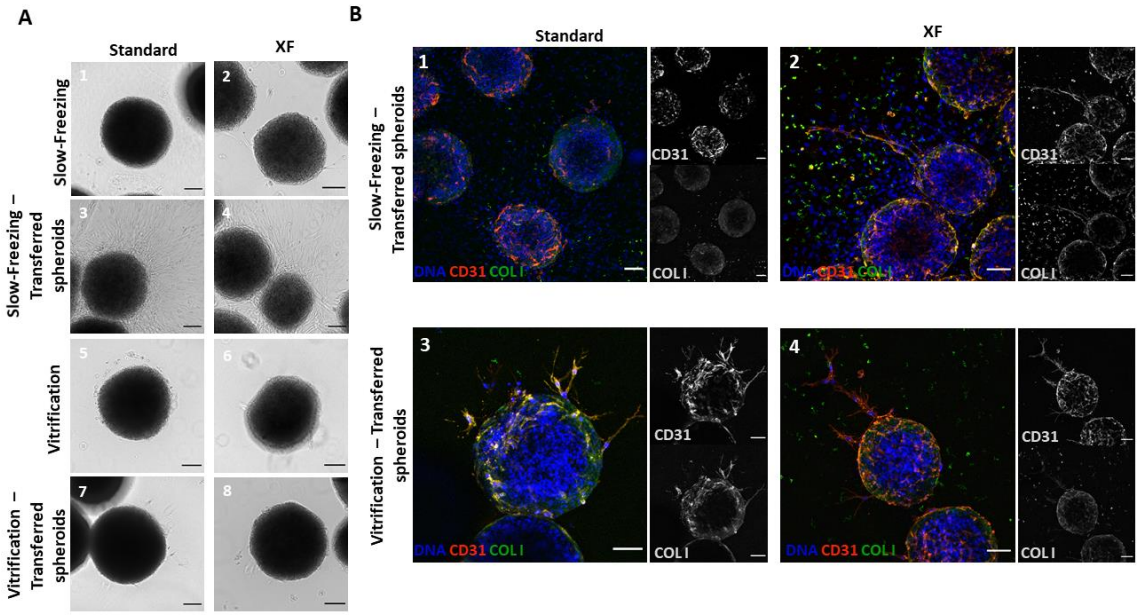

Figure 24 - HDFn-OEC co-culture cryopreserved spheroids spheroids sprouting assay. (A) Brightfield images of HDFn-OEC spheroids after 72 h in fibrin. Immunostaining of CD31 (red), COL I (green) and counterstained with DAPI (blue). Images were acquired using a 20x objective. Scale bar 100 µm.

Effect of CPA exposure time

To determine if the time of exposure to the cryopreservation solution was enough to allow CPA action an extra timepoint of 5 min exposure was performed. Also, to evaluate if increasing the post-cryopreservation incubation time would increase cells viability, by allowing cell recovery, spheroids were left for 18 h and 42 h at 37ºC before analysis.

CPA Cytotoxicity Control with 3 min and 5 min exposure presented higher metabolic activity than control in both mediums, with no significant difference between the two days (Figure 25). Overall, all cryopreservation conditions presented low metabolic activity levels. Nevertheless, Slow Freezing spheroids demonstrated a higher metabolic activity when

compared to the others conditions, in both days. Vitrification with 3 min and 5 min presented decreased metabolic activity at day 2 (Figure 25).

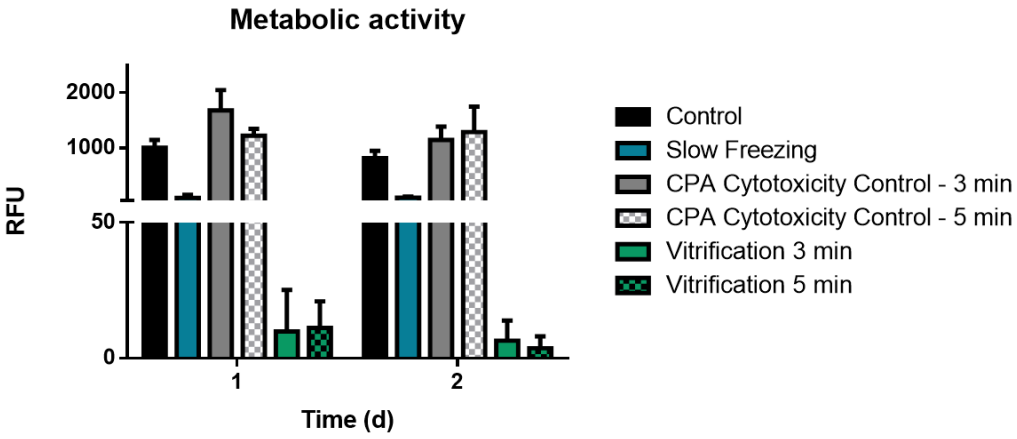

Figure 25 - HDFn-OEC spheroids metabolic activity (n=1). RFU stands for relative fluorescence units.

Spheroids sprouting potential

After 72 h incubated in fibrin, spheroids were stained for EC-marker CD31 and COL I. CPA Cytotoxicity Control and Control spheroids showed similar levels of endothelial spouting for both days (Figure 26B). However, in CPA Cytotoxicity Control spheroids, COL I expression was more co-localized with the OEC sprouts (Figure 26B). At day 2, CPA Cytotoxicity Control spheroids exhibit more OEC sprouting than the Control (Figure 26B-4).

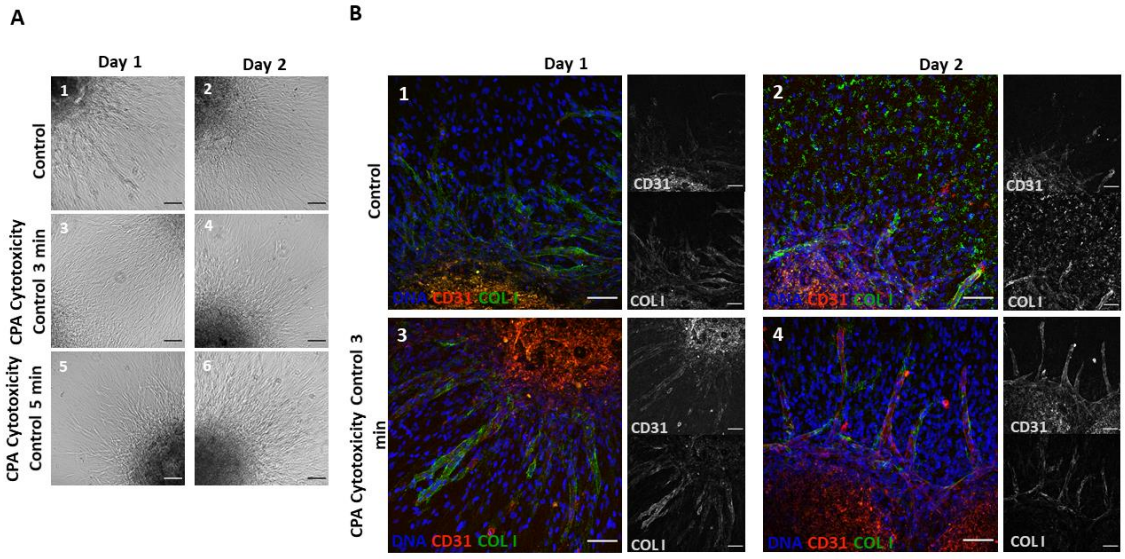

Figure 26 - HDFn-OEC co-culture spheroids sprouting potential. (A) Brightfield images of HDFn-OEC spheroids after 72 h in fibrin. (B) Immunostaining of CD31 (red), COLI (green) and counterstained with DAPI (blue). Images were acquired using a 20x objective. Scale bar 100 µm.

When cultured in fibrin, in brightfield images Slow Freezing spheroids showed high level of sprouting, particularly at day 2 (Figure 27A-1,2). In fact, spheroids seem to show more

sprouting when cultured for 2 days than just 1. Vitrification spheroids with 5 min, showed no sprouting formation, in both conditions (Figure 27A-5,6). Also, we were not able to see sprouting in Vitrification 3 min spheroids, probably due to experimental constraints, nevertheless additional experiments should be performed. The immunofluorescence showed no endothelial sprouting formation in both days (Figure 27B). There was only CD31 expression inside the spheroids. While in day 1 this expression was more visible in the periphery (Figure 27B-1), in day 2 it was more evenly distributed (Figure 27B-2). On day 2, Slow Freezing spheroids presented more cells migrating out from spheroids (DAPI) and dividing cells were visible (Figure 27B-3). These observations are not in agreement with our first results.

Since no sprouting was seen in brightfield images of Vitrification experiments with 3 min and 5 min, no fibrin gel immunofluorescence was performed.

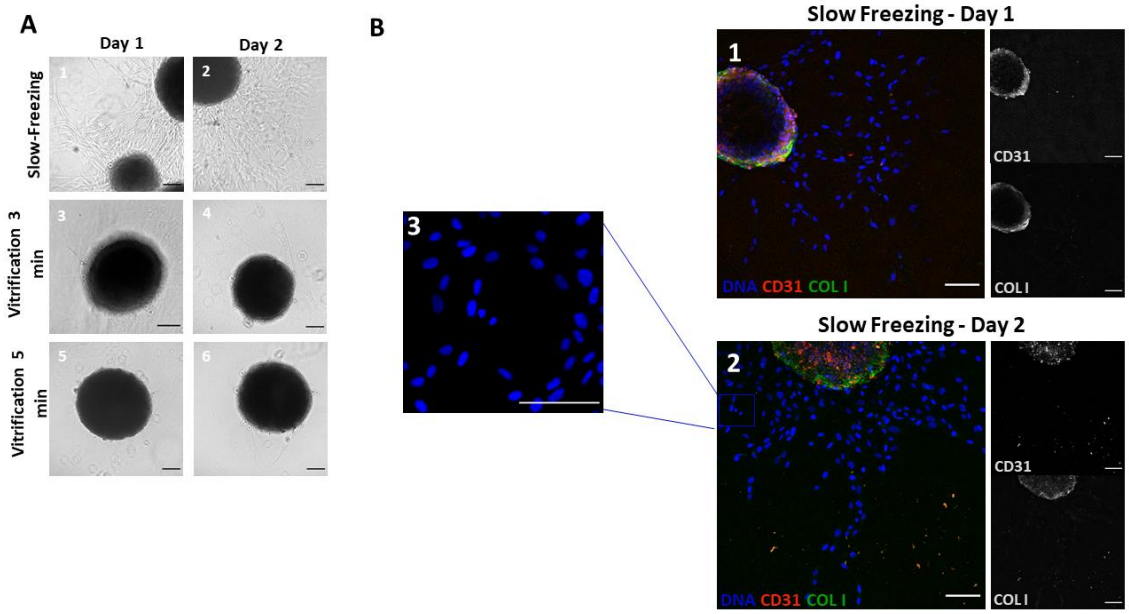

Figure 27 – HDFn-OEC cryopreserved co-culture spheroids sprouting potential. (A) Brightfield images of HDFn-OEC spheroids after 72 h in fibrin. (B) Immunostaining of CD31 (red), COL I (green) and counterstained with DAPI (blue). Images were acquired using a 20x objective. Scale bar 100 µm.

3.2.2. Cryopreservation in nylon mesh

To evaluate how the cryocarrier used could affect spheroids viability, we cryopreserved, and tested a new approach based on the use of a nylon mesh device. We used the 10 mL flasks as cryocarriers to be able to compare results (Figure 28). In this experimental set up only Standard medium was used.

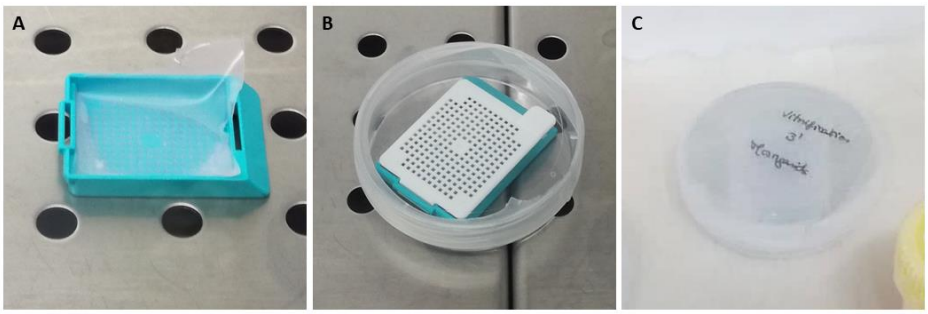

Figure 28 - Nylon Mesh protocol setup. (A) Histological cassette with spheroids between two nylon meshes. (B) Histological cassette closed and stored inside a Petri Dish with Parafilm. (C) Petri Dish with nylon mesh spheroids after 1-week storage in LN.

Metabolic activity

After thawing, spheroids were exposed to sucrose dilution solutions and then washed in fresh medium. Metabolic activity was measured 18 h and 42 h post-cryopreservation.

Spheroids vitrified in nylon mesh presented higher metabolic activity than spheroids vitrified in flasks. This difference was more accentuated on day 1. Nevertheless, again, both cryopreservation conditions had low metabolic activity compared to Control and CPA Cytotoxicity Control spheroids for both days. Additionally, the metabolic activity of CPA Cytotoxicity Control spheroids was higher than Control for both days (figure 29).

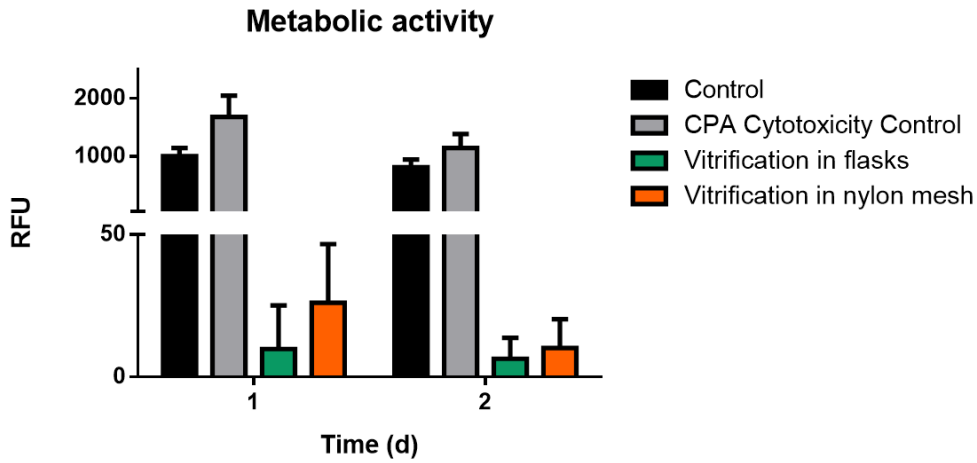

Figure 29 - HDFn-OEC spheroids metabolic activity (n=1). RFU stands for relative fluorescence units.

Spheroids sprouting potential

Spheroids were cultured in fibrin gel for 72 h to evaluate their sprouting potential. Even though, Nylon mesh vitrified spheroids presented higher metabolic activity than Vitrification in flasks, we did not see any sprouting in none of the days (Figure 30DH). Vitrified spheroids in flasks also did not present any sprouting. No fibrin gel immunofluorescence was performed in cryopreserved spheroids since no sprouting was detected in brightfield images.

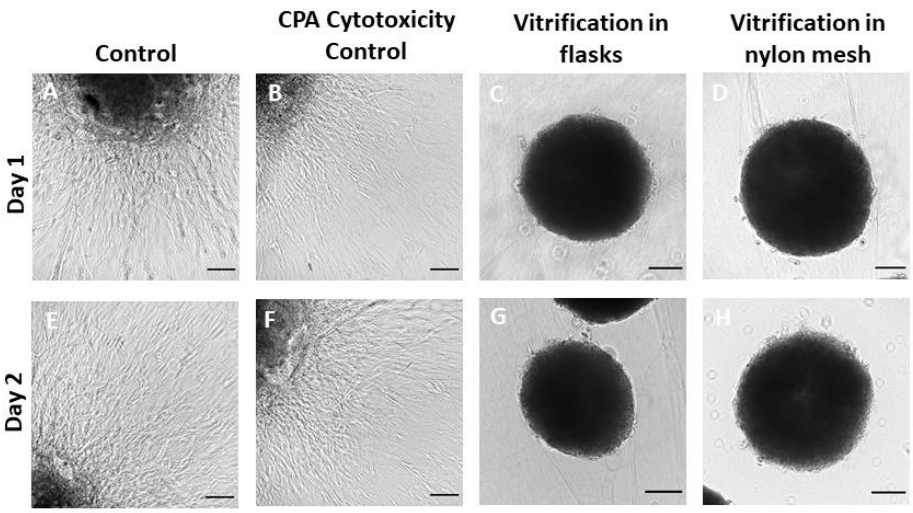

Figure 30 - HDFn-OEC spheroids sprouting assay. Brightfield images of HDFn-OEC spheroids after 72 h in fibrin. Scale bar 100 µm.

This page was intentionally left on blank.

Chapter 4

Discussion

CT aim at restoring the structure and function of damaged or diseased tissues, by using cells as a therapeutic tool tissue repair (Buzhor *et al.*, 2014). In the last few years several studies regarding this type of therapies have shown promising results. One of the most promising CT approaches is the use of pre-vascularized spheroids. These multicellular structures have shown to have greater protection against cell death, produce higher amounts of GF and ECM proteins. In these structures, EC are able be organize in vascular-like network before implantation, which will increase the chances of cell survival and anastomoses with the host tissue. These therapies have not still reached the clinic stage, and there are still some challenges ahead. One of the processes still to be overcome is the production of these spheroids in a high-throughput manner for pre-clinical or clinical trials and, ultimately, in clinical practice with patients.

Cryopreservation is a technique which allows the preservation of biological material at subzero temperatures for short or long periods of time. Cryopreservation has been used for decades, however, tissue engineered constructs have showed to be difficult to cryopreserve, due to its size, multicellular composition and other components involved, such as ECM. In this context, the present study aimed to produce and cryopreserve in a HT manner, stromal/vascular cells spheroids and analyzed their activity, viability and sprouting potential. Herein, OEC were used as vascular cells source, while MSC or HDFn were used as stromal cells source. OEC have shown to contribute for neo-vessel formation (Hendrickx *et al.*, 2010) and have been used for co-culture spheroids where they were extensively characterized (Bauman *et al.*, 2018). MSC were described to display enhanced anti-inflammatory and angiogenic activities. Since they are able to produce high amounts ECM proteins, it makes them essential for EC viability, when in co-culture. HDFn are also known to produce high amounts of ECM, and studies showed that they promote EC organization into vascular structures (Guerreiro *et al.*, 2014).

Vitrification is a highly used cryopreservation technique, which has been extensively used in oocyte cryopreservation. Few studies also used vitrification successfully in cryopreserving tissue engineered constructs (Magalhaes *et al.*, 2008) (Bhakta *et al.*, 2009; Tian *et al.*, 2019).

In this study we used MSC-OEC co-cultured spheroids in a 1:1 ratio, since it has been already reported that OEC were able to organize in tubular-like structures and have sprouting potential when cultured in fibrin gels, both in Standard and XF conditions (Bauman *et al.*, 2018). Additionally, we used 5:1 ratio HDFn-OEC co-cultured spheroids, since our preliminary results showed an endothelial organization similar to MSC-OEC spheroids as well as sprouting potential.

Metabolic activity of MSC-OEC spheroids cryopreserved in cryovials indicated that cells remained active, even though cryopreserved and CPA Cytotoxicity Control spheroids metabolic activity was low in both mediums. Additionally, cells in XF medium presented almost half the metabolic activity of the Standard medium. This was not unexpected, as our group had previously reported that co-culture spheroids with XF medium have in general low metabolic activity than control medium (Bauman *et al.*, 2018). To determine if cells preserved their sprouting potential, an *in vitro* angiogenic potential assay was performed 18 h after LN retrieval. Spheroids were cultured in fibrin gel for 72 h and sprouting was evaluated. When cryopreserving MSC-OEC co-cultured spheroids in cryovials, cells showed little sprouting after thawing, in both Slow Freezing and Vitrification conditions. Cytotoxicity CPA Control spheroids were used as a solution control, regarding vitrification solutions. It is well described that this type of solutions is toxic to the cells due to its high pCPA concentrations (Karow, 1969). Also, the osmotic shock upon retrieval of vitrification solutions is often referred as an important factor to cell survival (Meryman, 1971). The fact that cells were active but were not able to form sprouts means that cells might have remained viable but lost their capacity to migrate and organize in tubular-like structures. In fact, it is reported that, after cryopreservation there is a high level of continued cell death, which is not apparent right after thawing, but manifests over a 24 h to 48 h period, as a result of delayed apoptosis and necrosis (J. Baust *et al.*, 2002; Fu *et al.*, 2001; Heng *et al.*, 2006). This phenomenon has been named cryopreservation-induced delayed-onset cell death (CIDOCD) (J. M. Baust *et al.*, 2001) and could explain the presence of metabolic activity after 18 h of incubation, but the lack of cell sprouting 72 h after fibrin culture.

Endothelial cells are more sensitive than MSC, which means they were probably more affected by cryopreservation procedures than MSC. Larman *et al.* reported that exposing mouse and human oocytes to vitrification solutions with high concentrations of CPA, at RT, resulted in spindle disruption, however the same did not happen at 38ºC (Larman *et al.*, 2007). Moreover, longer exposures (7-10 min) to EG have shown to cause actin filament disruption (Hotamisligil *et al.*, 1996). In our first experimental setup, the Vitrification and CPA Cytotoxicity Control spheroids were subject to high levels of cell manipulation, such as centrifugation cycles and up and down pipetting, which represents a high level of cell

manipulation. Previous works showed that in MSC-EC spheroids, EC formed a concentric layer around the spheroid, and were the ones mostly involved in sprouting (Saleh *et al.*, 2011) (Bauman *et al.*, 2018). Our results may indicate that the manipulation of spheroids was too aggressive, or that spheroids exposure to the cryopreserved solutions was too toxic resulting in OEC dead and/or loss. In fact, our data suggest that the last hypothesis might be valid, as levels of CD31 expression at the outer layer of thawed spheroids were effectively low. For that reason, cryopreservation in cryovials was abandoned.

To investigate if spheroid manipulation was one major factor accounting for the poor outcome, MSC-OEC spheroids were exposed to the solutions and cryopreserved while still in the agarose molds, which were then transferred to 10 mL flasks as cryocarriers. When cryopreserved this way, the integrity and diameter of MSC-OEC spheroids were maintained, which led us to believe that ECM matrix architecture was preserved, at least to some extent. One of the main constrains, while cryopreserving tissue engineered constructs, is maintenance of the different cellular elements, along with ECM architecture and composition In some types of spheroid, integrity and viability is intrinsically dependent on ECM production, which provides biochemical and biomechanical cues for tissue morphogenesis, differentiation and homeostasis (Frantz *et al.*, 2010). Also, upon spheroid formation, cells express high levels of cadherins which facilitates cells compaction and stronger cell-cell adhesions (Giannotta *et al.*, 2013). Thus, the preservation of ECM proteins, cell-cell and cell-ECM adhesions during cryopreservation is highly important to maintain cells viability after thawing. In fact, most studies in TE have been more focused in preserving ECM architecture during tissue cryopreservation than cell viability post-thawing (Brockbank *et al.*, 2015; Eisenberg *et al.*, 2014). The metabolic activity of CPA Cytotoxicity Control spheroids, when cryopreserved in molds within flasks, was similar to the Control, in both mediums. This means that manipulation of spheroids is indeed a very important factor and should be taken into account. Moreover, high sprouting formation, as well as MSC migration, was observed in fibrin gels, comparable to the control condition and for both mediums.

Co-cultured HDFn-OEC spheroids in a 5:1 ratio were also cryopreserved in agarose molds. In the first experiment, cells were exposed for 3 min to each cryopreservation solution. The retention of toxic compounds in agarose molds was one major concern relatively to cell viability. So, after thawing in different sucrose dilutions, spheroids were moved to new molds. Metabolic activity was slightly higher in the transferred spheroids conditions (for both Slow Freezing and Vitrification spheroids) in Standard medium, which suggests that agarose molds could indeed absorb and retain some toxicity of cryopreservation solutions. However, this was not observed in XF medium regarding vitrification spheroids. It can be hypothesized that the results observed in XF conditions could be due to a technical error, and further experiments should be done to clarify this point.

For MSC-OEC spheroids in Standard medium, Slow Freezing spheroids presented higher metabolic activity than Vitrification spheroids. This might be because Vitrification solutions

were not penetrating enough into the spheroids. On one hand, this would result in lower cytotoxicity but, on the other hand, cells might be insufficiently protected against cryopreservation.

In literature, Vitrification is often referred as the most appropriate cryopreservation technique in the case of TE products (Dahl *et al.*, 2006; Fahy *et al.*, 2004; Kuleshova *et al.*, 2007; M. Taylor *et al.*, 2019). The use of high concentrations of pCPA allow cells to enter a vitreous state without ice formation, which avoids ice injury, while npCPA act as an osmotic buffer, especially during thawing. However, results presented here show otherwise. Both in MSC-OEC and HDFn-OEC spheroids, the ones exposed to Slow Freezing solutions and cooling rates presented higher overall metabolic activity and sprouting potential than the ones exposed to Vitrification, when cryopreserved in agarose molds. EG has been found to be less toxic than DMSO and has a lower molecular weight, penetrating quicker into cells (Songsasen *et al.*, 1995; Valdez *et al.*, 1992). This means that Vitrification spheroids should be more protected against cryopreservation than Slow Freezing spheroids. In order to clarify the reason behind this observation, we further investigated if the cooling and thawing processes were affecting metabolic activity and sprouting potential. Spheroids were exposed to vitrification solutions with a Slow Freezing cooling rate, which turned out to be no different from the normal Vitrification. In what concerns warming rates, after retrieved from LN, spheroids were thaw in a 37ºC bath, a step that should be quick and took about 5 to 10 min. Eventually, the time spent in the thawing process could have been too long, impairing cell viability and sprouting potential due to high pCPA concentrations or osmotic shock. In fact, some reports have showed that warming rates could be more important to oocyte viability than cooling rates (Leibo & Pool, 2011; Seki & Mazur, 2009).

Our results have also shown increased sprouting potential in HDFn-OEC spheroids in post-cryopreservation, when compared to MSC-OEC spheroids, which exhibit almost no sprouting. In an attempt to improve the spheroids sprouting potential, 5 min of exposure to Vitrification solutions was performed, only in HDFn-OEC spheroids. This increment seemed to have no effect in both CPA Cytotoxicity Control and Vitrification spheroids. In fact, no sprouting was found in spheroids exposed to vitrification solutions for 3 min in the second experiment. Nevertheless, this could have been due to experimental constraints and more experiments should be performed to validate our results.

Additionally, spheroids were cultured for 1 and 2 days, pre and post-cryopreservation. Interestingly, Slow Freezing spheroids had high values of metabolic activity and were able to form sprouts throughout fibrin culture. Also, brightfield images showed more sprouting when spheroids were in culture for 2 days post-cryopreservation. This could mean that cells after cryopreservation need time to reactivate and properly become functional. Moreover, it was also possible to observe mitotic cells, a good indicative of cell viability and functionality. Still, CPA Cytotoxicity Control spheroids were similar to Control spheroids, in both days and both timepoints (3 and 5 min exposure), presenting high metabolic activity and high levels of

sprouting, which strengths the fact that, like in MSC-OEC spheroids, the process of warming in Vitrification could be the main reason for the poor outcome. Petrenko and colleagues used a perfusion bioreactor for the exposal and removal of CPA in collagen scaffolds seeded with MSC (Petrenko *et al.*, 2017). With this type of equipment, CPA solutions are perfused directly into the pores of the constructs, allowing a constant and homogeneous diffusion of CPA through cells. This had an increased in recovery rate compared to standard diffusion methods (59 ± 4.2% vs 42.3 ± 4.5%, respectively).

Even though there was not much sprouting in cryopreserved spheroids, some cells were able to migrate and colonize the fibrin gel, in this case fibroblasts, that expressed collagen type I, providing another indication of cellular viability and functionality. Unfortunately, we did not perform any Live/Dead assay herein to confirm these results, since this assay is not very reliable in dense, spheroid-based 3D constructs.

Another vitrification approach was tested, Liquidus-Tracking. LT is a recent approach, more suitable for higher-volume samples, which is usually the case in TE. There are still very few reports using LT technique as a cryopreservation technique. Recently, Alginate-encapsulated liver cells, with average diameter of 450 µm, were successfully cryopreserved using LT (Puschmann *et al.*, 2017). In the present study, HFDn-OEC spheroids were exposed to DMSO at 6 different concentrations, which were increased as temperature decreased. Our results have shown that LT CPA Cytotoxicity Control spheroids were metabolic active but, showed no sprouting formation when cultured in fibrin gel. LT is a highly automated process, and Puschmann *et al* recommended that automatizing even more the process would be a priority (Puschmann *et al.*, 2014). Since that kind of equipment was not available in the lab, all the protocol was performed manually. Even though all efforts were made to strictly control temperature between solution changes, it was very difficult to avoid oscillations. When removed from -20 and -80ºC freezers to the cell culture rooms, samples increased almost +10ºC in temperature. As the premises of this protocol is to increase CPA concentration as the temperature is lowered, it can be concluded that our set-up did not adequately fulfilled such requisites. For that reasons, this approach was abandoned, and LT spheroids were not recovered from LN.

As an attempt to understand if the cryocarrier could affect cells viability, experiments with agarose molds and a nylon mesh were performed. Nylon meshes have been used for oocyte cryopreservation (Matsumoto *et al.*, 2001), and more recently in TE (Tian *et al.*, 2019). Tian and colleagues used a nylon mesh device to cryopreserve alginate microfibers containing MSC. Microfibers cryopreserved in nylon mesh had 85-89% more viability than microfibers cryopreserved in cryovials. Since the device setup design reported by Tian and co-workers was not fully described, we tried to develop an equivalent approach. The metabolic activity of Nylon Mesh spheroids was significantly lower than in Control spheroids, even though it was slightly higher than Vitrification spheroids in flasks. Yet, when cultured in fibrin, both conditions showed no signs of sprouting. Additionally, Nylon Mesh in day 1 had a visible

swelling compared with other conditions. This phenomenon could be due to the difficulties in spheroids thawing. The histological cassette could not be immersed in a 37ºC bath, since the Petri Dish was not properly sealed. Instead, Petri Dish was placed on top of a support and the thawing process took several minutes. Another challenge was faced when retrieving spheroids from the nylon mesh. Even though they were visible to the naked eye, spheroids attached to the nylon mesh, making it very difficult to recover them. Overall this whole process should be optimized, especially spheroids thawing and retrieval

Overall, these findings suggest that a slow cooling rate with a freezing solution of 10% v/v DMSO could be a better approach for 3D multicellular spheroids cryopreservation. Also, XF medium remains as a viable option for producing and cryopreserving spheroids in a HT manner. In the present study, HDFn-OEC spheroids presented an overall increased viability post-cryopreservation, comparing to MSC-OEC spheroids. Nevertheless, more studies should be performed, in both cell type spheroids, regarding CPA solutions optimization as well as cooling and thawing rates.

Chapter 5

Concluding remarks and future perspectives

The present study aimed at producing stromal-vascular co-culture spheroids in a HT manner; cryopreserve them by vitrification; and evaluate their viability and function post-retrieval. For that purpose, HDFn-OEC and MSC-OEC spheroids were produced using agarose micromold arrays, cultured in both Standard and XF medium, exposed to different cryopreservation solutions under different conditions, and stored in LN.

Similar to what has been previously described for MSC-OEC spheroids, HDFn-OEC spheroids culture promoted OEC organization into two different types of vascular structures: surface monolayers and internal clusters, with ability to sprout and form vascular-like networks.

MSC-OEC spheroids were cryopreserved by Slow Freezing method and by Vitrification, first in suspension inside cryovials and then in agarose molds inside flasks. Even though spheroids cryopreserved in cryovials presented metabolic activity, *in vitro* pro-angiogenic assay showed that cells had no sprouting potential, even prior to cryopreservation. Spheroids that did not experienced manipulation (agarose molds inside flasks setup) had higher metabolic activity levels and sprouting potential similar to control spheroids before cryopreservation. However, after retrieval from LN both their metabolic activity and sprouting potential decreased drastically.

Regarding culture mediums, there was no significant differences of metabolic activity and sprouting potential in cryopreserved spheroids.

When cryopreserved in agarose molds, HDFn-OEC spheroids that were cryopreserved by Slow Freezing demonstrated higher viability than spheroids cryopreserved by Vitrification, probably due to higher toxicity of vitrification solutions. Interestingly the same was not observed for MSC-OEC spheroids. In addition, cells presented a higher degree of sprouting when cultured in a fibrin gel 42 h after retrieved from LN instead of 18 h. This could mean that cells took time to recover from cryopreservation conditions and regain optimal functional potential. Also, a new and recent vitrification protocol was tested, LT. Despite presenting some metabolic

activity, spheroids did not sprout when cultured in fibrin gel. Nevertheless, LT remains a viable option for tissue engineered constructs, and should be tested in the future, ideally with appropriate equipment. HDFn-OEC spheroids vitrification in a Nylon Mesh device presented low metabolic activity and no sprouting formation. Further optimizations should be performed, namely in terms of the thawing procedure.

Overall, additional optimization of cryopreservation protocols should be explored. Specifically, it would be worthwhile to test different CPA solutions (with lower CPA concentrations), longer exposure time and different temperatures. Interestingly, the cryocarrier has showed to be an important factor for successful cryopreservation, so different cryocarriers should be tested. Inclusion of polymers such as dextran and ficoll in vitrification solutions have shown improved results in cell viability and should be encouraged.

In conclusion, collectively, our results suggest that Slow Freezing cryopreservation technique is more suited to HDFn-OEC pre-vascularized spheroids than Vitrification. Unfortunately, successful cryopreservation of MSC-OEC spheroids was not achieved. Nevertheless, this study represented one step forward towards the development of adequate protocols for the cryopreservation of pre-vascularized constructs. If successful, this would greatly facilitate the translation of these types of CT into the clinics.

Chapter 6

Bibliography

Abbott, R. D., & Kaplan, D. L. (2015). Strategies for improving the physiological relevance of human engineered tissues. *Trends Biotechnol, 33*(7), 401-407. doi:10.1016/j.tibtech.2015.04.003

Alajati, A., Laib, A. M., Weber, H., Boos, A. M., Bartol, A., Ikenberg, K., Korff, T., Zentgraf, H., Obodozie, C., Graeser, R., Christian, S., Finkenzeller, G., Stark, G. B., Heroult, M., & Augustin, H. G. (2008). Spheroid-based engineering of a human vasculature in mice. *Nat Methods, 5*(5), 439-445. doi:10.1038/nmeth.1198

Amann, A., Zwierzina, M., Koeck, S., Gamerith, G., Pechriggl, E., Huber, J. M., Lorenz, E., Kelm, J. M., Hilbe, W., Zwierzina, H., & Kern, J. (2017). Development of a 3D angiogenesis model to study tumour - endothelial cell interactions and the effects of anti-angiogenic drugs. *Sci Rep, 7*(1), 2963. doi:10.1038/s41598-017-03010-6

Annabi, N., Rana, D., Shirzaei Sani, E., Portillo-Lara, R., Gifford, J. L., Fares, M. M., Mithieux, S. M., & Weiss, A. S. (2017). Engineering a sprayable and elastic hydrogel adhesive with antimicrobial properties for wound healing. *Biomaterials, 139*, 229-243. doi:10.1016/j.biomaterials.2017.05.011

Arav, A., Aroyo, A., Yavin, S., & Roth, Z. (2009). Embryo cryopreservation in the presence of low concentration of vitrification solution with sealed pulled straws in liquid nitrogen slush. *Human Reproduction, 24*(4), 797-804. doi:10.1093/humrep/den397

Arav, A., Yavin, S., Zeron, Y., Natan, D., Dekel, I., & Gacitua, H. (2002). New trends in gamete's cryopreservation. *Mol Cell Endocrinol, 187*(1-2), 77-81.

Arav, A., & Zeron, Y. (1997). Vitrification of bovine oocytes using modified minimum drop size technique (MDS) is effected by the composition and the concentration of the vitrification solution and by the cooling conditions. *Theriogenology, 47*(1), 341. doi:10.1016/S0093-691X(97)82468-5

Arav, A., Zeron, Y., & Ocheretny, A. (2000). *A new device and method for vitrification increases the cooling rate and allows successful cryopreservation of bovine oocytes* (Vol. 53).

Argyle, C. E., Harper, J. C., & Davies, M. C. (2016). Oocyte cryopreservation: where are we now? *Hum Reprod Update, 22*(4), 440-449. doi:10.1093/humupd/dmw007

Asahara, T., Murohara, T., Sullivan, A., Silver, M., van der Zee, R., Li, T., Witzenbichler, B., Schatteman, G., & Isner, J. M. (1997). Isolation of Putative Progenitor Endothelial Cells for Angiogenesis. *Science, 275*(5302), 964-966. doi:10.1126/science.275.5302.964

Au, P., Tam, J., Fukumura, D., & Jain, R. K. (2008). Bone marrow-derived mesenchymal stem cells facilitate engineering of long-lasting functional vasculature. *Blood, 111*(9), 4551-4558. doi:10.1182/blood-2007-10-118273

Aurora, A., Wrice, N., Walters, T. J., Christy, R. J., & Natesan, S. (2018). A PEGylated platelet free plasma hydrogel based composite scaffold enables stable vascularization and targeted cell delivery for volumetric muscle loss. *Acta Biomater, 65*, 150-162. doi:10.1016/j.actbio.2017.11.019

Bartosh, T. J., et al. (2010). Aggregation of human mesenchymal stromal cells (MSCs) into 3D spheroids enhances their antiinflammatory properties. *Proceedings of the National Academy of Sciences, 2010. 107(31): p. 13724-13729.* doi: 10.1073/pnas.1008117107

Battaglia, R. A., Delic, S., Herrmann, H., & Snider, N. T. (2018). Vimentin on the move: new developments in cell migration. *F1000Res, 7*. doi:10.12688/f1000research.15967.1
Bauman, E., Feijao, T., Carvalho, D. T. O., Granja, P. L., & Barrias, C. C. (2018). Xeno-free pre-vascularized spheroids for therapeutic applications. *Sci Rep, 8*(1), 230. doi:10.1038/s41598-017-18431-6
Baust, J., Van Buskirk, R., & Baust, J. (2002). *Gene Activation of the Apoptotic Caspase Cascade Following Cryogenic Storage* (Vol. 1).
Baust, J. M., Vogel, M. J., Van Buskirk, R., & Baust, J. G. (2001). A molecular basis of cryopreservation failure and its modulation to improve cell survival. *Cell Transplant, 10*(7), 561-571.
Becker, J. L., & Souza, G. R. (2013). Using space-based investigations to inform cancer research on Earth. *Nat Rev Cancer, 13*(5), 315-327. doi:10.1038/nrc3507
Beebe, L. F., Cameron, R. D., Blackshaw, A. W., & Keates, H. L. (2005). Changes to porcine blastocyst vitrification methods and improved litter size after transfer. *Theriogenology, 64*(4), 879-890. doi:10.1016/j.theriogenology.2004.12.014
Benien, P., & Swami, A. (2014). 3D tumor models: history, advances and future perspectives. *Future Oncol, 10*(7), 1311-1327. doi:10.2217/fon.13.274
Berthod, F., Germain, L., Tremblay, N., & Auger, F. A. (2006). Extracellular matrix deposition by fibroblasts is necessary to promote capillary-like tube formation in vitro. *J Cell Physiol, 207*(2), 491-498. doi:10.1002/jcp.20584
Bhakta, G., Lee, K. H., Magalhaes, R., Wen, F., Gouk, S. S., Hutmacher, D. W., & Kuleshova, L. L. (2009). Cryopreservation of alginate-fibrin beads involving bone marrow derived mesenchymal stromal cells by vitrification. *Biomaterials, 30*(3), 336-343. doi:10.1016/j.biomaterials.2008.09.030
Bianco, P., Cao, X., Frenette, P. S., Mao, J. J., Robey, P. G., Simmons, P. J., & Wang, C. Y. (2013). The meaning, the sense and the significance: translating the science of mesenchymal stem cells into medicine. *Nat Med, 19*(1), 35-42. doi:10.1038/nm.3028
Boldt, J., Cline, D., & McLaughlin, D. (2003). Human oocyte cryopreservation as an adjunct to IVF-embryo transfer cycles. *Hum Reprod, 18*(6), 1250-1255. doi:10.1093/humrep/deg242
Borini, A., Bonu, M. A., Coticchio, G., Bianchi, V., Cattoli, M., & Flamigni, C. (2004). Pregnancies and births after oocyte cryopreservation. *Fertil Steril, 82*(3), 601-605. doi:10.1016/j.fertnstert.2004.04.025
Brockbank, K. G. M., Chen, Z., Greene, E. D., & Campbell, L. H. (2015). Vitrification of Heart Valve Tissues. In W. F. Wolkers & H. Oldenhof (Eds.), *Cryopreservation and Freeze-Drying Protocols* (pp. 399-421). New York, NY: Springer New York.
Brophy, C. M., Luebke-Wheeler, J. L., Amiot, B. P., Remmel, R. P., Rinaldo, P., & Nyberg, S. L. (2009). Rat hepatocyte spheroids formed by rocked technique maintain differentiated hepatocyte gene expression and function. *Hepatology (Baltimore, Md.), 49*(2), 578-586. doi:10.1002/hep.22674
Brouzes, E., Medkova, M., Savenelli, N., Marran, D., Twardowski, M., Hutchison, J. B., Rothberg, J. M., Link, D. R., Perrimon, N., & Samuels, M. L. (2009). Droplet microfluidic technology for single-cell high-throughput screening. *Proc Natl Acad Sci U S A, 106*(34), 14195-14200. doi:10.1073/pnas.0903542106
Buzhor, E., Leshansky, L., Blumenthal, J., Barash, H., Warshawsky, D., Mazor, Y., & Shtrichman, R. (2014). Cell-based therapy approaches: the hope for incurable diseases. *Regen Med, 9*(5), 649-672. doi:10.2217/rme.14.35
Cai, X. Y., Chen, G. A., Lian, Y., Zheng, X. Y., & Peng, H. M. (2005). Cryoloop vitrification of rabbit oocytes. *Hum Reprod, 20*(7), 1969-1974. doi:10.1093/humrep/deh805
Camus, A., Clairaz, P., Ersham, A., Van Kappel, A. L., Savić, G., & Staub, C. (2006). Principe de la vitrification : cinétiques comparatives. *Gynécologie Obstétrique & Fertilité, 34*(9), 737-745. doi:10.1016/j.gyobfe.2006.07.017
Chan, H. F., Zhang, Y., Ho, Y. P., Chiu, Y. L., Jung, Y., & Leong, K. W. (2013). Rapid formation of multicellular spheroids in double-emulsion droplets with controllable microenvironment. *Sci Rep, 3*, 3462. doi:10.1038/srep03462
Chen, C. (1986). Pregnancy after human oocyte cryopreservation. *Lancet, 1*(8486), 884-886.
Chen, J., Li, Y., Katakowski, M., Chen, X., Wang, L., Lu, D., Lu, M., Gautam, S. C., & Chopp, M. (2003). Intravenous bone marrow stromal cell therapy reduces apoptosis and promotes endogenous cell proliferation after stroke in female rat. *J Neurosci Res, 73*(6), 778-786. doi:10.1002/jnr.10691

Chen, J., Zhang, Z. G., Li, Y., Wang, L., Xu, Y. X., Gautam, S. C., Lu, M., Zhu, Z., & Chopp, M. (2003). Intravenous administration of human bone marrow stromal cells induces angiogenesis in the ischemic boundary zone after stroke in rats. *Circ Res, 92*(6), 692-699. doi:10.1161/01.res.0000063425.51108.8d

Chen, S. U., Lien, Y. R., Cheng, Y. Y., Chen, H. F., Ho, H. N., & Yang, Y. S. (2001). Vitrification of mouse oocytes using closed pulled straws (CPS) achieves a high survival and preserves good patterns of meiotic spindles, compared with conventional straws, open pulled straws (OPS) and grids. *Hum Reprod, 16*(11), 2350-2356.

Chen, X., Aledia, A. S., Popson, S. A., Him, L., Hughes, C. C., & George, S. C. (2010). Rapid anastomosis of endothelial progenitor cell-derived vessels with host vasculature is promoted by a high density of cotransplanted fibroblasts. *Tissue Eng Part A. 2010 Feb;16(2):585-94.*

Cheng, N. C., Chen, S. Y., Li, J. R., & Young, T. H. (2013). Short-term spheroid formation enhances the regenerative capacity of adipose-derived stem cells by promoting stemness, angiogenesis, and chemotaxis. *Stem Cells Transl Med, 2*(8), 584-594. doi:10.5966/sctm.2013-0007

Chian, R. C., Son, W. Y., Huang, J. Y., Cui, S. J., Buckett, W. M., & Tan, S. L. (2005). High Survival Rates and Pregnancies of Human Oocytes Following Vitrification: Preliminary Report. *Fertility and Sterility, 84*, S36. doi:10.1016/j.fertnstert.2005.07.086

Choi, C. W., Kim, B. S., Seo, J. H., Shin, S. W., Kim, Y. H., & Kim, J. S. (2001). Long-term engraftment stability of peripheral blood stem cells cryopreserved using the dump-freezing method in a -80 degrees C mechanical freezer with 10% dimethyl sulfoxide. *Int J Hematol, 73*(2), 245-250.

Cobo, A., Romero, J. L., Perez, S., de los Santos, M. J., Meseguer, M., & Remohi, J. (2010). Storage of human oocytes in the vapor phase of nitrogen. *Fertil Steril, 94*(5), 1903-1907. doi:10.1016/j.fertnstert.2009.10.042

Criado, E., Moalli, F., Polentarutti, N., Albani, E., Morreale, G., Menduni, F., & Levi-Setti, P. E. (2011). Experimental contamination assessment of a novel closed ultravitrification device. *Fertil Steril, 95*(5), 1777-1779. doi:10.1016/j.fertnstert.2010.12.044

Cuello, C., Gil, M. A., Parrilla, I., Tornel, J., Vazquez, J. M., Roca, J., Berthelot, F., Martinat-Botte, F., & Martinez, E. A. (2004). Vitrification of porcine embryos at various developmental stages using different ultra-rapid cooling procedures. *Theriogenology, 62*(1-2), 353-361. doi:10.1016/j.theriogenology.2003.10.007

Cui, X., Hartanto, Y., & Zhang, H. (2017). Advances in multicellular spheroids formation. *J R Soc Interface, 14*(127). doi:10.1098/rsif.2016.0877

Curcio, E., Salerno, S., Barbieri, G., De Bartolo, L., Drioli, E., & Bader, A. (2007). Mass transfer and metabolic reactions in hepatocyte spheroids cultured in rotating wall gas-permeable membrane system. *Biomaterials, 28*(36), 5487-5497. doi:10.1016/j.biomaterials.2007.08.033

Dahl, S. L., Chen, Z., Solan, A. K., Brockbank, K. G., Niklason, L. E., & Song, Y. C. (2006). Feasibility of vitrification as a storage method for tissue-engineered blood vessels. *Tissue Eng, 12*(2), 291-300. doi:10.1089/ten.2006.12.291

Desai, N. N., Goldberg, J. M., Austin, C., & Falcone, T. (2013). The new Rapid-i carrier is an effective system for human embryo vitrification at both the blastocyst and cleavage stage. *Reprod Biol Endocrinol, 11*, 41. doi:10.1186/1477-7827-11-41

Dinnyés, A. s., Jiang, S., Dai, Y., & Yang, X. (2000). High Developmental Rates of Vitrified Bovine Oocytes Following Parthenogenetic Activation, In Vitro Fertilization, and Somatic Cell Nuclear Transfer1. *Biol Reprod, 63*(2), 513-518. doi:10.1095/biolreprod63.2.513

Dissanayaka, W. L., Zhu, L., Hargreaves, K. M., Jin, L., & Zhang, C. (2014). Scaffold-free Prevascularized Microtissue Spheroids for Pulp Regeneration. *J Dent Res, 93*(12), 1296-1303. doi:10.1177/0022034514550040

Dittrich, A., Grimm, D., Sahana, J., Bauer, J., Kruger, M., Infanger, M., & Magnusson, N. E. (2018). Key Proteins Involved in Spheroid Formation and Angiogenesis in Endothelial Cells After Long-Term Exposure to Simulated Microgravity. *Cell Physiol Biochem, 45*(2), 429-445. doi:10.1159/000486920

Duguay, D., Foty, R. A., & Steinberg, M. S. (2003). Cadherin-mediated cell adhesion and tissue segregation: qualitative and quantitative determinants. *Developmental Biology, 2003. 253(2): p. 309-323.*

Duttenhoefer, F., Lara de Freitas, R., Meury, T., Loibl, M., Benneker, L. M., Herrmann, M., Richards, R. G., Alini, M., & Verrier, S. (2013). 3D scaffolds co-seeded with human endothelial progenitor and mesenchymal stem cells: Evidence of prevascularisation within 7 days. *European Cells and Materials, 26*, 59-65. doi:10.22203/eCM.v026a04

Eisenberg, D. P., Taylor, M. J., Jimenez-Rios, J. L., & Rabin, Y. (2014). Thermal expansion of vitrified blood vessels permeated with DP6 and synthetic ice modulators. *Cryobiology, 68*(3), 318-326. doi:10.1016/j.cryobiol.2014.04.010

Elliott, G. D., Wang, S., & Fuller, B. J. (2017). Cryoprotectants: A review of the actions and applications of cryoprotective solutes that modulate cell recovery from ultra-low temperatures. *Cryobiology, 76*, 74-91. doi:10.1016/j.cryobiol.2017.04.004

Fahy, G. M., MacFarlane, D. R., Angell, C. A., & Meryman, H. T. (1984). Vitrification as an approach to cryopreservation. *Cryobiology, 21*(4), 407-426.

Fahy, G. M., & Wowk, B. (2015). Principles of cryopreservation by vitrification. *Methods Mol Biol, 1257*, 21-82. doi:10.1007/978-1-4939-2193-5_2

Fahy, G. M., Wowk, B., Wu, J., Phan, J., Rasch, C., Chang, A., & Zendejas, E. (2004). Cryopreservation of organs by vitrification: perspectives and recent advances. *Cryobiology, 48*(2), 157-178. doi:10.1016/j.cryobiol.2004.02.002

Feremans, W. W., Bastin, G., Moine, F. L., Ravoet, C., Delville, J. P., Pradier, O., Wallef, G., Dupont, E., Capel, P., & Lambermont, M. (1996). Simplification of the blood stem cell transplantation (BSCT) procedure: large volume apheresis and uncontrolled rate cryopreservation at -80 degrees C. *Eur J Haematol, 56*(5), 278-282.

Foty, R. A., & Steinberg, M. S. (2004). Cadherin-mediated cell-cell adhesion and tissue segregation in relation to malignancy. *Int J Dev Biol, 48*(5-6), 397-409. doi:10.1387/ijdb.041810rf

Foty, R. A., & Steinberg, M. S. (2005). The differential adhesion hypothesis: a direct evaluation. *Dev Biol, 278*(1), 255-263. doi:10.1016/j.ydbio.2004.11.012

Frantz, C., Stewart, K. M., & Weaver, V. M. (2010). The extracellular matrix at a glance. *J Cell Sci, 123*(Pt 24), 4195-4200. doi:10.1242/jcs.023820

Fu, T., Guo, D., Huang, X., O'Gorman, M. R., Huang, L., Crawford, S. E., & Soriano, H. E. (2001). Apoptosis occurs in isolated and banked primary mouse hepatocytes. *Cell Transplant, 10*(1), 59-66.

Fuchs, S., Hermanns, M. I., & Kirkpatrick, C. J. (2006). Retention of a differentiated endothelial phenotype by outgrowth endothelial cells isolated from human peripheral blood and expanded in long-term cultures. *Cell Tissue Res, 326*(1), 79-92. doi:10.1007/s00441-006-0222-4

Fuchs, S., Motta, A., Migliaresi, C., & Kirkpatrick, C. J. (2006). Outgrowth endothelial cells isolated and expanded from human peripheral blood progenitor cells as a potential source of autologous cells for endothelialization of silk fibroin biomaterials. *Biomaterials, 27*(31), 5399-5408. doi:10.1016/j.biomaterials.2006.06.015

G Larman, M., B Sheehan, C., & Gardner, D. (2006). *Calcium-free vitrification reduces cryoprotectant-induced zona pellucida hardening and increases fertilization rates in mouse oocytes* (Vol. 131).

Galmes, A., Gutierrez, A., Sampol, A., Canaro, M., Morey, M., Iglesias, J., Matamoros, N., Duran, M. A., Novo, A., Bea, M. D., Galan, P., Balansat, J., Martinez, J., Bargay, J., & Besalduch, J. (2007). Long-term hematological reconstitution and clinical evaluation of autologous peripheral blood stem cell transplantation after cryopreservation of cells with 5% and 10% dimethylsulfoxide at -80 degrees C in a mechanical freezer. *Haematologica, 92*(7), 986-989.

Giannotta, M., Trani, M., & Dejana, E. (2013). VE-cadherin and endothelial adherens junctions: active guardians of vascular integrity. *Dev Cell, 26*(5), 441-454. doi:10.1016/j.devcel.2013.08.020

Gouk, S. S., Tan, F., Hande, P., Poonepalli, A., S. Dawe, G., & Kuleshova, L. (2006). *51. Protein and serum-free vitrification of neural stem cells* (Vol. 53).

Grimm, D., Wehland, M., Pietsch, J., Aleshcheva, G., Wise, P., van Loon, J., Ulbrich, C., Magnusson, N. E., Infanger, M., & Bauer, J. (2014). Growing Tissues in Real and Simulated Microgravity: New Methods for Tissue Engineering. *Tissue Engineering. Part B, Reviews, 20*(6), 555-566. doi:10.1089/ten.teb.2013.0704

Guerreiro, S. G., Brochhausen, C., Negrao, R., Barbosa, M. A., Unger, R. E., Kirkpatrick, C. J., Soares, R., & Granja, P. L. (2012). Implanted neonatal human dermal fibroblasts

influence the recruitment of endothelial cells in mice. *Biomatter, 2*(1), 43-52. doi:10.4161/biom.20063
Guerreiro, S. G., Oliveira, M. J., Barbosa, M. A., Soares, R., & Granja, P. L. (2014). Neonatal human dermal fibroblasts immobilized in RGD-alginate induce angiogenesis. *Cell Transplant, 23*(8), 945-957. doi:10.3727/096368913x670183
Guerrero, J., Catros, S., Derkaoui, S. M., Lalande, C., Siadous, R., Bareille, R., Thebaud, N., Bordenave, L., Chassande, O., Le Visage, C., Letourneur, D., & Amedee, J. (2013). Cell interactions between human progenitor-derived endothelial cells and human mesenchymal stem cells in a three-dimensional macroporous polysaccharide-based scaffold promote osteogenesis. *Acta Biomater, 9*(9), 8200-8213. doi:10.1016/j.actbio.2013.05.025
Hamawaki, A., Kuwayama, M., & Hamano, S. (1999). Minimum volume cooling method for bovine blastocyst vitrification. *Theriogenology, 51*(1), 165. doi:10.1016/S0093-691X(99)91724-7
Hamilton, G. A., Westmorel, C., & George, A. E. (2001). Effects of medium composition on the morphology and function of rat hepatocytes cultured as spheroids and monolayers. *In Vitro Cell Dev Biol Anim, 37*(10), 656-667.
Han, Y., Liu, X.-M., Liu, H., Li, S.-C., Wu, B.-C., Ye, L.-L., Wang, Q.-W., & Chen, Z.-L. (2006). Cultivation of Recombinant Chinese hamster ovary cells grown as suspended aggregates in stirred vessels. *Journal of Bioscience and Bioengineering, 102*(5), 430-435.
Hendrickx, B., Verdonck, K., Van den Berge, S., Dickens, S., Eriksson, E., Vranckx, J. J., & Luttun, A. (2010). Integration of blood outgrowth endothelial cells in dermal fibroblast sheets promotes full thickness wound healing. *Stem Cells, 28*(7), 1165-1177. doi:10.1002/stem.445
Heng, B. C., Ye, C. P., Liu, H., Toh, W. S., Rufaihah, A. J., Yang, Z., Bay, B. H., Ge, Z., Ouyang, H. W., Lee, E. H., & Cao, T. (2006). Loss of viability during freeze-thaw of intact and adherent human embryonic stem cells with conventional slow-cooling protocols is predominantly due to apoptosis rather than cellular necrosis. *J Biomed Sci, 13*(3), 433-445. doi:10.1007/s11373-005-9051-9
Heo, D. N., Hospodiuk, M., & Ozbolat, I. T. (2019). Synergistic interplay between human MSCs and HUVECs in 3D spheroids laden in collagen/fibrin hydrogels for bone tissue engineering. *Acta Biomater*. doi:10.1016/j.actbio.2019.02.046
Hirschhaeuser, F., Menne, H., Dittfeld, C., West, J., Mueller-Klieser, W., & Kunz-Schughart, L. A. (2010). Multicellular tumor spheroids: an underestimated tool is catching up again. *J Biotechnol, 148*(1), 3-15. doi:10.1016/j.jbiotec.2010.01.012
Hotamisligil, S., Toner, M., & Douglas Powers, R. (1996). Changes in Membrane Integrity, Cytoskeletal Structure, and Developmental Potential of Murine Oocytes after Vitrification in Ethylene Glycol1. *Biol Reprod, 55*(1), 161-168. doi:10.1095/biolreprod55.1.161
Hunt, C. J. (1984). Studies on cellular structure and ice location in frozen organs and tissues: the use of freeze-substitution and related techniques. *Cryobiology, 21*(4), 385-402.
Hurley, J. R., Balaji, S., & Narmoneva, D. A. (2010). Complex temporal regulation of capillary morphogenesis by fibroblasts. *Am J Physiol Cell Physiol, 299*(2), C444-453. doi:10.1152/ajpcell.00572.2009
Ingram, M., Techy, G., Saroufeem, R., Yazan, O., Narayan, K., Goodwin, T., & Spaulding, G. (1997). Three-dimensional growth patterns of various human tumor cell lines in simulated microgravity of a NASA bioreactor. *In Vitro Cell Dev Biol Anim. 33(6):459-66.*
Isachenko, V., Alabart, J. L., Nawroth, F., Isachenko, E., Vajta, G., & Folch, J. (2001). The open pulled straw vitrification of ovine GV-oocytes: positive effect of rapid cooling or rapid thawing or both? *Cryo Letters, 22*(3), 157-162.
Isachenko, V., Folch, J., Isachenko, E., Nawroth, F., Krivokharchenko, A., Vajta, G., Dattena, M., & Alabart, J. L. (2003). Double vitrification of rat embryos at different developmental stages using an identical protocol. *Theriogenology, 60*(3), 445-452. doi:10.1016/S0093-691X(03)00039-6
Jahn, K., Richards, R. G., Archer, C. W., & Stoddart, M. J. (2010). Pellet culture model for human primary osteoblasts. *Eur Cell Mater, 20*, 149-161.
Jain, R. K., Au, P., Tam, J., Duda, D. G., & Fukumura, D. (2005). Engineering vascularized tissue. *Nature Biotechnology, 23*, 821. doi:10.1038/nbt0705-821

Karow, A. M., Jr. (1969). Cryoprotectants--a new class of drugs. *J Pharm Pharmacol, 21*(4), 209-223.
Kasai, M., Hamaguchi, Y., Zhu, S. E., Miyake, T., Sakurai, T., & Machida, T. (1992). High survival of rabbit morulae after vitrification in an ethylene glycol-based solution by a simple method. *Biol Reprod, 46*(6), 1042-1046. doi:10.1095/biolreprod46.6.1042
Kay, A. G., Hoyland, J. A., Rooney, P., Kearney, J. N., & Pegg, D. E. (2015). A liquidus tracking approach to the cryopreservation of human cartilage allografts. *Cryobiology, 71*(1), 77-84. doi:10.1016/j.cryobiol.2015.05.005
Kelm, J. M., Diaz Sanchez-Bustamante, C., Ehler, E., Hoerstrup, S. P., Djonov, V., Ittner, L., & Fussenegger, M. (2005). VEGF profiling and angiogenesis in human microtissues. *J Biotechnol, 118*(2), 213-229. doi:10.1016/j.jbiotec.2005.03.016
Kelm, J. M., Djonov, V., Ittner, L. M., Fluri, D., Born, W., Hoerstrup, S. P., & Fussenegger, M. (2006). Design of custom-shaped vascularized tissues using microtissue spheroids as minimal building units. *Tissue Eng, 12*(8), 2151-2160. doi:10.1089/ten.2006.12.2151
Kelm, J. M., & Fussenegger, M. (2004). Microscale tissue engineering using gravity-enforced cell assembly. *Trends in Biotechnology, 22*(4), 195-202. doi:10.1016/j.tibtech.2004.02.002
Kelm, J. M., Lorber, V., Snedeker, J. G., Schmidt, D., Broggini-Tenzer, A., Weisstanner, M., Odermatt, B., Mol, A., Zund, G., & Hoerstrup, S. P. (2010). A novel concept for scaffold-free vessel tissue engineering: self-assembly of microtissue building blocks. *J Biotechnol, 148*(1), 46-55. doi:10.1016/j.jbiotec.2010.03.002
Kelm, J. M., Timmins, N. E., Brown, C. J., Fussenegger, M., & Nielsen, L. K. (2003). Method for generation of homogeneous multicellular tumor spheroids applicable to a wide variety of cell types. *Biotechnol Bioeng, 83*(2), 173-180. doi:10.1002/bit.10655
Khaoustov, V., Darlington, G., Soriano, H., Krishnan, B., Risin, D., Pellis, N., & Yoffe, B. (1999). Induction of three-dimensional assembly of human liver cells by simulated microgravity. *In Vitro Cell Dev Biol Anim. 35(9):501-9.*
Kitazato. Retrieved from https://www.kitazato.co.jp/en/products/cryo/cryotop.html. Accessed June 16, 2019
Konc, J., Kanyo, K., Kriston, R., Somoskoi, B., & Cseh, S. (2014). Cryopreservation of embryos and oocytes in human assisted reproduction. *Biomed Res Int, 2014*, 307268. doi:10.1155/2014/307268
Korff, T., & Augustin, H. G. . (1998). Integration of Endothelial Cells in Multicellular Spheroids Prevents Apoptosis and Induces Differentiation. *The Journal of Cell Biology, 143(5), 1341–1352.*
Korff, T., et al. (2001). Blood vessel maturation in a 3-dimensional spheroidal coculture model: direct contact with smooth muscle cells regulates endothelial cell quiescence and abrogates VEGF responsiveness. *FASEB J. ;15(2):447-57.*
Kuleshova, L., Gianaroli, L., Magli, C., Ferraretti, A., & Trounson, A. (1999). Birth following vitrification of a small number of human oocytes: case report. *Hum Reprod, 14*(12), 3077-3079.
Kuleshova, L. L., Gouk, S. S., & Hutmacher, D. W. (2007). Vitrification as a prospect for cryopreservation of tissue-engineered constructs. *Biomaterials, 28*(9), 1585-1596. doi:10.1016/j.biomaterials.2006.11.047
Kuleshova, L. L., MacFarlane, D. R., Trounson, A. O., & Shaw, J. M. (1999). Sugars exert a major influence on the vitrification properties of ethylene glycol-based solutions and have low toxicity to embryos and oocytes. *Cryobiology, 38*(2), 119-130. doi:10.1006/cryo.1999.2153
Kuleshova, L. L., Shaw, J. M., & Trounson, A. O. (2001). Studies on replacing most of the penetrating cryoprotectant by polymers for embryo cryopreservation. *Cryobiology, 43*(1), 21-31. doi:10.1006/cryo.2001.2335
Kuwayama, M., Vajta, G., Ieda, S., & Kato, O. (2005). Comparison of open and closed methods for vitrification of human embryos and the elimination of potential contamination. *Reproductive BioMedicine Online, 11*(5), 608-614. doi:10.1016/S1472-6483(10)61169-8
Kuwayama, M., Vajta, G., Kato, O., & Leibo, S. P. (2005). Highly efficient vitrification method for cryopreservation of human oocytes. *Reprod Biomed Online, 11*(3), 300-308.

Laib, A. M., Bartol, A., Alajati, A., Korff, T., Weber, H., & Augustin, H. G. (2009). Spheroid-based human endothelial cell microvessel formation in vivo. *Nat Protoc, 4*(8), 1202-1215. doi:10.1038/nprot.2009.96

Landry J, B. D., Ouellet C, Goyette R, Marceau N. (1985). Spheroidal aggregate culture of rat liver cells: histotypic reorganization, biomatrix deposition, and maintenance of functional activities. *The Journal of Cell Biology, 101*(3), 914-923.

Lane, M., Forest, K. T., Lyons, E. A., & Bavister, B. D. (1999). Live births following vitrification of hamster embryos using a novel containerless technique. *Theriogenology, 51*(1), 167. doi:10.1016/S0093-691X(99)91726-0

Lane, M., Schoolcraft, W. B., Gardner, D. K., & Phil, D. (1999). Vitrification of mouse and human blastocysts using a novel cryoloop container-less technique. *Fertility and Sterility, 72*(6), 1073-1078. doi:10.1016/S0015-0282(99)00418-5

Larman, M. G., Minasi, M. G., Rienzi, L., & Gardner, D. K. (2007). Maintenance of the meiotic spindle during vitrification in human and mouse oocytes. *Reproductive BioMedicine Online, 15*(6), 692-700. doi:10.1016/S1472-6483(10)60537-8

Laschke, M. W., & Menger, M. D. (2016). Prevascularization in tissue engineering: Current concepts and future directions. *Biotechnol Adv, 34*(2), 112-121. doi:10.1016/j.biotechadv.2015.12.004

Laschke, M. W., & Menger, M. D. (2017). Life is 3D: Boosting Spheroid Function for Tissue Engineering. *Trends Biotechnol, 35*(2), 133-144. doi:10.1016/j.tibtech.2016.08.004

Lazar, A., J.Mann, H., Remmel, R. P., Shatford, R. A., Cerra, F. B., & Hu, W.-S. (1995). Extended liver-specific functions of porcine hepatocyte spheroids entrapped in collagen gel. *In Vitro Cell Dev Biol Anim ;31(5):340-6.*

Lee, D. R., Yang, Y. H., Eum, J. H., Seo, J. S., Ko, J. J., Chung, H. M., & Yoon, T. K. (2007). Effect of using slush nitrogen (SN2) on development of microsurgically manipulated vitrified/warmed mouse embryos. *Hum Reprod, 22*(9), 2509-2514. doi:10.1093/humrep/dem206

Leibo, S. P., & Pool, T. B. (2011). The principal variables of cryopreservation: solutions, temperatures, and rate changes. *Fertility and Sterility, 96*(2), 269-276. doi:10.1016/j.fertnstert.2011.06.065

Leno, G. H., Sun, X., Yi, Y., Chen, J., Li, Z., & Engelhardt, J. F. (2008). Efficient Term Development of Vitrified Ferret Embryos Using a Novel Pipette Chamber Technique1. *Biol Reprod, 79*(5), 832-840. doi:10.1095/biolreprod.107.067371

Li, Q., Chen, C., Kapadia, A., Zhou, Q., Harper, M. K., Schaack, J., & LaBarbera, D. V. (2011). 3D models of epithelial-mesenchymal transition in breast cancer metastasis: high-throughput screening assay development, validation, and pilot screen. *J Biomol Screen, 16*(2), 141-154. doi:10.1177/1087057110392995

Li, Y., Chen, J., Chen, X. G., Wang, L., Gautam, S. C., Xu, Y. X., Katakowski, M., Zhang, L. J., Lu, M., Janakiraman, N., & Chopp, M. (2002). Human marrow stromal cell therapy for stroke in rat: neurotrophins and functional recovery. *Neurology, 59*(4), 514-523. doi:10.1212/wnl.59.4.514

Liebermann, J., Tucker, M. J., Graham, J. R., Han, T., Davis, A., & Levy, M. J. (2002). Blastocyst development after vitrification of multipronuclear zygotes using the Flexipet denuding pipette. *Reproductive BioMedicine Online, 4*(2), 146-150. doi:10.1016/S1472-6483(10)61932-3

Lin, K., Matsubara, Y., Masuda, Y., Togashi, K., Ohno, T., Tamura, T., Toyoshima, Y., Sugimachi, K., Toyoda, M., Marc, H., & Douglas, A. (2008). Characterization of adipose tissue-derived cells isolated with the Celution system. *Cytotherapy, 10*(4), 417-426. doi:10.1080/14653240801982979

Lin, R. Z., & Chang, H. Y. (2008). Recent advances in three-dimensional multicellular spheroid culture for biomedical research. *Biotechnol J, 3*(9-10), 1172-1184. doi:10.1002/biot.200700228

Lin, Y., Weisdorf, D. J., Solovey, A., & Hebbel, R. P. (2000). Origins of circulating endothelial cells and endothelial outgrowth from blood. *J Clin Invest, 105*(1), 71-77. doi:10.1172/JCI8071

Loibl, M., Binder, A., Herrmann, M., Duttenhoefer, F., Richards, R. G., Nerlich, M., Alini, M., & Verrier, S. (2014). Direct cell-cell contact between mesenchymal stem cells and endothelial progenitor cells induces a pericyte-like phenotype in vitro. *Biomed Res Int, 2014*, 395781. doi:10.1155/2014/395781

Lovelock, J. E., & Bishop, M. W. (1959). Prevention of freezing damage to living cells by dimethyl sulphoxide. *Nature, 183*(4672), 1394-1395.
Magalhaes, R., Wang, X. W., Gouk, S. S., Lee, K. H., Ten, C. M., Yu, H., & Kuleshova, L. L. (2008). Vitrification successfully preserves hepatocyte spheroids. *Cell Transplant, 17*(7), 813-828.
Makino, S., Harada, M., Akashi, K., Taniguchi, S., Shibuya, T., Inaba, S., & Niho, Y. (1991). A simplified method for cryopreservation of peripheral blood stem cells at -80 degrees C without rate-controlled freezing. *Bone Marrow Transplant, 8*(4), 239-244.
Martino, A., Songsasen, N., & Leibo, S. P. (1996). Development into blastocysts of bovine oocytes cryopreserved by ultra-rapid cooling. *Biol Reprod, 54*(5), 1059-1069.
Matsumoto, H., Jiang, J. Y., Tanaka, T., Sasada, H., & Sato, E. (2001). Vitrification of Large Quantities of Immature Bovine Oocytes Using Nylon Mesh. *Cryobiology, 42*(2), 139-144. doi:10.1006/cryo.2001.2309
Mazur, P. (1963). KINETICS OF WATER LOSS FROM CELLS AT SUBZERO TEMPERATURES AND THE LIKELIHOOD OF INTRACELLULAR FREEZING. *J Gen Physiol, 47*, 347-369.
McMillan, K. S., McCluskey, A. G., Sorensen, A., Boyd, M., & Zagnoni, M. (2016). Emulsion technologies for multicellular tumour spheroid radiation assays. *Analyst, 141*(1), 100-110. doi:10.1039/c5an01382h
Medina, R. J., O'Neill, C. L., Sweeney, M., Guduric-Fuchs, J., Gardiner, T. A., Simpson, D. A., & Stitt, A. W. (2010). Molecular analysis of endothelial progenitor cell (EPC) subtypes reveals two distinct cell populations with different identities. *BMC Med Genomics, 3*, 18. doi:10.1186/1755-8794-3-18
Meryman, H. T. (1971). Cryoprotective agents. *Cryobiology, 8*(2), 173-183.
Meryman, H. T., & Hornblower, M. (1972). A Method for Freezing and Washing Red Blood Cells Using a High Glycerol Concentration. *Transfusion, 12*(3), 145-156. doi:10.1111/j.1537-2995.1972.tb00001.x
Meyer, D., PiÉTu, G., Fressinaud, E., & Girma, J.-P. (1991). Von Willebrand Factor: Structure and Function. *Mayo Clinic Proceedings, 66*(5), 516-523. doi:10.1016/s0025-6196(12)62394-5
Mohamadnejad, M., Alimoghaddam, K., Mohyeddin-Bonab, M., Bagheri, M., Bashtar, M., Ghanaati, H., Baharvand, H., Ghavamzadeh, A., & Malekzadeh, R. (2007). Phase 1 trial of autologous bone marrow mesenchymal stem cell transplantation in patients with decompensated liver cirrhosis. *Arch Iran Med, 10*(4), 459-466. doi:07104/aim.008
Mueller-Klieser, W. (1984). Method for the determination of oxygen consumption rates and diffusion coefficients in multicellular spheroids. *Biophysical Journal, 46*(3), 343-348.
Mukaida, T., Takahashi, K., & Kasai, M. (2003). Blastocyst cryopreservation: ultrarapid vitrification using cryoloop technique. *Reprod Biomed Online, 6*(2), 221-225.
Mukaida, T., Wada, S., Takahashi, K., Pedro, P. B., An, T. Z., & Kasai, M. (1998). Vitrification of human embryos based on the assessment of suitable conditions for 8-cell mouse embryos. *Hum Reprod, 13*(1o), 2874-2879. doi:10.1093/humrep/13.10.2874
Muller, A. M., Hermanns, M. I., Skrzynski, C., Nesslinger, M., Muller, K. M., & Kirkpatrick, C. J. (2002). Expression of the endothelial markers PECAM-1, vWf, and CD34 in vivo and in vitro. *Exp Mol Pathol, 72*(3), 221-229. doi:10.1006/exmp.2002.2424
Muthukumar, K., Mangalaraj, A. M., Kamath, M. S., & George, K. (2008). Blastocyst cryopreservation: vitrification or slow freeze. *Fertility and Sterility, 90*, S426-S427. doi:10.1016/j.fertnstert.2008.07.1306
Newman, A. C., N., N. M., W, C., Gershon, P. D., & Hughes, C. C. (2011). The requirement for fibroblasts in angiogenesis: fibroblast-derived matrix proteins are essential for endothelial cell lumen formation. *Mol Biol Cell. 2011 Oct;22(20):3791-800.* doi:10.1091/mbc.E11-05-0393)
Noguchi, R., Nakayama, K., Itoh, M., Kamohara, K., Furukawa, K., Oyama, J., Node, K., & Morita, S. (2016). Development of a three-dimensional pre-vascularized scaffold-free contractile cardiac patch for treating heart disease. *J Heart Lung Transplant, 35*(1), 137-145. doi:10.1016/j.healun.2015.06.001
Nyberg, S. L., Hardin, J., Amiot, B., Argikar, U. A., Remmel, R. P., & Rinaldo, P. (2005). Rapid, large-scale formation of porcine hepatocyte spheroids in a novel spheroid reservoir bioartificial liver. *Liver Transpl, 11*(8), 901-910. doi:10.1002/lt.20446
Origio. Retrieved from https://fertility.coopersurgical.com/wp-content/uploads/McGill_0236-02_Canada.pdf. Accessed June 16, 2019.

Paixao, C. L., Pereira, P. C., Minguetti-Camara, V. C., & Almodin, C. G. (2010). Embryo development and gestation using fresh and vitrified oocytes. *Human Reproduction, 25*(5), 1192-1198. doi:10.1093/humrep/deq042

Pampaloni, F., E.H.K. Reynaud Eg Fau - Stelzer, and E.H. Stelzer. (2007). The third dimension bridges the gap between cell culture and live tissue. *Nat Rev Mol Cell Biol. 8(10):839-45.*

Papis, K., Korwin-Kossakowski, M., & Wenta-Muchalska, E. (2009). Comparison of traditional and modified (VitMaster) methods of rabbit embryo vitrification. *Acta Vet Hung, 57*(3), 411-416. doi:10.1556/AVet.57.2009.3.7

Park, S., DiMaio, T. A., Scheef, E. A., Sorenson, C. M., & Sheibani, N. (2010). PECAM-1 regulates proangiogenic properties of endothelial cells through modulation of cell-cell and cell-matrix interactions. *Am J Physiol Cell Physiol, 299*(6), C1468-1484. doi:10.1152/ajpcell.00246.2010

Pegg, D. E. (1984). Red cell volume in glycerol/sodium chloride/water mixtures. *Cryobiology, 21*(2), 234-239.

Pegg, D. E. (2010). The relevance of ice crystal formation for the cryopreservation of tissues and organs. *Cryobiology, 60*(3 Suppl), S36-44. doi:10.1016/j.cryobiol.2010.02.003

Pegg, D. E. (2015). Principles of cryopreservation. *Methods Mol Biol, 1257*, 3-19. doi:10.1007/978-1-4939-2193-5_1

Pegg, D. E., Wang, L., & Vaughan, D. (2006). Cryopreservation of articular cartilage. Part 3: The liquidus-tracking method. *Cryobiology, 52*(3), 360-368. doi:10.1016/j.cryobiol.2006.01.004

Peng, L., Xie, D. Y., Lin, B. L., Liu, J., Zhu, H. P., Xie, C., Zheng, Y. B., & Gao, Z. L. (2011). Autologous bone marrow mesenchymal stem cell transplantation in liver failure patients caused by hepatitis B: short-term and long-term outcomes. *Hepatology, 54*(3), 820-828. doi:10.1002/hep.24434

Petrenko, Y. A., Petrenko, A. Y., Martin, I., & Wendt, D. (2017). Perfusion bioreactor-based cryopreservation of 3D human mesenchymal stromal cell tissue grafts. *Cryobiology, 76*, 150-153. doi:10.1016/j.cryobiol.2017.04.001

Petyim, S., Makemahar, O., Kunathikom, S., Choavaratana, R., Laokirkkiat, P., & Penparkkul, K. (2009). The successful pregnancy and birth of a healthy baby after human blastocyst vitrification using Cryo-E, first case in Siriraj Hospital. *J Med Assoc Thai, 92*(8), 1116-1121.

Polge, C., Smith, A. U., & Parkes, A. S. (1949). Revival of Spermatozoa after Vitrification and Dehydration at Low Temperatures. *Nature, 164*(4172), 666-666. doi:10.1038/164666a0

Pollock, G. A., Pegg, D. E., & Hardie, I. R. (1986). An isolated perfused rat mesentery model for direct observation of the vasculature during cryopreservation. *Cryobiology, 23*(6), 500-511.

Pope, C. E., Pope, V. Z., & Beck, L. R. (1986). Cryopreservation and transfer of baboon embryos. *Journal of in Vitro Fertilization and Embryo Transfer, 3*(1), 33-39. doi:10.1007/bf01131378

Porcu, E., Fabbri, R., Seracchioli, R., Ciotti, P. M., Magrini, O., & Flamigni, C. (1997). Birth of a healthy female after intracytoplasmic sperm injection of cryopreserved human oocytes. *Fertil Steril, 68*(4), 724-726.

Privratsky, J. R., & Newman, P. J. (2014). PECAM-1: regulator of endothelial junctional integrity. *Cell Tissue Res, 355*(3), 607-619. doi:10.1007/s00441-013-1779-3

Puschmann, E., Selden, C., Butler, S., & Fuller, B. (2014). *Liquidus Tracking: Controlled Rate Vitrification for the Cryopreservation of Larger Volumes and Tissues* (Vol. 35).

Puschmann, E., Selden, C., Butler, S., & Fuller, B. (2017). Liquidus Tracking: Large scale preservation of encapsulated 3-D cell cultures using a vitrification machine. *Cryobiology, 76*, 65-73. doi:10.1016/j.cryobiol.2017.04.006

Qihao, Z., Xigu, C., Guanghui, C., & Weiwei, Z. (2007). Spheroid formation and differentiation into hepatocyte-like cells of rat mesenchymal stem cell induced by co-culture with liver cells. *DNA Cell Biol, 26*(7), 497-503. doi:10.1089/dna.2006.0562

Quinn, P., & Kerin, J. F. P. (1986). Experience with the cryopreservation of human embryos using the mouse as a model to establish successful techniques. *Journal of in Vitro Fertilization and Embryo Transfer, 3*(1), 40-45. doi:10.1007/bf01131379

Rakszewska, A., Tel, J., Chokkalingam, V., & Huck, W. T. S. (2014). One drop at a time: toward droplet microfluidics as a versatile tool for single-cell analysis. *NPG Asia Materials, 6*(10), e133-e133. doi:10.1038/am.2014.86

Rall, W. F. (1987). Factors affecting the survival of mouse embryos cryopreserved by vitrification. *Cryobiology, 24*(5), 387-402. doi:10.1016/0011-2240(87)90042-3

Rall, W. F., & Fahy, G. M. (1985). Ice-free cryopreservation of mouse embryos at -196 degrees C by vitrification. *Nature, 313*(6003), 573-575.

Rosenfeld, C. S., Gremba, C., Shadduck, R. K., Zeigler, Z. R., & Nemunaitis, J. (1994). Engraftment with peripheral blood stem cells using noncontrolled-rate cryopreservation: comparison with autologous bone marrow transplantation. *Exp Hematol, 22*(3), 290-294.

Saleh, F. A., Whyte, M., & Genever, P. G. (2011). Effects of endothelial cells on human mesenchymal stem cell activity in a three-dimensional in vitro model. *Eur Cell Mater, 22*, 242-257; discussion 257. doi:10.22203/eCM.v022a19

Salmenpera, P., Kankuri, E., Bizik, J., Siren, V., Virtanen, I., Takahashi, S., Leiss, M., Fassler, R., & Vaheri, A. (2008). Formation and activation of fibroblast spheroids depend on fibronectin-integrin interaction. *Exp Cell Res, 314*(19), 3444-3452. doi:10.1016/j.yexcr.2008.09.004

Santos, R. M. d., Barreta, M. H., Frajblat, M., Cucco, D. C., Mezzalira, J. C., Bunn, S., Cruz, F. B., Vieira, A. D., & Mezzalira, A. (2006). Vacuum-cooled liquid nitrogen increases the developmental ability of vitrified-warmed bovine oocytes. *Ciência Rural, 36*, 1501-1506.

Saragusty, J., & Arav, A. (2011). Current progress in oocyte and embryo cryopreservation by slow freezing and vitrification. *Reproduction, 141*(1), 1-19. doi:10.1530/rep-10-0236

Schmeichel, K. L., & Bissell, M. J. (2003). Modeling tissue-specific signaling and organ function in three dimensions. *J Cell Sci, 116*(Pt 12), 2377-2388. doi:10.1242/jcs.00503

Schwartz, M. A., & Chen, C. S. (2013). Cell biology. Deconstructing dimensionality. *Science, 339*(6118), 402-404. doi:10.1126/science.1233814

Seki, S., & Mazur, P. (2009). The dominance of warming rate over cooling rate in the survival of mouse oocytes subjected to a vitrification procedure. *Cryobiology, 59*(1), 75-82. doi:10.1016/j.cryobiol.2009.04.012

Shi, Q., S, R., Wu, M. H., Wijelath, E. S., Yu, C., Ishida, A., Fujita, Y., Kothari, S., Mohle, R., Sauvage, L. R., Moore, M. A., Storb, R. F., & Hammond, W. P. (1998). Evidence for circulating bone marrow-derived endothelial cells. *Blood. 1998 Jul 15;92(2):362-7.*

Sieme, H., Oldenhof, H., & Wolkers, W. F. (2016). Mode of action of cryoprotectants for sperm preservation. *Anim Reprod Sci, 169*, 2-5. doi:10.1016/j.anireprosci.2016.02.004

Sloviter, H. A. (1951). IN-VIVO SURVIVAL OF RABBIT'S RED CELLS RECOVERED AFTER FREEZING. *The Lancet, 257*(6669), 1350-1351. doi:10.1016/S0140-6736(51)92800-0

Song, H., David, O., Clejan, S., Giordano, C., Pappas-Lebeau, H., Xu, L., & O'Connor, K. (2004). Spatial composition of prostate cancer spheroids in mixed and static cultures. *Tissue Eng. ;10(7-8):1266-76.*

Songsasen, N., Buckrell, B. C., Plante, C., & Leibo, S. P. (1995). In vitro and in vivo survival of cryopreserved sheep embryos. *Cryobiology, 32*(1), 78-91. doi:10.1006/cryo.1995.1007

Souza, G. R., Molina, J. R., Raphael, R. M., Ozawa, M. G., Stark, D. J., Levin, C. S., Bronk, L. F., Ananta, J. S., Mandelin, J., Georgescu, M.-M., Bankson, J. A., Gelovani, J. G., Killian, T. C., Arap, W., & Pasqualini, R. (2010). Three-dimensional tissue culture based on magnetic cell levitation. *Nature Nanotechnology, 5*, 291. doi:10.1038/nnano.2010.23

Stahl, A., Wenger, A., Weber, H., Stark, G. B., Augustin, H. G., & Finkenzeller, G. (2004). Bi-directional cell contact-dependent regulation of gene expression between endothelial cells and osteoblasts in a three-dimensional spheroidal coculture model. *Biochem Biophys Res Commun, 322*(2), 684-692. doi:10.1016/j.bbrc.2004.07.175

Steponkus, P. L., Myers, S. P., Lynch, D. V., Gardner, L., Bronshteyn, V., Leibo, S. P., Rall, W. F., Pitt, R. E., Lin, T. T., & MacIntyre, R. J. (1990). Cryopreservation of Drosophila melanogaster embryos. *Nature, 345*(6271), 170-172. doi:10.1038/345170a0

Stiff, P. J., Koester, A. R., Weidner, M. K., Dvorak, K., & Fisher, R. I. (1987). Autologous bone marrow transplantation using unfractionated cells cryopreserved in dimethylsulfoxide and hydroxyethyl starch without controlled-rate freezing. *Blood, 70*(4), 974-978.

Sugiyama, R., Nakagawa, K., Shirai, A., Sugiyama, R., Nishi, Y., Kuribayashi, Y., & Inoue, M. (2010). Clinical outcomes resulting from the transfer of vitrified human embryos using a new device for cryopreservation (plastic blade). *Journal of Assisted Reproduction and Genetics, 27*(4), 161-167. doi:10.1007/s10815-010-9390-y

Sun, Y., Wang, Y., Zhou, L., Zou, Y., Huang, G., Gao, G., Ting, S., Lei, X., & Ding, X. (2018). Spheroid-cultured human umbilical cord-derived mesenchymal stem cells attenuate hepatic ischemia-reperfusion injury in rats. *Sci Rep, 8*(1), 2518. doi:10.1038/s41598-018-20975-0

Syed-Picard, F. N., Du, Y., Hertsenberg, A. J., Palchesko, R., Funderburgh, M. L., Feinberg, A. W., & Funderburgh, J. L. (2018). Scaffold-free tissue engineering of functional corneal stromal tissue. *J Tissue Eng Regen Med, 12*(1), 59-69. doi:10.1002/term.2363

Tan, F., Heng Lee, K., Siam Gouk, S., Magalhaes, R., Poonepalli, A., Hande, P., S Dawe, G., & Kuleshova, L. (2007). *Optimization of cryopreservation of stem cells cultured as neurospheres: Comparison between vitrification, slow-cooling and raped cooling "freezing" protocols* (Vol. 28).

Tateishi-Yuyama, E., Matsubara, H., Murohara, T., Ikeda, U., Shintani, S., Masaki, H., Amano, K., Kishimoto, Y., Yoshimoto, K., Akashi, H., Shimada, K., Iwasaka, T., & Imaizumi, T. (2002). Therapeutic angiogenesis for patients with limb ischaemia by autologous transplantation of bone-marrow cells: a pilot study and a randomised controlled trial. *Lancet, 360*(9331), 427-435. doi:10.1016/s0140-6736(02)09670-8

Taylor, M., Song, Y. C., & Brockbank, K. (2019). Vitrification in Tissue Preservation: New Developments.

Taylor, M. J., & Pegg, D. E. (1983). The effect of ice formation on the function of smooth muscle tissue stored at −21 or −60 °C. *Cryobiology, 20*(1), 36-40. doi:10.1016/0011-2240(83)90057-3

Tekkatte, C., Gunasingh, G. P., Cherian, K. M., & Sankaranarayanan, K. (2011). "Humanized" stem cell culture techniques: the animal serum controversy. *Stem Cells Int, 2011*, 504723. doi:10.4061/2011/504723

Tian, C., Zhang, X., & Zhao, G. (2019). Vitrification of stem cell-laden core-shell microfibers with unusually low concentrations of cryoprotective agents. *Biomater Sci, 7*(3), 889-900. doi:10.1039/c8bm01231h

Trounson, A., & Mohr, L. (1983). Human pregnancy following cryopreservation, thawing and transfer of an eight-cell embryo. *Nature, 305*(5936), 707-709.

Tsang, W. H., & Chow, K. L. (2009). Mouse embryo cryopreservation utilizing a novel high-capacity vitrification spatula. *BioTechniques, 46*(7), 550-552. doi:10.2144/000113125

Tucker, M. J., Morton, P. C., Wright, G., Sweitzer, C. L., & Massey, J. B. (1998). Clinical application of human egg cryopreservation. *Hum Reprod, 13*(11), 3156-3159.

Tzanakakis, E. S., Hansen, L. K., & Hu, W. S. (2001). The role of actin filaments and microtubules in hepatocyte spheroid self-assembly. *Cell Motil Cytoskeleton, 48*(3), 175-189. doi:10.1002/1097-0169(200103)48:3<175::aid-cm1007>3.0.co;2-2

Vajta, G., Holm, P., Kuwayama, M., Booth, P. J., Jacobsen, H., Greve, T., & Callesen, H. (1998). Open Pulled Straw (OPS) vitrification: a new way to reduce cryoinjuries of bovine ova and embryos. *Mol Reprod Dev, 51*(1), 53-58. doi:10.1002/(sici)1098-2795(199809)51:1<53::aid-mrd6>3.0.co;2-v

Vajta, G., Rienzi, L., & Ubaldi, F. M. (2015). Open versus closed systems for vitrification of human oocytes and embryos. *Reprod Biomed Online, 30*(4), 325-333. doi:10.1016/j.rbmo.2014.12.012

Valdez, C. A., Abas Mazni, O., Takahashi, Y., Fujikawa, S., & Kanagawa, H. (1992). Successful cryopreservation of mouse blastocysts using a new vitrification solution. *J Reprod Fertil, 96*(2), 793-802.

van Uem, J. F., Siebzehnrubl, E. R., Schuh, B., Koch, R., Trotnow, S., & Lang, N. (1987). Birth after cryopreservation of unfertilized oocytes. *Lancet, 1*(8535), 752-753.

Vanderzwalmen, P., Bertin, G., Debauche, C., Standaart, V., & Schoysman, E. (2000). “In Vitro” Survival of Metaphase II Oocytes (MII) and Blastocysts After Vitrification in a Hemi-Straw (HS) System. *Fertility and Sterility, 74*(3, Supplement 1), S215-S216. doi:10.1016/S0015-0282(00)01358-3

Vantangoli, M. M., Madnick, S. J., Huse, S. M., Weston, P., & Boekelheide, K. (2015). MCF-7 Human Breast Cancer Cells Form Differentiated Microtissues in Scaffold-Free Hydrogels. *PLoS ONE, 10*(8), e0135426. doi:10.1371/journal.pone.0135426

Wartenberg, M., DÖNMEZ, F., LING, F. C., ACKER, H., HESCHELER, J., & SAUER, H. (2001). Tumor-induced angiogenesis studied in confrontation cultures of multicellular tumor spheroids and embryoid bodies grown from pluripotent embryonic stem cells. *The FASEB Journal, 15*(6), 995-1005. doi:10.1096/fj.00-0350com

Whittingham, D. G., Leibo, S. P., & Mazur, P. (1972). Survival of Mouse Embryos Frozen to -196° and -269°C. *Science, 178*(4059), 411-414. doi:10.1126/science.178.4059.411

Williams, P. A., Stilhano, R. S., To, V. P., Tran, L., Wong, K., & Silva, E. A. (2015). Hypoxia augments outgrowth endothelial cell (OEC) sprouting and directed migration in response to sphingosine-1-phosphate (S1P). *PLoS ONE, 10*(4), e0123437. doi:10.1371/journal.pone.0123437

Winslow, K. L., Yang, D., Blohm, P. L., Brown, S. E., Jossim, P., & Nguyen, K. (2001). Oocyte cryopreservation/a three year follow up of sixteen births. *Fertility and Sterility, 76*(3), S120-S121. doi:10.1016/S0015-0282(01)02354-8

Wu, M.-Y., Chen, S.-U., Chen, T.-H., Yang, Y.-S., Chien, C.-L., Lai, S.-M., & Lin, C.-W. (2006). Novel direct cover vitrification for cryopreservation of ovarian tissues increases follicle viability and pregnancy capability in mice. *Human Reproduction, 21*(11), 2794-2800. doi:10.1093/humrep/del210

Wu, Y., Yu, H., Chang, S., Magalhaes, R., & Kuleshova, L. L. (2007). Vitreous cryopreservation of cell-biomaterial constructs involving encapsulated hepatocytes. *Tissue Eng, 13*(3), 649-658. doi:10.1089/ten.2006.0075

Yavin, S., & Arav, A. (2007). Measurement of essential physical properties of vitrification solutions. *Theriogenology, 67*(1), 81-89. doi:10.1016/j.theriogenology.2006.09.029

Yu, X., Chen, G., & Zhang, S. (2013). A model for predicting the permeation of dimethyl sulfoxide into articular cartilage, and its application to the liquidus-tracking method. *Cryobiology, 67*(3), 332-338. doi:10.1016/j.cryobiol.2013.09.168

Yuhas, J. M., Li, A. P., Martinez, A. O., & Ladman, A. J. (1977). A Simplified Method for Production and Growth of Multicellular Tumor Spheroids. *Cancer Research, 37*(10), 3639-3643.

Zhang, P., Baxter, J., Vinod, K., Tulenko, T. N., & Di Muzio, P. J. (2009). Endothelial differentiation of amniotic fluid-derived stem cells: synergism of biochemical and shear force stimuli. *Stem Cells Dev, 18*(9), 1299-1308. doi:10.1089/scd.2008.0331

Zhao, X., Qiu, X., Zhang, Y., Zhang, S., Gu, X., & Guo, H. (2016). Three-Dimensional Aggregates Enhance the Therapeutic Effects of Adipose Mesenchymal Stem Cells for Ischemia-Reperfusion Induced Kidney Injury in Rats. *Stem Cells Int, 2016*, 9062638. doi:10.1155/2016/9062638